Expression and Functional Role of the Immune-Checkpoint Molecules CD200 and CD200R in Neonatal Sepsis

Dissertation

der Mathematisch-Naturwissenschaftlichen Fakultät

der Eberhard Karls Universität Tübingen

zur Erlangung des Grades eines

Doktors der Naturwissenschaften

(Dr. rer. nat.)

vorgelegt von

Janine Hebel (M. Sc.)

aus Göppingen

Tübingen

2025

Gedruckt mit Genehmigung der Mathematisch-Naturwissenschaftlichen Fakultät der Eberhard Karls Universität Tübingen.

Tag der mündlichen Qualifikation:	13.03.2026
Dekan:	Prof. Dr. Thilo Stehle
1. Berichterstatter/-in:	Prof. Dr. Katja Schenke-Layland
2. Berichterstatter/-in:	PD Dr. med. Natascha Köstlin-Gille

Erklärung

Hiermit erkläre ich, Janine Hebel, dass ich die zur Promotion eingereichte Arbeit mit dem Titel: „*Expression and Functional Role of the Immune-Checkpoint Molecules CD200 and CD200R in Neonatal Sepsis*“ selbstständig verfasst, nur die angegebenen Quellen und Hilfsmittel benutzt und wörtlich oder inhaltlich übernommene Stellen als solche gekennzeichnet habe. Ich erkläre, dass die Richtlinien zur Sicherung guter wissenschaftlicher Praxis der Universität Tübingen (Beschluss des Senats vom 25.05.2000) beachtet wurden. Ich versichere an Eides statt, dass die Angaben wahr sind und dass ich nichts verschwiegen habe. Mir ist bekannt, dass die falsche Abgabe einer Versicherung an Eides statt mit Freiheitsstrafe bis zu drei Jahren oder mit Geldstrafe bestraft wird.

Tübingen, den 14.10.2025

Table of Content

Summary

Almost 40% of childhood deaths occur within the first 28 days of life, with neonatal sepsis being a major contributor to morbidity and mortality, particularly among preterm infants. Newborns are highly susceptible to infections, as their immune responses, compared to those of adults, are still characterized by anti-inflammatory and immunosuppressive mechanisms originating from fetal life. On the other hand, newborns have an impaired ability to resolve inflammatory reactions once they have been initiated. Immune-checkpoint molecules (ICMs) control inflammatory responses and may contribute to immune adaptations in early life, but their role in neonatal sepsis has been poorly defined so far. The ICM CD200 and its receptor CD200R have been suggested to play an important part in regulating inflammatory responses in various murine models of inflammatory diseases and human inflammatory diseases. However, its expression pattern on many neonatal immune cells and its potential role in regulating neonatal responses in inflammatory diseases has not been described so far.

In this study, we investigated the role of CD200/CD200R for the pathogenesis of neonatal sepsis. In a murine *E. coli* sepsis model, neonatal mice required lower bacterial doses to reach mortality comparable to adults and showed higher bacterial burden in lungs and blood, alongside pro-inflammatory cytokine levels. Neonates displayed higher CD200R but lower CD200 expression on monocytes, while neonatal T-cells expressed more CD200 than CD200R. Additionally, neonates had elevated soluble CD200 (sCD200) levels. Recombinant CD200 (rCD200) administration significantly increased mortality in neonatal mice without affecting bacterial load, cytokine levels or immune cell composition, while CD200 blockade had no clear effect in preliminary experiments.

A cross-species analysis of CD200 and CD200R expression of mice and humans revealed notable differences between species. Human neonates (pre-term and full-term) expressed more CD200 on T-cells than adults, with similarly high CD200R expression across groups, while sCD200 levels were lower in newborns compared to adults. Functional assays were unable to elucidate the functional relevance of CD200/CD200R on neonatal immune cells.

Differential CD200/CD200R expression in neonates could reflect developmental immune adaptations that limit excessive inflammation after birth but may predispose neonates to the development of severe infections after pathogen encounter. This provides a basis for further studies on how immune checkpoint pathways shape early-life immunity and transition from fetal to postnatal life. Although rCD200 worsened sepsis outcomes in neonatal mice, immune checkpoint pathways remain a potential target for novel therapeutic approaches in neonatal inflammatory disease.

Zusammenfassung

Fast 40 % aller Todesfälle von Kindern ereignen sich in den ersten 28 Lebenstagen, dabei ist die Sepsis eine der Hauptursachen für Morbidität und Mortalität, vor allem bei Frühgeborenen. Neugeborene sind sehr viel anfälliger für Infektionen als Erwachsene, da die Immunantwort Neugeborener noch durch anti-inflammatorische und immunsuppressive Reaktionen geprägt ist, die aus der Zeit *in utero* stammen. Gleichzeitig ist das neonatale Immunsystem aber auch schlechter in der Lage einmal begonnene Inflammationsreaktionen wieder zu beenden. Immune-Checkpoint Moleküle (ICMs) sind Oberflächenmoleküle auf Immunzellen, die Entzündungsreaktionen regulieren. Über ihre Rolle bei der Immunentwicklung des Neugeborenen und im Rahmen der neonatalen Sepsis ist bisher noch wenig bekannt. Das ICM CD200 und sein Rezeptor CD200R spielen eine wichtige Rolle in der Regulation der Immunreaktion im Rahmen inflammatorischer Erkrankungen, wie bereits in Studien mit Erwachsenen Mäusen und Menschen gezeigt werden konnte. Die Expressionsmuster von CD200 und CD200R auf vielen neonatalen Immunzellen, sowie ihre Rolle in der Regulation der neonatale Immunreaktion auf inflammatorische Erkrankungen wurden bisher noch nicht ausführlich untersucht.

In dieser Studie untersuchten wir die Bedeutung von CD200 und CD200R für die Pathogenese der neonatalen Sepsis. In einem Mausmodell der *E. coli* induzierten Sepsis benötigten neugeborene Mäuse eine deutlich niedrigere Bakteriendosis als adulte Mäuse, um eine vergleichbare Sepsis Mortalität zu erleiden. Neugeborene Mäuse hatten im Rahmen der Sepsis eine höhere Bakterienlast in Lungen und Blut, begleitet von erhöhten Konzentrationen proinflammatorischer Zytokine. Monozyten Neugeborener zeigten eine höhere CD200R aber eine niedrigere CD200 Expression, während neonatale T-Zellen mehr CD200 als CD200R exprimierten. Darüber hinaus hatten Neugeborene erhöhte Level von löslichem CD200 (sCD200) im Blut. Die Gabe von rekombinantem CD200 (rCD200) erhöhte die Mortalität der Sepsis bei neugeborenen Mäusen signifikant, während Bakterienlast, Zytokin-Konzentrationen und die Immunzellkomposition nicht beeinflusst wurden. Eine Blockade von CD200 in Pilotexperimenten zeigte keinen Effekt.

Eine Analyse der CD200 und CD200R Expression auch beim Menschen zeigte deutliche Unterschiede im Vergleich zu den Expressionsmustern in Mäusen. Neugeborene (Früh- und Reifgeborene) exprimierten hier mehr CD200 auf T-Zellen als Erwachsene, wobei die CD200R Expression sich nicht unterschied. Die Level von sCD200 waren bei Neugeborenen verringert. Funktionale Assays konnten die funktionelle Bedeutung der CD200/CD200R Expression auf Neugeborenen-Immunzellen in unserem Setting nicht aufklären.

Unterschiede in der CD200/CD200R Expression bei Neugeborenen im Vergleich zu Erwachsenen könnten eine Rolle bei der Immunadaptionen des Neugeborenen spielen und dazu beitragen, übermäßige Entzündungsreaktionen zu bremsen, aber gleichzeitig mitverantwortlich für die erhöhte Infektionsanfälligkeit Neugeborener sein. Unsere Arbeit bildet eine Grundlage für weiter Studien, die sich mit der Frage beschäftigen sollten, wie Immune-Checkpoint-Signalwege die frühkindliche Immunität und den Übergang vom fetalen in den postnatalen und dann adulten Zustand beeinflussen. Die Arbeit zeigt, dass ICMs ein interessantes Ziel für die Entwicklung neuer therapeutischer Ansätze im Zusammenhang mit inflammatorischen Erkrankungen bei Neugeborenen sind.

List of Abbreviations

-	not present
+	present
°C	Degree Celsius
µg	Microgram
µl	Microliter
µM	Micromolar
ACK	Ammonium chloride
ADAM28	Disintegrin and metallopeptidase domain 28
AmCyan	Anemonia viridis cya
ANOVA	Analysis of Variance
APC	Antigen Presenting Cell
APC (FACS)	Allophycocyanin
APC-Cy7	Allophycocyanin-cyanine7
ARDS	Acute respiratory distress syndrome
Arg-1	Arginase-1
BPD	Bronchopulmonary dysplasia
BV421	Brilliant violet 421
c	Concentration
CBMC	Cord blood mononuclear cells
CD	Cluster of differentiation
CD200R	CD200 receptor
$CD4^+$	T-helper cells
$CD8^+$	Cytotoxic T-cells
cDNA	Complementary DNA
CFDA-SE	Carboxyfluorescein diacetate succinimidyl ester
CFSE	Carboxyfluorescein succinimidyl ester
CFU	Colony forming unit
CLP	Cecal ligation and puncture
CO_2	Carbon dioxide
CRP	C-reactive protein
CS	Cecal slurry
CTLA-4	Cytotoxic T-lymphocyte-associated antigen 4
DAMPs	Camage associated molecular patterns

DC	Dendritic cell
DMEM	Dulbecco's Modified Eagle Medium
DMSO	Dimethyl sulfoxide
DNA	Deoxyribonucleic acid
Dok1/Dok2	Docking protein 1/2
DPBS	Dulbecco's Phosphate Buffered Saline
E	Embryonic day
E. coli	*Escherichia coli*
EDTA	Ethylenediaminetetraacetic acid
ELISA	Enzyme linked immunosorbent assay
EOS	Early onset sepsis
eppi	Eppendorf tubes
ERK	Extracellular signal-related kinase
FACS	Fluorescence-activated cell sorting
FBS	Fetal bovine serum
FITC	Fluorescein isothiocyanate
FoxP3	Forkhead box P3
FSC	Forward scatter
FVS510	Fixable viability stain 510
G	Gauge
g	Gram
GBS	Group B streptococcus
GC	Germinal center
G-CSF	Granulocyte colony-stimulating factor
GM-CSF	Granulocyte-macrophage colony stimulating factor
G-MDSC	Granulocytic myeloid-derived suppressor cells
Gr-1	Granulocyte differentiation antigen-1
h	Hours
H_2O	Dihydrogen monoxide/water
HLA-DR	Human leucocyte antigen DR
HLA-G	Human leucocyte antigen G
i.p.	Intraperitoneal
i.v.	Intravenous
ICM	Immune checkpoint molecules
IDO	Indoleamine 2,3 dioxygenase

IFNγ	Interferone γ
IgSF	Immunoglobulin superfamily
IL-1β	Interleukin-1β
IL-2/4/6/8/10/12/15/17	Interleukin-2/4/6/8/10/12/15/17
iNOS	Inducible Nitric Oxide Synthase
ITIM	Inhibitory receptor motif
JNK	Jun N-terminal kinase
$KHCO_3$	Potassium hydrogen carbonate
LAIR-1	Leukocyte associated immunoglobulin like receptor-1
LB	Lysogeny Broth
LD30	Lethal dose 30
LD90	Lethal dose 90
LOS	Late onset sepsis
LOS (discussion)	Lipooligosaccharide
LPS	Lipopolysaccharide
LTA	Lipoteichoic acid
Ly6-C	Lymphocyte antigen 6 complex, locus C
Ly6-G	Lymphocyte antigen 6 complex, locus G
MACS	Magentic activated cell sorting
MAPK	Mitogen-activated protein kinase
MDSC	Myeloid derived supressor cell
MHC	Major histocompatibility complex
ml	Mililiter
mM	Milimolar
M-MDSC	Monocytic myeloid-derived suppressor cells
MOI	Multiplicity of infection
MyD88	Myeloid differentiation factor 88
NaN_3	Sodiumazide
NEC	Necrotizing enterocolitis
NETs	Neutrophil extracelullar traps
ng	Nanogram
NH_4Cl	Ammonium chloride
NK-cell	Natural killer-cells
nm	Nanometers
NOS	Nitric oxide synthase

OD	Optical density
P	Postnatal day
p	p-value
p38	p38 mitogen-activated protein kinase
P/S	Penicillin/streptomycin
PAMPs	Pathogen associated molecular patterns
PBMC	Peripheral blood mononuclear cell
PD-1	Programmed cell death protein 1
PD-L1	Programmed cell death protein ligand 1
PE	Phycoerythrin
PE-Cy7	Phycoerythrin-cyanine7
PerCP	Peridinin chlorophyll-A protein
pg	Picogram
PHA	Phytohemagglutinin
PorB	Porin protein
pPROM	Preterm premature rupture of membranes
PRR	Pattern recognition receptors
PTB	Phosphotyrosine binding domain
PVL	Periventricular leukomalacia
qPCR	Quantitative polymerase chain reaction
RasGAP	Ras GTPase-activating protein
RasGDP	Ras guanosine diphosphate
RasGTP	Ras guanosine triphosphate
rCD200	Recombinant CD200 protein
rcf	Relative centrifugal force
RNA	Ribonucleic acid
ROS	Reactive oxygen species
RPMI-medium	Roswell Park Memorial Institute-medium
RPS13	Ribosomal protein S13
s.c.	Subcutaneous
sCD200	Soluble CD200
SD	Standard deviation
Src kinase family	Sarcoma kinase family
SSC	Sideward scatter
TGF-β	Transforming growth factor β

Th1	T helper cell 1
Th2	T helper cell 2
TLR	Toll like receptor
TNF-α	Tumor necrosis factor α
Treg	T regulatory cell
TRIF	TIR-domain adaptor-inducing IFN-β
U	Unit
VLBW	Very low birth weight
VLBWI	Very low birth weight infants
vs.	versus
w	with

List of Figures

List of Tables

1. Introduction

1.1. Neonatal sepsis

Almost 40% of all childhood deaths occur during the first 28 days of life, with neonatal sepsis being one of the leading causes of death in the neonatal period [1]. Despite advances in medical care, neonatal sepsis remains a major cause of morbidity and mortality in newborns globally, with an estimated 3 million cases annually and a mortality rate between 11-19% [2,3]. In term infants (≥ 37 weeks gestation), the incidence of sepsis is low, with roughly 0.05%, but it increases in pre-term infants and very low birth weight infants (VLBWI) by up to 40% (**Figure 1**) [4–8].

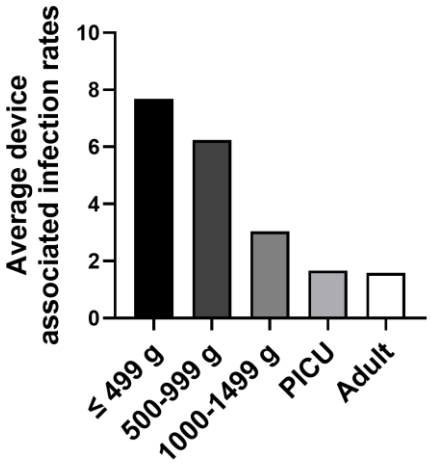

Figure 1. Age and weight dependent rates of sepsis.
Bar graph shows pooled arithmetic means of device associated infection rates of central venous catheter associated sepsis rates in VLBWI (≤499 g, 500-999 g and 1000-1499 g), pediatric intensive care units (PICU) and adults (left to right). Bar graph shows collective data reported by the German National Reference Center for Surveillance of Nosocomial Infections (NRZ) in their NEO- and ITS-KISS reports [9–11]. Graph was created by Janine Hebel.

In adults, according to the 3rd international consensus definition of sepsis, sepsis is defined as a 'life threatening organ dysfunction caused by a dysregulated host response to infection' [12]. In contrast to adults, neonatal sepsis is characterized by many unspecific symptoms. A combination of clinical signs, including changes in body temperature, skin coloration or heart rate, laboratory signs, such as elevated levels of the C-reactive protein (CRP) and/or the cytokines IL-6 or IL-8 and microbial growth in blood cultures is used to identify sepsis in neonates [13–16]. A clear definition is further complicated by the two different categories of, early- and late-onset neonatal sepsis. Early-onset sepsis (EOS) usually occurs within the first 72 hours after birth and is caused by pathogens from the vaginal tract, in particular group B streptococci (GBS) and *Escherichia coli* (*E. coli*) [16,17]. Risk factors for EOS include low

gestational age, intraamniotic infections and preterm premature rupture of the membranes (pPROM)[18]. On the other hand, late-onset sepsis (LOS) occurs after 72 hours post birth and is caused by pathogens from the hospital environment (so called nosocomial pathogens). The most important risk factors for LOS are low gestational age and low birth weight as well as invasive procedures such as intubation or central venous or central arterial lines [3,16,19,20]. In addition to the high mortality rate already mentioned, neonatal sepsis can lead to further health complications including brain injury, the lung disease bronchopulmonary dysplasia (BPD) and the gastrointestinal disease necrotizing enterocolitis (NEC) [21–23]. Deviations in susceptibility and mortality rates of neonatal and adult sepsis most likely stem from differences in the neonatal and adult immune response due to many different immune adaptations of neonates necessary for survival before and after birth.

1.2. The immune system

The immune system represents one of the most important defense mechanisms of the body. It consists of the first line of defense, the physical and chemical barriers like the skin and mucous membranes of the lung and intestinal tract [24–26], followed by two functional components, the innate and the adaptive immune system. The innate immune system develops early in life and remains relatively constant over its course. It acts fast but in an unspecific manner [26,27]. Most cellular components of the innate immune system belong to the myeloid cell lineage such as monocytes, macrophages, granulocytes and dendritic cells (DCs) with the addition of natural killer (NK) cells, as lymphoid cells. They can recognize unspecific pathogen structures, the pattern-associated molecular patterns (PAMPs), or damage-associated molecular patterns (DAMPs) via pattern recognition receptors (PRRs) [26–29]. This leads to phagocytosis of pathogens and/or the secretion of cytokines and chemokines, which activate and recruit other immune cells to the site of infection, where cells like neutrophils kill bacteria using various mechanisms such as phagocytosis and degranulation [26,30,31]. Additionally, antigen presenting cells (APCs) such as monocytes, macrophages, B-cells or DCs internalize pathogens and present small fragments, so called antigens, on their cell surface through major histocompatibility complex (MHC) II molecules to cells of the adaptive immune system. The adaptive immune system develops over the course of life and is characterized by a specific and targeted but slower immune response. Cells of the adaptive

immune system are lymphoid B-cells and T-cells, which first recognize the specific pathogenic antigens, presented by APCs though MHC II molecules via their T- or B-cell receptors. Activation of T-cells further requires signaling through co-stimulatory molecules like CD28 on T-cells with CD80 or CD86 on APCs or, for B-cells, co-stimulation by T-helper cells via CD40/CD40L. These signals are followed by the release of cytokines that further promote T- and B-cell survival and differentiation from naïve T- or B-cells to effector cells [26,32–34]. $CD8^+$ T-cells can induce apoptosis in cell targets, killing infected cells efficiently. $CD4^+$ T-cells can differentiate into, for example, effector T-helper cells 1 (Th1) or T-helper cell 2 (Th2) cells. Both cell types have many important functions. Th1 cells can, for example, activate phagocytes and $CD8^+$ T-cells through the release of interferon γ (IFNγ) and target and eliminate intracellular pathogens, while Th2 cells eliminate extracellular pathogens through the release of, for example, interleukin 4 (IL-4). Th1 and Th2 cells also play an important role in regulating inflammatory responses of the immune system and can induce B-cell differentiation and antibody production. Several other Th-cell sub-sets have been described, which will not be discussed in detail here. B-cells can differentiate into plasma cells, who produce specific antibodies against detected pathogens to neutralize and eliminate them. B-cells and T-cells can also differentiate into long-lived memory cells, that help to provide a faster and enhanced immune response to subsequent exposure to the same antigen [26,33,35,36]. To regulate the immune response, activating signals for T- and B-cells can also be counteracted by signaling via inhibitory molecules, so called immune-checkpoint molecules (ICMs) who provide anti-inflammatory and/or immune inhibitory signals to cells, dampening the pro-inflammatory immune response to infections (more details see chapter 1.4. ICMs). An effective immune response decreases the bacterial load, leading to reduced inflammatory signals. This process is further promoted by, for example, T regulatory cells (Tregs) that can produce anti-inflammatory cytokines to suppress immune cell activation. Another important aspect in the resolution of inflammation is the apoptosis and phagocytosis of activated immune cells such as neutrophils to reduce pro-inflammatory signaling, prevent tissue damage and restore homeostasis [26,37].

1.2.1. Characteristics of the neonatal immune response

Compared to the adult immune system, the neonatal immune system faces particularly great challenges. During pregnancy, the fetus lives in a sterile environment and is protected from infections by the maternal immune system. At this stage, the primary task of the fetal immune system is the prevention of rejection by maternal immune cells, a process called maternal-fetal tolerance. Our group was the first to discover the important role of immunosuppressive myeloid-derived suppressor cells (MDSCs) in maternal-fetal tolerance. MDSCs accumulate both in the mother and the child and play an important part in modulating innate and adaptive immune responses of both [38–42]. During birth, the newborn transfers from the sterile environment of the uterus into the non-sterile environment outside. To protect the newborns sensitive skin from potential harmful pathogens during this vulnerable phase, the neonatal skin is covered in a waxy coating called vernix caseosa, which contains anti-microbial factors such as lysozymes and defensins to kill microorganisms [43]. Due to its limited exposure to antigens *in utero*, the newborn relies primarily on its innate immunity, while the adaptive immunity develops over the first weeks of postnatal life [44,45]. Rapid colonization of the newborns skin and mucous membranes by a huge number of microorganisms immediately after birth, to establish the newborn's microbiome, is another important aspect requiring adaptations of the neonatal immune system [46]. As the innate immune system has to avoid an over-reaction to colonization with commensal bacteria [47,48]. However, these effects are likely also responsible for the high susceptibility to infections of neonates compared to adults [1,16]. Specifically, it has been shown that neonatal monocytes have a reduced ability to process and present antigens due to reduced MHC II expression, which can impact their ability to activate other immune cells [49]. Compared to adult cells, altered expression patterns of co-stimulatory molecules CD80, CD86 and CD40 have been observed in neonatal APCs including DCs, monocytes and macrophages, limiting immune cell activation [50–53]. On top of their reduced co-stimulatory molecule expression, neonatal innate immune cells display further phenotypic and functional differences from adult innate immune cells. Dendritic cell sub-set composition, for example, differs between neonates and adults [54], while NK-cell numbers are elevated at birth [55]. NK-cells are responsible for killing of cells during viral infections, a function that is impaired in neonates due to reduced degranulation of NK-cells and their about three times reduced cytotoxic efficiency compared to adult NK-cells [56,57].

Further, neonatal neutrophils have been reported to be impaired in their antimicrobial defense due to a reduced ability to form neutrophil extracellular traps (NETs) [58] and due to reduced phagocytic capabilities [59,60]. Neonates also possess high amounts of unique immunosuppressive and immunoregulatory neutrophilic immune cells (MDSCs), only present in small numbers in healthy adults [39,61–63].

Important regulatory signaling for innate and adaptive immunity in response to pathogens is triggered by a sub-group of PRRs, the toll-like receptors (TLRs) [64,65]. Among them, TLR2 and TLR4 recognize PAMPs in the form of cell wall components of Gram-positive (e.g. lipoteichoic acid or LTA from group B streptococci) or Gram-negative (e.g. lipopolysaccharide or LPS from *E. coli*) bacteria [64,65]. Multiple studies reported impaired TLR mediated immunity in neonates compared to adults [66–68]. However, for most TLRs, this impaired signaling was not due to lower TLR expression, but rather due to reduced expression of the downstream adaptor molecule myeloid differentiation factor 88 (MyD88) [52,67,69].

Even cytokine secretion by neonatal immune cells has been found to be vastly different from adult immune cells. Activated neonatal innate and adaptive immune cells secrete lower levels of the pro-inflammatory cytokines interleukin 1β (IL-1β), tumor necrosis factor α (TNF-α), IL-12 and IFNγ but higher amounts of the pro-inflammatory IL-6 and the anti-inflammatory IL-10 and IL-4 [52,66,68,70–72]. Reduced TNF-α secretion can impact the recruitment of monocytes to the site of infection or, in combination with reduced IFNγ and granulocyte-macrophage colony-stimulating factor (GM-CSF), can impact macrophage activation [73,74]. Further, lower secretion of IL-12 and IL-15 has been described to lead to reduced neonatal NK-cell activity, resulting in their decreased IFNγ and TNF-α production, thereby impairing T-cell activation and the phagocytic response of innate immune cells [75–80].

Regarding adaptive immunity, it has been shown that the cytokine profile of newborns favors increased secretion of Th2-associated cytokines like IL-10, IL-4 and IL-2 over Th1 related cytokines TNF-α, IFNγ and IL-12. This shift in the cytokine profile of neonates skews the immune system towards an overall anti-inflammatory (Th2) over a pro-inflammatory (Th1) immune response to inflammatory stimuli, which is also observed in neonatal mice [52,71,79–83]. During severe infections associated with strong pro-inflammatory immune responses like sepsis, a high anti-inflammatory IL-10 secretion, that has been observed in newborns, can result in impaired neutrophil recruitment leading to severe disease progression [84].

Another special characteristic of the neonatal immune response is the neonate's disturbed ability to effectively terminate pro-inflammatory immune responses, leading to sustained inflammation and increased risk of organ damage [85,86]. Apoptosis of activated immune cells is an important mechanism to control inflammation and tissue damage during infection. In that context, neonatal neutrophils have been found to be less efficient in their response to apoptotic stimuli leading to prolonged cell survival [87–89].

Despite many advances in understanding neonatal immunity in recent years, many aspects of the neonatal immune system and their relation to higher disease susceptibility and more severe inflammatory disease progression in full-term and especially pre-term infants remain unclear and require further research.

1.3. The immune response to sepsis

In adults, the immune response to bacteria starts out normally as described above (see chapter 1.2. the immune system) with an early pro-inflammatory response. Due to the high bacterial load during sepsis, over time, this leads to hyper-inflammation caused by the uncontrolled release of pro-inflammatory cytokines like TNF-α, IL-6, IL-1β, IFNγ and IL-8, a reaction known as 'cytokine storm' that leads to severe organ dysfunctions [90–95]. In adults, the hyperinflammatory reaction is often followed by an immunosuppressive stage [96,97]. The severe immunosuppression observed in later stages of sepsis is most likely due to increased depletion of many immune cell types, such as T-cells, B-cells and DCs, via apoptosis and an increased secretion of anti-inflammatory cytokines like IL-10, which impairs immune cell functions [93,98–102]. An expansion of immune regulatory Tregs and MDSCs has also been observed in septic patients leading to reduced immune cell activation and T-cell expansion during infection and therefore higher mortality rates [103–107]. Additionally, T-cell exhaustion, a dysfunctional state of T-cells, and reduced expression of antigen presenting cell surface markers like human leucocyte antigen DR (HLA-DR), which are needed for T-cell activation, have been observed in adults with sepsis [97,108]. All of this prevents effective clearance of bacteria and the resolution of inflammation without excessive tissue damage leading to high mortality rates of sepsis. Interestingly, women seem to tolerate sepsis better than men, with lower rates of organ failure and mortality noted in women [109–112].

1.3.1. The neonatal immune response to sepsis

As mentioned before, neonates are much more susceptible to severe infections like sepsis and experience a higher mortality rate compared to adults. This has been associated with differences in the immune response of neonates leading to an impaired initial reaction to pathogens. For example, reduced cell surface expression of HLA-DR has been observed on monocytes and DCs of septic neonates, leading to reduced T-cell activation and impaired immune functions [113,114]. Impaired immune response to sepsis in neonates can also be attributed to high numbers of the immune regulatory MDSCs and Tregs, which polarize the immune system towards an anti-inflammatory Th2 response (**Figure 2**) [62,115,116]. Impaired immune responses and increased mortality in neonatal sepsis can also be linked to the increased depletion of neutrophils (neutropenia) during sepsis due reduced bone marrow storage pools of neonates compared to adults [117–120].

On the other hand, neonates often develop further health complications associated with sepsis like BPD and NEC. The development of these complications has been associated with a decreased ability to terminate pro-inflammatory responses in neonates, an effect called sustained inflammation. For example, it has been reported, that neonatal monocytes have a reduced sensitivity to apoptosis and phagocytosis-induced cell death after bacterial clearance, leading to continuous pro-inflammatory signaling by these cells [85,121–123]. In fact, an increased release of pro-inflammatory cytokines including IL-6, TNF-α, IL-8 and IFNγ as well as anti-inflammatory cytokines IL-10 and IL-4 (known as cytokine storm) has been observed in human neonates and in murine models of neonatal sepsis [124–126].

The treatment of adult, and in particular, neonatal sepsis remains challenging. In addition to antibiotic therapy and supportive approaches targeting clinical symptoms, various immunomodulatory strategies including cytokine modulators, TLR antagonists and targeting of immune-checkpoint molecules have been tested to improve outcomes [127–131]. However, none has demonstrated a clear benefit so far.

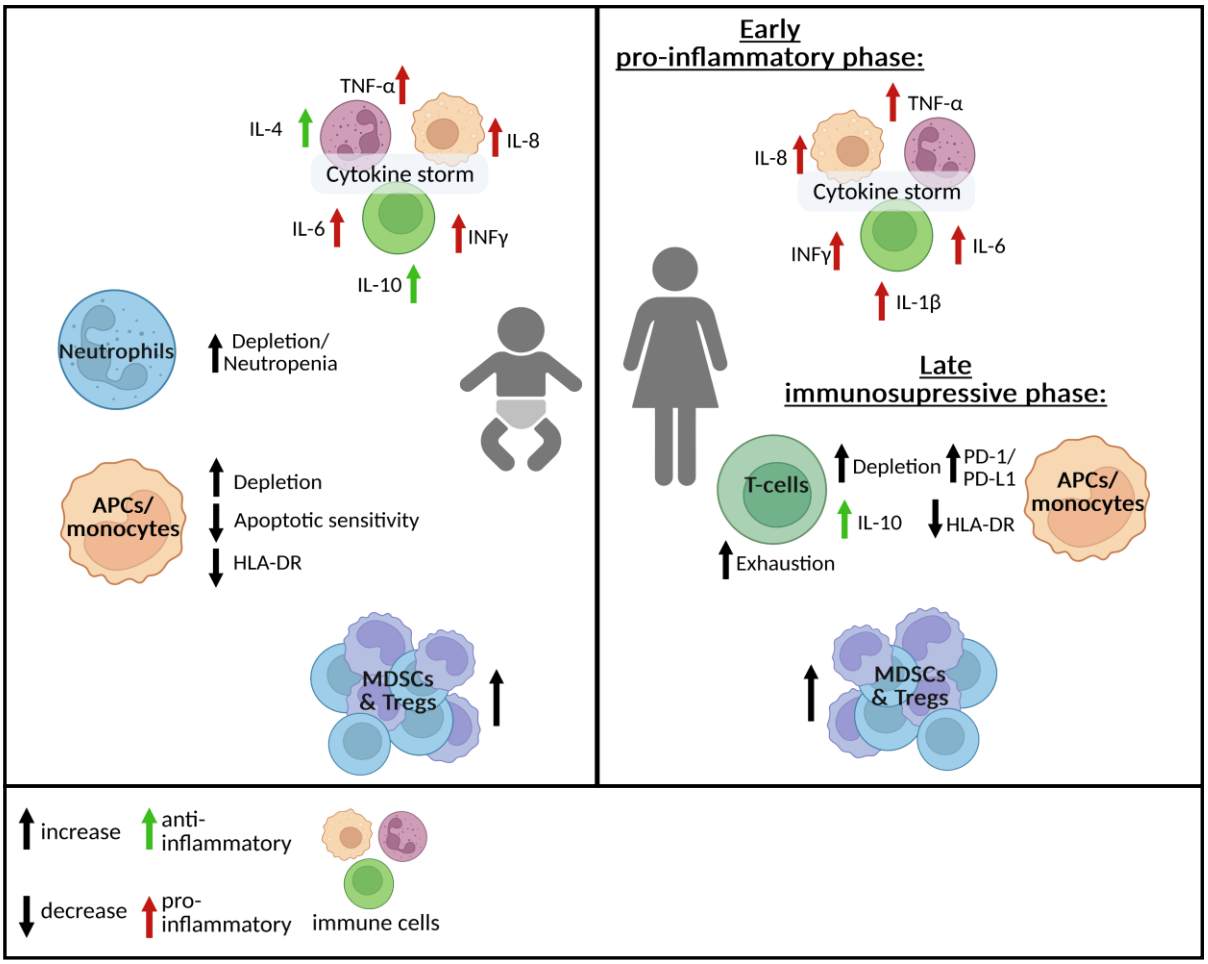

Figure 2. The immunology of sepsis in neonates and adults.

The immune system undergoes many changes during severe sepsis infections in neonates (left) and adults (right). This includes increased cytokine release by immune cells known as cytokine storm, immune cell depletion, changes in cell surface marker expression and accumulation of MDSCs and Tregs among other changes. Created with BioRender.com.

1.4. Immune-checkpoint molecules (ICMs)

Immune-checkpoint molecules (ICMs) are a group of immune-regulatory molecules expressed on the surface of different cell types [132–134]. ICMs play an important role in maintaining self-tolerance and controlling immune responses, and a disturbed balance between stimulatory and inhibitory signals can lead to pathologies such as autoimmune disorders [135,136]. ICMs also play an important role in immune escape of malignant diseases. Here tumors can regulate ICM expression to inhibit, for example, T-cell activation thereby avoiding killing of malignant cells. One of the most studied ICM pairs is programmed cell death protein 1 (PD-1) and its ligand PD-L1. They have been found to be expressed on a variety of different immune cell types including T-cells, B-cells, monocytes, NK-cells and DCs [137–141]. PD-1 and PD-L1 provide an inhibitory signal for the adaptive immune response by regulating T-cell activation and cytokine production and inducing immune tolerance [137,138,142,143]. The inhibitory signaling of PD-1 has also been found to be an important regulator of innate immune responses [144]. Another widely expressed ICM is cytotoxic T-lymphocyte-associated antigen 4 (CTLA-4), a negative regulator of T-cell function that binds to CD80 and CD86 on APCs [145,146]. Blocking of ICMs including PD-1 and CTLA-4 has been successfully used before in malignant diseases to reactivate T-cells to eliminate malignant cells [147–149].

ICMs also play a role in regulating inflammation in the context of infections. Many studies reported increased expression of PD-1 and PD-L1 in patients or mice with sepsis [140,144,150,151]. These increased ICM expressions may be linked to sepsis-induced immunosuppression [152]. PD-1 and PD-L1 expression during sepsis has been associated with reduced proliferative capacity of T-cells and therefore an increased risk for secondary infections [97]. Targeting of PD-1/PD-L1 or CTLA-4 in murine sepsis models by either knock-out or blocking antibodies has been shown to improve survival, reduce organ damage and lower T-cell apoptosis [153–157]. However, despite the benefit of ICM blockade in septic mice, adverse effects of targeting ICMs have to be considered and no ICM blocking antibody has been approved for sepsis treatment in humans so far. In fact, clinical studies of PD-1 or PD-L1 blocking antibody treatment in human sepsis have been limited to early phase 1 trials with a focus on analyzing toxicities and dose-ranging [158–160].

Differences in the expression pattern of ICMs between adult and neonatal cells have been

reported for some ICMs. For example, Walk et al. observed differential expression of several ICMs on neonatal T-cells and monocytes compared to adults [161]. Our group found reduced expression of PD-L1, PD-L2 and CTLA-4 on neonatal $CD4^+$ and to a lesser extent $CD8^+$ T-cells compared to adult cells after activation of the T-cell receptor and after bacterial stimulation [141]. In neonatal mice PD-1 knock-out led to lower mortality rates after sepsis induction [151,155]. However, the role of other ICMs in the neonatal immune response has not been explored in depth so far.

1.4.1. CD200 and CD200R

The ICM CD200, formerly known as OX-2, is a type 1 transmembrane glycoprotein with a size of 48 kDa [162,163]. The structure of CD200 consists of three parts, two immunoglobulin superfamily (IgSF) extracellular domains, a single transmembrane region and a short cytoplasmic tail that lacks any signaling motifs [163–165]. Its structure is closely related to the family of B7 co-stimulatory receptors [166]. CD200 is highly conserved and has been described in humans [167], mice [168] and rats [162], with amino acid sequence homology ranging between 74-96% [165]. CD200 is expressed on various epithelial cells in, for example, the lung and blood vessels [167,169,170], as well as tumor cells [171].

Due to the lack of any signaling motifs in the short intracellular region of CD200, its functionality depends on the engagement with its binding partner, the CD200 receptor (CD200R) [172]. Genes encoding CD200 and CD200R are closely related both in humans and in mice, indicating that these genes evolved by gene duplication [173]. Just like CD200, the structure of CD200R consists of two IgSF domains and a single transmembrane region [174]. However, CD200R has a significantly longer cytoplasmic tail [174] that, in contrast to most inhibitory receptors of the IgSF, does not contain an immunoreceptor tyrosine-based inhibitory receptor motif (ITIM) for signaling [175]. Instead, the cytoplasmic tail of CD200R contains three conserved tyrosine (Y) residues Y291, Y294 and Y302 in humans [176,177] and Y286, Y289 and Y297 in mice [178,179]. Out of the three tyrosine residues, Y302/Y297 and, to a lesser extent, Y291/Y286 are required for CD200R signaling, with Y302/Y297 being located within a recognition motif (NPxY) of a phosphotyrosine binding (PTB) domain [174,176,178,179]. Interaction of CD200 with CD200R leads to phosphorylation of these tyrosine residues mediated by members of the Src (sarcoma) kinase family [178]. This leads to

binding of docking-protein 1 (Dok1) and (with a higher affinity) docking-protein 2 (Dok2) at the PTB domain of Y302/Y297 and their subsequent phosphorylation by Src kinases [176,178,179]. Dok2 has been shown to be essential for CD200R mediated signaling while Dok1 signaling seems to be less important in this context [176]. After binding of Dok2 to the PTB domain of the CD200R cytoplasmic tail and its subsequent phosphorylation, Dok2 recruits Ras GTPase-activating protein (RasGAP), which hydrolyses RasGTP to its inactive form RasGDP. This inhibits Ras signaling to multiple mitogen-activated protein kinase (MAPK) pathways, including extracellular signal-regulated kinase (ERK), p38 mitogen-activated protein kinase (p38) and Jun N-terminal kinase (JNK), thereby suppressing their activation and leading to inhibition of cell functions (**Figure 3**) [176,179,180].

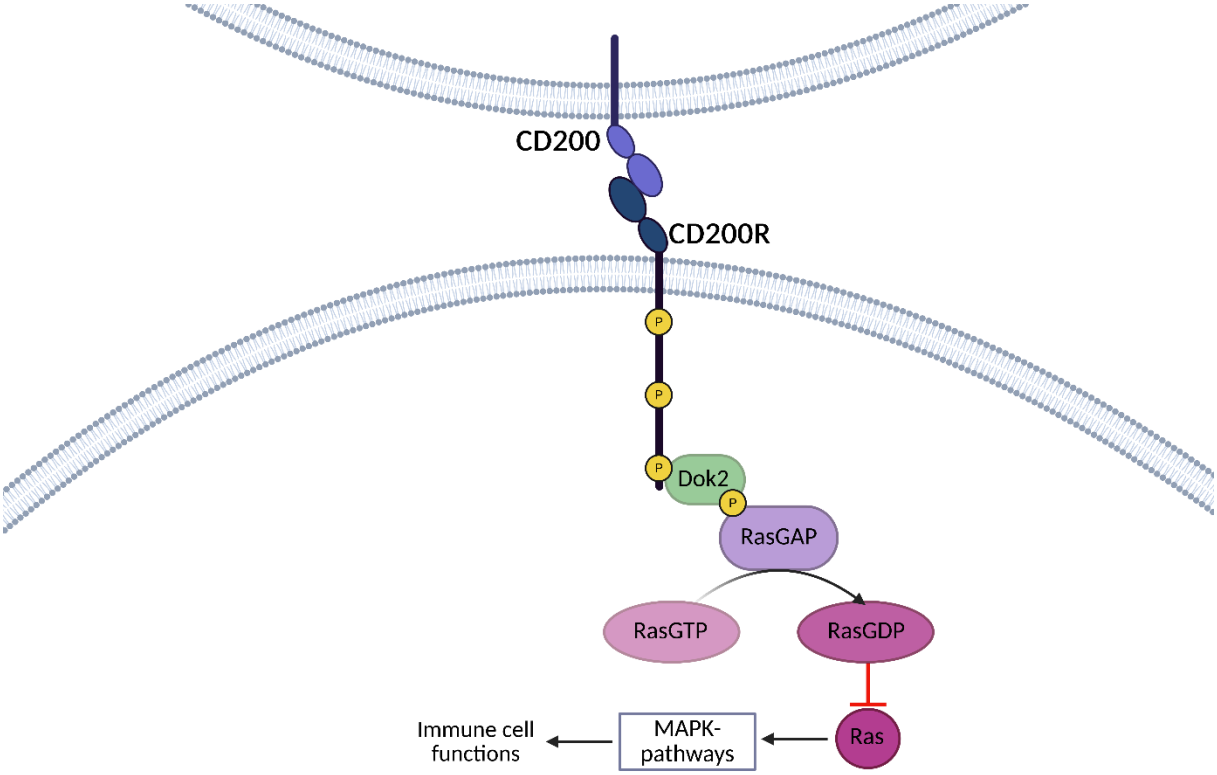

Figure 3. CD200R signaling pathway.
Simplified overview of the CD200R pathway signaling cascade of immune cells. Created with BioRender.com.

Over the years, multiple isoforms of CD200R have been discovered, with at least two isoforms (CD200R1, CD200R2) found in humans and five (CD200R1-R5) in mice [173,181–183]. Gorczynski et al. reported that all CD200R isoforms can bind CD200, while multiple other groups found weaker or no binding of CD200 to CD200R2-R4 isoforms, highlighting isoform CD200R1 as the functionally most important [173,184,185].

Compared to CD200, CD200R expression is more restricted to immune cells and has been reported to be highly expressed on cells of the myeloid lineage, including macrophages, DCs, monocytes, neutrophils, NK-cells, MDSCs and mast cells [161,169,173,174,178,186]. To a lesser extent, CD200R expression has also been observed on immune cells of the lymphoid lineage like B-cells and T-cells and on brain microglia cells [161,168,173,186,187].

Throughout the years, numerous studies have been conducted to reveal the functional consequences of CD200 and CD200R interaction. Using CD200 -/- (knock-out) mice, Hoek et al. observed increased macrophage and microglia activation in the absence of CD200, indicating its importance in regulating myeloid cell activity [168]. A role for CD200-CD200R signaling in modulating myeloid cell functions has also been suggested by Zhang et al., who observed reduced degranulation and cytokine production by mast cells after CD200 engagement with its receptor [179], and Jenmalm et al., who reported inhibition of IFNγ and IL-17 secretion by myeloid cells of humans and mice after CD200R activation [188]. Regarding lymphoid cells, CD200 -/- mice displayed a shift from Th1- to Th2-associated cytokine production after antigen challenge, indicating a potential role of CD200 in regulating Th1/Th2 cells balance [189,190]. Further, multiple studies revealed a correlation between the abundance of CD200 and the induction of forkhead box P3 $(FoxP3)^{+}$ Tregs *in vitro* and in myeloid malignancies [191–194]. A potential role of CD200 and CD200R in regulating lung homeostasis has also been suggested, whereby CD200R-expressing alveolar macrophages are functionally arrested by binding to CD200-expressing alveolar epithelial cells [169,195,196]. Interestingly, CD200 also seems to have a protective effect on pregnancy as injection of an anti-CD200 antibody increased fetal loss in a mouse model of abortion, while overexpression of CD200 in mice reduced the rates of pregnancy failure [197]. Multiple studies reported CD200 to be a prognostic or diagnostic marker for several malignant diseases such as multiple myeloma, chronic lymphoid leukemia and acute myeloid leukemia [198–200]. Expression of

CD200 by cells in the tumor microenvironment was demonstrated to play a role in immune evasion of tumors by, for example, interaction with CD200R-expressing MDSCs.

In the context of infectious diseases, it has been shown that absence of CD200 increased susceptibility to and mortality during influenza infection [169] or LPS-induced lung inflammation [201] due to increased activation of myeloid cells. A role for CD200 in immune regulation during sepsis has also been suggested. Mukhopadhyay et al. observed reduced CD200R but increased CD200 expression on macrophages in a mouse sepsis model with *Neisseria meningitidis* and showed that CD200 knock-out led to higher numbers of activated leukocytes, higher levels of pro-inflammatory cytokine secretion and significantly increased mortality [202]. The role of CD200 and CD200R for the pathogenesis of neonatal sepsis has not yet been investigated.

1.4.2. sCD200

Soluble CD200 (sCD200) is produced by ectodomain shedding of the cell bound CD200 [203]. CD200 is cleaved by the disintegrin and metallopeptidase domain ADAM28 to create sCD200 in humans [203,204]. sCD200 has been shown to be bioactive, since its binding to the CD200 receptor is followed by downstream phosphorylation of molecules in the CD200R1 signaling cascade [205]. Due to its ability to activate CD200R signaling, sCD200 may also play a role in the control of anti-inflammatory immune cell functions and needs to be considered when studying the CD200/CD200R pathway. Indeed, elevated levels of sCD200 have been observed in some malignancies and in patients with inflammatory diseases like lupus erythematosus and endometriosis, where sCD200 was found to correlate with disease severity [203,206,207].

1.5. Aim of the study

Various immune-checkpoint molecules have been studied in the context of inflammatory diseases over the past years. Their importance in regulating pro- and anti-inflammatory immune responses has been made clear in multiple studies analyzing the effect of ICM blockade or stimulation on survival and immune responses to severe infections like sepsis.

In recent years, the anti-inflammatory signaling ICM CD200 and its receptor CD200R have been studied in relation to inflammatory diseases and cancer in mice and humans. In this context, the loss of CD200 has been reported to be detrimental for survival and outcome in adult septic mice.

The expression of CD200 and CD200R on a broad spectrum of neonatal immune cells and its functional role in relation to neonatal *E. coli* sepsis infections has not been analyzed before. In this study the following hypotheses were investigated:

- CD200 and/or CD200R expression on immune cells differs between adults and neonates and is regulated in response to *E. coli* infection
- Differential CD200/CD200R expression in murine neonates negatively impacts sepsis outcomes

The aim of this study was to analyze and characterize potential differences in the expression patterns of CD200 and CD200R on healthy and *E. coli* infected immune cells of adults and neonates in humans and mice as well as to explore a functional role of CD200/CD200R in septic mice.

2. Materials

2.1. Animals

Mice of the inbred strain C57BL/6J (strain code 632) were originally purchased from Charles River Laboratories in Sulzfeld, Germany. At the time of delivery, mice were six to eight weeks old and received an adaptation period of at least two weeks in our facilities before the start of experiments or breeding. All mice were kept in a designated animal facility. Mice were kept in open type II cages (530 cm^2) in a light-dark cycle of 12 hours. Animal husbandry and breeding of all mice used for experiments in this study were performed in close collaboration with the animal caretakers at the facility. Due to its inbred status, C57BL/6J mice are genetically identical, which reduces discrepancies in research result due to genetic differences and enhances reproducibility of studies [208,209]. These mice have been widely used in studies on the effect of inflammatory diseases on the immune system, which provides good resources to compare and discuss newly obtained results of this study with existing literature [151,169,202,210].

All animal experiments were approved by the regional council Tübingen, Germany (approval numbers K02/20G, K02/23G and K02/24M)

2.1.1. Murine antibodies

Antibody concentrations were titrated before the start of the experiments.

Antibodies for flow cytometry (**Table 1**):

Table 1. List of murine antibodies for flow cytometry.

Antibody	Clone	Fluorochrome	REF	Manufacturer
CD3e	145-2C11	FITC	553062	BD Bioscience, Heidelberg, Germany
CD4	GK1.5	APC-Cy7	100414	BioLegend, San Diego, Ca, USA
CD4	RM4-5	APC	561091	BD Bioscience, Heidelberg, Germany
CD8a	QA17A07	APC-Cy7	155015	BioLegend, San Diego, Ca, USA
CD11b	M1/70	FITC	553310	BD Bioscience, Heidelberg, Germany
CD11c	N418	BV421	117343	BioLegend, San Diego, Ca, USA

CD19	1D3	PE	557399	BD Bioscience, Heidelberg, Germany
CD25	PC61	APC	102012	BioLegend, San Diego, Ca, USA
CD45	30-F11	PerCP-Cy5.5	550994	BD Bioscience, Heidelberg, Germany
CD62L	MEL-14	BV421	562910	BD Bioscience, Heidelberg, Germany
CD200	OX-90	BV421	565547	BD Bioscience, Heidelberg, Germany
CD200R	OX-110	Alexa Fluor 647	566345	BD Bioscience, Heidelberg, Germany
CD335 (NKp46)	29A1.4	PE-Cy7	137618	BioLegend, San Diego, Ca, USA
F4/80	T45-2342	PE	565410	BD Bioscience, Heidelberg, Germany
F4/80	BM8	APC	123116	BioLegend, San Diego, Ca, USA
Fixable Viability Stain 510		AmCyane	564406	BD Bioscience, Heidelberg, Germany
FoxP3	FJK-16s	PE	12-5773-80	Invitrogen by Thermofisher Scientific, Waltham, MA, USA
Ly-6G/ Ly-6C (Gr-1)	RB6-8C5	PE-Cy7	108416	BioLegend, San Diego, Ca, USA
Ly-6C	KHK1.4	PE-Cy7	128018	BioLegend, San Diego, Ca, USA
Ly-6C	AL-21	APC-Cy7	560596	BD Bioscience, Heidelberg, Germany
Ly-6G	1A8	PE-Cy7	127617	BioLegend, San Diego, Ca, USA
Ly-6G	1A8	APC	127614	BioLegend, San Diego, Ca, USA

Functional antibodies (**Table 2**):

Table 2. List of murine antibodies for functional experiments.

Antibody	Clone	REF	Manufacturer
InVivoMAb^{TM} anti-mouse CD200 (OX2)	OX-90	BE0299	Bio X Cell, Lebanon, NH, USA
InVivoMAb^{TM} rat IgG2a isotype control	2A3	BE0089	Bio X Cell, Lebanon, NH, USA

2.2. Patient samples

Adult peripheral blood was collected from healthy volunteers after informed consent in 30 ml syringes with 2 ml heparin sodium (c = 100 U/ml) via percutaneous venipuncture. Cord blood of term-infants (≥ 37 weeks gestation) and pre-term infants (25 4/7 to 34 4/7 weeks gestation) was collected from the umbilical cord directly after cesarean section at the University Women´s Hospital Tübingen. Cord blood samples were collected in 50 ml Falcon tubes containing 2 ml heparin sodium. For full-term infants, mothers gave their written informed consent before the cesarean section. These studies were approved by the local ethics committee (682/2016B0 and 542/2023B01). Peripheral blood (~100-200µl) of pre-term infants was collected 14 days after birth by trained neonatologists at the University Children´s Hospital Tübingen in blood collection tubes containing ethylenediaminetetraacetic acid (EDTA). Cord blood and peripheral blood collection of pre-term infants was approved by the local ethics committee (542/2023B01). All blood samples were collected between October 2022 and September 2025.

2.2.1. Human antibodies

Antibody concentrations were titrated before the start of the experiments.

Antibodies for flow cytometry (**Table 3**):

Table 3. List of human antibodies for flow cytometry.

Antibody	Clone	Fluorochrome	REF	Manufacturer
CD3	REA613 / SK7	FITC	130-113-138	Miltenyi Biotec, Bergisch Gladbach, Germany
CD3	UCHT1	FITC	300406	BioLegend, San Diego, Ca, USA
CD3	HIT3a	PerCP	300326	BioLegend, San Diego, Ca, USA
CD3	HIT3a	PE-Cy7	300316	BioLegend, San Diego, Ca, USA
CD4	RPA-T4	Pacific Blue	300524	BioLegend, San Diego, Ca, USA
CD4	SK3	FITC	345768	BD Bioscience, Heidelberg, Germany
CD8	SK1	APC-Cy7	344713	BioLegend, San Diego, Ca, USA
CD14	M5E2	PE-Cy7	301814	BioLegend, San Diego, Ca, USA

CD19	HIB19	PerCP	302227	BioLegend, San Diego, Ca, USA
CD45	2D1	APC-Cy7	368516	BioLegend, San Diego, Ca, USA
CD45RO	UCHL1	PerCP-Cy5.5	304221	BioLegend, San Diego, Ca, USA
CD62L	DREG-56	BV421	304827	BioLegend, San Diego, Ca, USA
CD66b	G10F5	FITC	561927	BD Bioscience, Heidelberg, Germany
CD80	L307.4	PE	340294	BD Bioscience, Heidelberg, Germany
CD86	2331 (FUN-1)	FITC	555657	BD Bioscience, Heidelberg, Germany
CD183 (CXCR3)	G025H7	APC-Cy7	353721	BioLegend, San Diego, Ca, USA
CD194 (CCR4)	205410	FITC	FAB1567-F	R&D Systems, Minneapolis, MN, USA
CD196 (CCR6)	G034E3	PE-Cy7	353417	BioLegend, San Diego, Ca, USA
CD197 (CCR7)	G043H7	FITC	353215	BioLegend, San Diego, Ca, USA
CD200 (OX2)	A18042B	PE	399804	BioLegend, San Diego, Ca, USA
CD200R	OX-108	APC	329308	BioLegend, San Diego, Ca, USA
CD279 (PD-1)	NAT105	APC	367406	BioLegend, San Diego, Ca, USA
CD282 (TLR-2)	11G7	Alexa Fluor 647	558319	BD Bioscience, Heidelberg, Germany
Fixable Viability Stain 510		AmCyane	564406	BD Bioscience, Heidelberg, Germany
HLA-DR	REA805 / L243	PerCP	130-111-793	Miltenyi Biotec, Bergisch Gladbach, Germany
HLA-DR	L243	FITC	347363	BD Bioscience, Heidelberg, Germany
TCR γ/δ	B1	PerCP	331223	BioLegend, San Diego, Ca, USA
TLR4 (CD284)	TF901	PE	564215	BD Bioscience, Heidelberg, Germany

Functional antibodies (**Table 4**):

Table 4. List of human antibodies for functional experiments.

Antibody	Clone	REF	Manufacturer
Ultra-LEAF™ Purified anti-human CD200 (OX2) Antibody	OX-104	329227	BioLegend, San Diego, Ca, USA
Ultra-LEAF™ Purified anti-human CD200R Antibody	OX-108	329316	BioLegend, San Diego, Ca, USA
Ultra-LEAF™ Purified Mouse IgG1, κ Isotype Ctrl Antibody	MOPC-21	400166	BioLegend, San Diego, Ca, USA

2.3. Technical devices and software

Table 5. List of used devices and software.

Device or Software	Manufacturer
BD FACSCanto™ II	BD Bioscience, Heidelberg, Germany
BD FACSDiva™ Software (Version 9.0)	BD Bioscience, Heidelberg, Germany
Excel	Microsoft, Redmond, WA, USA
FlowJo™ (Version 10)	BD Bioscience, Heidelberg, Germany
GraphPad Prism (Version 10.1.1)	GraphPad Software LLC, San Diego, CA, USA
Quantstudio™ Design & Analysis Software (Version 10.1.1)	Thermofischer Scientific Inc., Waltham, MA, USA
Quantstudio™ 3	Thermofischer Scientific Inc., Waltham, MA, USA
SkanIt™ Software for Microplate Readers (Version 7.0.2)	Thermofischer Scientific Inc., Waltham, MA, USA
T100TM Thermal Cycler	BioRad, Hercules, CA, USA
Varioskan™ LUX Microplate reader	Thermofischer Scientific Inc., Waltham, MA, USA
XP-300™ Automated Hematology Analyzer	Sysmex, Nordstedt, Germany

2.4. Chemicals and reagent

Table 6. List of used chemicals and reagents.

Material	REF	Manufacturer
1.5ml Eppendorf Safelock Tubes	0030 120.086	Eppendorf, Hamburg, Germany
15 ml Cellstar Tubes	188 271-N	Greiner Bio-One, Frickenhausen, Germany
2 ml Eppendorf Safe lock Tubes	0030 120.094	Eppendorf, Hamburg, Germany
24-well Cell culture Plate, Costar	3524 REF	Corning Inc., Corning, NY, USA
2-Mercaptoethanol	M3148	Sigma Aldrich, St.Louis, MO, USA
48-well Cell culture Plate, Costar	3548	Corning Inc., Corning, NY, USA
50 ml Polypropylen Conical Tubes	352070	Corning Inc., Corning, NY, USA
96-well F-bottom Cell culture Plate	655 180	Greiner Bio-One, Frickenhausen, Germany
96-well U-bottom Cell culture Plate, Cellstar	650 180	Greiner Bio-One, Frickenhausen, Germany
Ammonium chloride (NH_4Cl)	09718-1KG	SigmaAldrich, St.Louis, MO, USA
Ampuwa ® Spüllösung	13RAP011	Fresenius Kabi GmbH, Bad Homburg, Germany
BD Cytofix/Cytoperm™ Fixation and Permeabilization Solution	554722	BD Bioscience, Heidelberg, Germany
BD Perm/Wash™ Perm/Wash Buffer	554723	BD Bioscience, Heidelberg, Germany
Blue S'Green qPCR Kit Separate ROX	331416	Biozym, Hessisch Olendorf, Germany
Bovine Serum Albumin (BSA) 20%	P06-1402500	PAN Biotech, Aidenbach, Germany
Brefeldin A from Penicillium brefeldianum	B7651	SigmaAldrich, St.Louis, MO, USA
Columbia Agar with 5% sheepblood	PB5039A	Thermofisher Scientific Inc., Waltham, MA, USA
DMEM	P04-04515	PAN Biotech, Aidenbach, Germany
DMSO	4720.4	Carl Roth GmbH+Co. KG, Karlsruhe, Germany
DPBS	P04-36500	PAN Biotech, Aidenbach, Germany
Dynabeads™ Mouse T-Activator (CD3/CD28)	11452D	Gibco by Thermofisher Scientific, Waltham, MA, USA
EASYstrainer™ 100µm	542000	Greiner Bio-One, Frickenhausen, Germany
EASYstrainer™ 100µm kleiner Druchmesser	542100	Greiner Bio-One, Frickenhausen, Germany
EASYstrainer™ 40µm	542040	Greiner Bio-One, Frickenhausen, Germany

eBioscience™ Foxp3/Transcription Factor Staining Buffer Set	00-5523-00	Invitrogen by Thermofisher Scientific, Waltham, MA, USA
EDTA	ED-500G	SigmaAldrich, St.Louis, MO, USA
Escherichia coli DH5α		Prof. Dr. Dehio, University of Basel, Switzerland
Escherichia coli K1		Dr. Matthias Marschal, University of Tuebingen, Germany
FACS Tubes	10186360	Thermofisher Scientific Inc., Waltham, MA, USA
FACS-Flow	342003	BD Bioscience, Heidelberg, Germany
FBS	S0115	PAN Biotech, Aidenbach, Germany
Fixation/Permeabilization Concentrate (eBioscience)	00-5123-43	Invitrogen by Thermofisher Scientific, Waltham, MA, USA
Formaldehyde (4.5 %)	FN10000-45-1	SAV Liquid Production GmbH, Flintsbach am Inn, Germany
Glycerol	G9012-100ML	SigmaAldrich, St.Louis, MO, USA
Hamilton syringe + 33Gx1/2", 0,21x15mm		Hamilton Company, Reno, NV, USA
Heparin-sodium-5000		Ratiopharm GmbH, Ulm, Germany
human recombinant IFNγ	78020	Stemcell technologies, Vancouver, BC, Canada
IL-2 IS (human)	130-097-742	Miltenyi Biotec, Bergisch Gladbach, Germany
InVivoPure pH 7.0 Dilution Buffer	IP0070	Bio X Cell, Lebanon, NH, USA
LB Broth base (Lennox)	12780052	Invitrogen by Thermofisher Scientific, Waltham, MA, USA
L-Glutamin-solution, 200mM	G7513	SigmaAldrich, St.Louis, MO, USA
MicroAmp® Fast 96-Well Reaction Plate (0.1 ml)	4346907	Applied biosystems by Thermofisher Scientific
MicroAmp™ Opical Adhesive Film	311971	Applied biosystems by Thermofisher Scientific
Microvette® APT 250 EDTA (Capillary blood collection)	201.331	Saerstedt, Nümbrecht, Germany
MojoSort™ Buffer 5X	480017	BioLegend, San Diego, CA, USA
Omnican® 100, 30G x1/2", 0.3mm x 12 mm, insulin syringe	9151141S	B. Braun, Melsungen, Germany
Pancoll human (density 1.077 g/ml)	P04-605000	PAN Biotech, Aidenbach, Germany
PBS Tablets	18912-014	Gibco by Thermofisher Scientific, Waltham, MA, USA
Penicillin-Streptomycin (P/S)	A2212	Biochrom GmbH, Berlin, Germany
Pipette 10 ml	607 160	Greiner Bio-One, Frickenhausen, Germany
Pipette 25 ml	760 160	Greiner Bio-One, Frickenhausen, Germany

Pipette 5 ml	606 160	Greiner Bio-One, Frickenhausen, Germany
Pipette Tips 10µl	720011	Biozym, Hessisch Olendorf, Germany
Pipette Tips 1000µl	2100610	Ratiolab, Dreieich, Germany
Pipette Tips 200µl	775350	Greiner Bio-One, Frickenhausen, Germany
Recombinant human CD200 (carrier free)	770002	BioLegend, San Diego, CA, USA
Recombinant Mouse CD200 FC Chimera Protein, CF (rCD200)	3355-CD-50	R&D Systems, Minneapolis, MN, USA
RPMI 1640	P04-17500	PAN Biotech, Aidenbach, Germany
Sodium azide (NaN_3)	609374-500MG	SigmaAldrich, St.Louis, MO, USA
Sodium bicarbonate ($NaHCO_3$)	60339-500g	SigmaAldrich, St.Louis, MO, USA
Trypanblue 0,4%	T8154-100ML	SigmaAldrich, St.Louis, MO, USA
Trypsin 0.5 %/EDTA 0.2 %,	P10-024100	PAN Biotech, Aidenbach, Germany
Vybrant® CFDA-SE Cell Tracer Kit	V12883	Invitrogen by Thermofisher Scientific, Waltham, MA, USA

2.5. Kits

Table 7. List of used kits.

Kit	REF	Manufacturer
Anti FITC MicroBeads + CD66b AK FITC [211]	130-048-701	Miltenyi Biotec
ELISA MAX™ Standard Set Mouse TNF-α [212]	430901	BioLegend
ELISA MAX™ Standard Set Mouse IL-6 [213]	431301	BioLegend
Human CD200 DuoSetELISA [214]	DY2724	R&D Systems
Human CD200 DuoSetELISA [214]	DY2724	R&D Systems
MojoSort ™ Human Pan Monocyte Isolation kit [215]	480059	BioLegend
Mouse CXCL1/KC DuoSetELISA [216]	DY453	R&D Systems
NucleoSpin RNA isolation kit [217]	740955.50	Macherey-Nagel
Pan T Cell Isolation Kit human [218]	130-096-535	Miltenyi Biotec
Pierce™ 660 nm Protein Assay Kit [219]	22662	Thermofischer Scientific Inc.
PicoKine™ ELISA Mouse CD200 [220]	EK1185	Boster Biological Technology
ProtoScript™ II, cDNA synthesis kit [221]	E6560L	New England Biolabs

2.6. Buffers and culture media

Table 8. List of compositions of used culture media and buffers.

Buffer or Medium	Function	Reagents	Concentration
Ammonium chloride buffer	Erythrocyte lysis	NH_4Cl $NaHCO_3$ EDTA (292.25 g) deionized water	83 g 10 g 0.377 g 900-950 ml
DMEM-medium	cell culture	DMEM FBS L-glutamine P/S	 10% 1% 1%
FACS-buffer	removal unbound antibodies	FACS-Flow NaN_3	 0.1%
Freezing medium	PBMC/CBMC freezing	RPMI FBS DMSO	 20% 20%
Heparin-solution	blood collection	NaCl 0.9% Heparin-sodium-5000	 50 ml 200 µl
LB-medium	liquid bacterial culture	LB Broth Base deionized water	5 g 250 ml
MACS-buffer	MACS	DPBS BSA EDTA	 0.5% 2 mM
RPMI-medium	cell culture	RPMI 1640 FBS L-glutamine (P/S)	 10% 1% 1%

3. Methods

All experiments were performed in a fully equipped biosafety level 1 (BSL-1) laboratory.

3.1. Bacterial culture

Escherichia coli strain K1 was used to induce sepsis in **mice** for our experiments. *E. coli* K1 is an encapsulated strain from a clinical meningitidis and was kindly gifted to us by Dr. Matthias Marschal, University of Tübingen, Germany. *E. coli* K1 is known to be a leading cause of neonatal meningitis [222] and is therefore an ideal strain to induce sepsis *in vivo*. *E. coli* stocks were stored at -80°C in 1 ml cryo-tubes in 500 µl LB-medium and 500 µl of 40% glycerol. *E. coli* for *in vivo* applications was regrown one to two days prior to the start of the experiments. For that, 10 µl of the *E. coli*-stock were added into 1 ml of Dulbecco´s phosphate buffered saline (DPBS) and 100 µl of this solution was plated onto Columbia agar plates containing 5% sheep blood. Plates were incubated at 37°C until the start of the sepsis experiments. For the experiments, *E. coli* was transferred from the agar plates into 1 ml DPBS using a cotton swab. *E. coli* was washed twice with DPBS by centrifugation at 13.000 relative centrifugal force (rcf) for three minutes. The supernatant was removed each time. Finally, *E. coli* was resuspended in 1 ml DPBS. The concentration of *E. coli* was determined by measuring the optical density (OD) of the *E. coli* solution at a wavelength of 600 nanometers (nm) (OD_{600}) using a 96-well flat bottom plate and the Varioskan™ LUX Microplate reader with the SkanIt™ Software. In our experiments, an OD_{600} of 1 corresponded to a concentration of $3.3x10^9$ *E. coli*/ml as determined by a previously established standard curve. For adult and neonatal sepsis experiments, *E. coli* K1 was diluted to reach an OD_{600} of 0.45 (equals $1.5x10^9$ *E. coli*/ml) and then further diluted with DPBS until the desired concentration for each experiment was reached. An example of a calculation for a desired concentration of $3.5x10^8$ *E. coli*/ml is shown below:

OD_{600} 0.45 = $1x10^9$ *E. coli*/ml

Dilution 1:2.5 = 400 µl *E.coli* solution + 600 µl = $6x10^8$ *E. coli*/ml

Dilution 1:7.1 ($6x10^8/3.5x10^8$) = 584 µl of 1:2.5 *E.coli* solution + 416 µl = $3.5x10^8$ *E. coli*/ml

All bacterial solutions were kept on ice until use to reduce duplication of bacteria and therefore changes in the concentration of the solutions.

For *in vitro* stimulation of **human** immune cells the *Escherichia coli* (*E. coli*) strain DH5α, an encapsulated K12 laboratory strain, which was generously gifted to us by Prof. Dr. Dehio (University of Basel, Switzerland) was used. To grow bacteria for the experiments, *E. coli* was transferred from a frozen stock at -80°C to 5 ml culture medium (LB-medium) and incubated overnight at 37°C in a shaker set to 200 rpm. The next day, 200 µl of the bacterial culture were transferred into 5 ml of new LB-medium and incubated at 37°C for additional 60-90 minutes to allow the bacteria to reach their logarithmic growth phase. Then, bacteria were kept on ice to slow down growth. To determine the concentration of the bacterial solution, the OD_{600} was measured using the Varioskan™ LUX Microplate reader. LB-medium without *E. coli* was used as a reference. The logarithmic growth phase of the *E. coli* culture lies between OD_{600} = 0.4 to 0.7. In the case of the *E. coli* strain DH5α, an OD_{600} of 0.5 equals $1x10^9$ *E. coli*/ml and the concentration of bacteria increase linearly with increasing OD-values between OD_{600} of 0.5 and OD_{600} of 1. Bacterial concentration used to stimulate cells is usually specified as multiplicity of infection (MOI). In our experiments, cells were stimulated with *E. coli* in a concentration of MOI 10:1. An example for calculating MOI is given below.

Formula to calculate MOI 10:1 for $1x10^6$ PBMCs with an OD_{600} of 0.4:

Concentration OD_{600} 0.4: $0.4 \times 2x10^9 = 8x10^8$ *E. coli*/ml or $0.8x10^6$ *E. coli*/µl

Concentration *E. coli* MOI 10:1 for $1x10^6$ PBMCS: $1x10^6 \times 10 = 10x10^6$ *E. coli*

$$\text{Volume of } \textit{E. coli} \text{ solution: } \frac{10x10^6}{0.8x10^6} = 12.5 \text{ µl}$$

E. coli was heat-inactivated before the start of experiments to prevent further bacterial growth during the *in vitro* experiments that would alter the ratio/MOI of cells to bacteria over time. For heat inactivation, bacterial solutions with a predetermined OD_{600} value were incubated in a water bath set to 70°C for 30 minutes.

3.2. Mouse experiments

For mouse experiments, a similar set up was used for all experiments. In general, neonatal mice aged postnatal day 1 (P1) to P8 were euthanized via decapitation. Mice aged P21 and up were euthanized in their home cages using CO_2, followed by cervical dislocation. Blood of neonatal mice was collected from the neck area after decapitation using a capillary blood collection tube containing ethylenediaminetetraacetic acid (EDTA). Blood from adult mice was collected by intracardial puncture with a 1 ml syringe containing ~20 µl heparin solution to avoid coagulation of blood. Spleens, livers and lungs of neonatal and adult mice were removed and placed into 1.5 ml Eppendorf tubes filled with DPBS and processed as described in chapter 3.3, unless stated otherwise. For all sepsis experiments, to verify the correct *E. coli* concentration was given to the mice, the prepared *E. coli* solution for each experiment was diluted 1:1.000.000 with DPBS. 100µl of the bacterial solution were plated onto a Columbia agar plate with 5%sheep blood. The plate was incubated at 37°C for at least 24h. Colony forming units (CFUs) grown on the plate were then counted and the *E. coli* concentration given to the mice was calculated (s. 3.1).

Age dependent CD200 and CD200R expression in mice

To determine age dependent differences in the expression patterns of CD200 and CD200R in murine immune cells, flow cytometry analysis of spleens and livers was performed. For this experiment, C57BL/6J mice of five different age groups were analyzed, which included mice aged P1, P3, P8, P21 and adults (8 weeks old). In order to easily compare differences in CD200 and CD200R expression patterns between groups, the ratio of CD200 to CD200R expression was calculated for each group and immune cell type. The formula for calculating this ratio is provided below.

3.2.1. *E. coli* sepsis model with adult mice

For the murine sepsis experiments with adult mice, 8- to 12-week-old C57BL/6J mice were used. Mice were separated into individual cages one day prior to the start of the experiment to reduce stress on the day of the experiment. Separation of mice was done to guarantee the best surveillance of each individual mouse over the course of the experiment and to reduce stress for the animals due to, for example, territorial fights between cage mates.

To induce sepsis, mice received an intraperitoneal (i.p.) injection of $6x10^7$ CFU *E. coli* in 200µl DPBS with an insulin syringe and a G 30 sized needle. *E. coli* concentration was determined as described in chapter 3.1. To study the effect of sepsis on CD200 and CD200R expression on immune cells, both male and female mice were used for this analysis. In a second experiment, to study the effect of high CD200 levels on sepsis progression and outcome, mice received an i.v. injection of 10 µg murine recombinant CD200 protein (rCD200) dissolved in 50µl DPBS 30 minutes before sepsis induction. The control group received a DPBS only injection. Due to the higher tolerance of female mice to sepsis [112], only male C57BL/6J mice were used for this experiment. After sepsis induction, mice were monitored and weighed at least every 12 hours for a maximum of 96 hours in total. Once the first symptoms became visible, the time between monitoring was reduced to 6-, 4-, 2- or 1-hour intervals depending on severity of symptoms and in accordance with a scoresheet and a point system, approved by the regional council in Tübingen (s. Appendix **Table 17**) that monitored the severity of sepsis based on symptom categories. Symptoms in adult animals started as early as six hours after sepsis induction and included loss of appetite and severe weight loss, reduced activity, piloerection (raised fur) on the back and bridge of the nose, mucus around the eyes, a hunched posture and reduced or no reaction to stimuli (for example, touching of the mouse or tapping on the outside of the cage) (**Figure 4**).

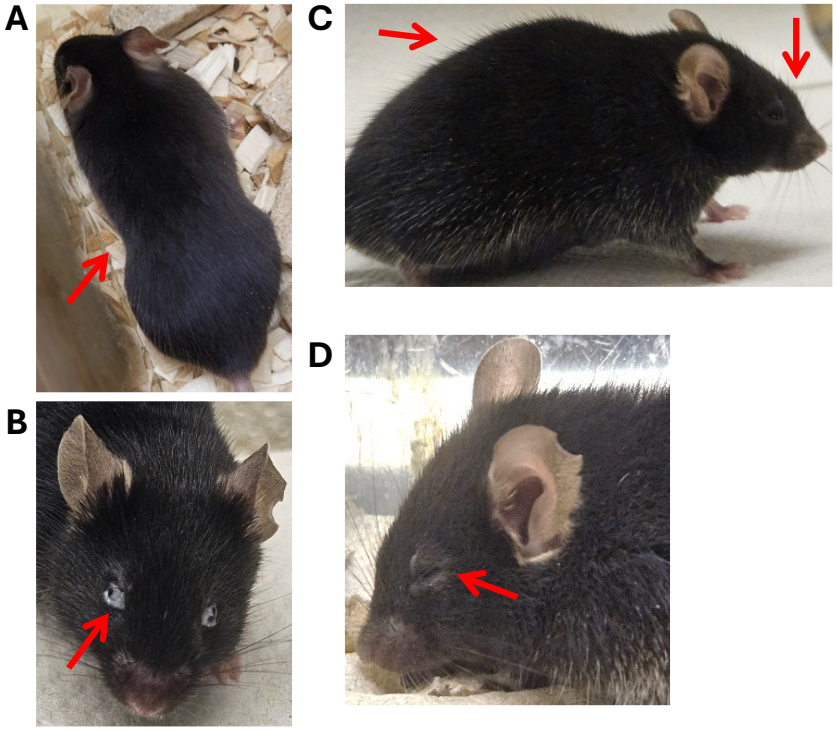

Figure 4. Symptoms of advanced sepsis in adult C57BL/6J mice.

A Picture shows significant weight loss and hunched posture of mouse (red arrow). **B** Picture shows mucus build-up around the eyes of the mouse (red arrow). **C** Picture show piloerection on the back of the mouse and building on the bridge of the nose (red arrows) and a hunched posture. **D** Picture shows closing of the eyelid (red arrow) as an indication of pain. Pictures were taken by Janine Hebel.

Mortality rates were noted during the experiments. At the end of the experiments (96h after sepsis induction) or earlier depending on their score, mice were euthanized as described above. Then, organs were prepared for flow cytometry and measurement of bacterial load as described in detail in chapters 3.4 and 3.5.

3.2.2. *E. coli* sepsis model with neonatal mice

For the induction of neonatal sepsis, two-day old mice (P2) received a subcutaneous (s.c.) injection of 40.000 - 50.000 *E. coli* in 30 µl DPBS into the neck fold (s. 3.1). The injection was performed using a Hamilton syringe with a 33 G needle. To study the effect of sepsis on CD200 and CD200R expression on immune cells of neonatal mice no further treatment was administered. In a second experiment, to study the effect of high CD200 levels on sepsis progression and outcome, neonatal mice additionally received an i.p. injection of 1 µg murine rCD200 reconstituted in 10 µl DPBS using a Hamilton syringe, half an hour before the induction of sepsis. The rCD200 concentration was chosen based on the paper of Snelgrove et al. who injected 10 µg rCD200 into adult mice and reduced our concentration to 1 µg according to average body weight differences between adult and neonatal mice [169]. The control group received a DPBS only injection. In a third experiment, to study the effect of CD200 blockade

on neonatal sepsis progression and outcome, neonatal mice additionally received a 10 µl i.p. injection of 15 µg InVivoMAb^{TM} anti-mouse CD200 (OX2) antibody (BioXCell) diluted in antibody diluent (InVivoPure pH 7.0 Dilution Buffer), 30 minutes before sepsis induction. The concentration was chosen based on manufacturer´s instructions for adult mice and adjusted to the lower weight of neonatal mice. The control group received the same injection using 15 µg InVivoMAb^{TM} rat IgG2a isotype control. Afterwards, sepsis was induced as described above. Neonatal mice stayed with their mothers and their respective litter mates over the course of the experiment. After sepsis induction, mice were monitored for symptoms and weighed every 6 hours over the course of the experiment. Once symptoms were detected, the time frame of monitoring was adjusted to 3- or 1-hour intervals according to the scoresheet and point system approved by the regional council in Tübingen (s. Appendix **Table 18**, **Figure 32**). On average, symptoms were first observed 24h after sepsis induction. Neonatal mice were euthanized at the end of the experiment (48 hours) or earlier if the respective score points were reached as described above. The mortality rate was noted during the experiments. Organs were then prepared for flow cytometry analysis and measurement of bacterial load respectively as described in chapters 3.2.3, 3.3 and 3.5.

3.2.3. Determining bacterial load in septic mice

Bacterial load in blood and organs of septic mice was used as a measure to determine variations in sepsis severity between treatment and control groups in the different experimental sepsis setups.

Spleen, liver and lungs of neonatal and adult mice were weighed using a precision scale. For adult mice, 50 µg of the spleen and 100 µg of each liver and lung were separated and used to determine bacterial load. Organs were homogenized and pushed through a 100 µm filter on top of a 1.5 ml Eppendorf Tube using a syringe plunger and 1 ml of DPBS. These organ solutions were set to be a 1:10 dilution for livers and lungs and a 1:20 dilution for spleens. 100 µl of blood were diluted 1:10 in DPBS. Each organ or blood solution was then diluted again to 1:100 and 1:1000 dilutions. 100 µl of each dilution was plated on Columbia agar plates with 5% sheep blood. Plating all dilutions was necessary to guarantee that CFU growth of at least one dilution could be counted even when the bacterial load of the organs was high. High bacterial load in combination with a low dilution of the organ solution could result in high density of bacterial growth on the plates, preventing an accurate CFU count (**Figure 5**). Plates were incubated at 37°C for 24h. After 24h, the CFUs on each plate were counted and bacterial load of each organ or blood was calculated as CFU/g organ or CFU/ml blood. Examples for calculation of bacterial load in organs and blood are provided below.

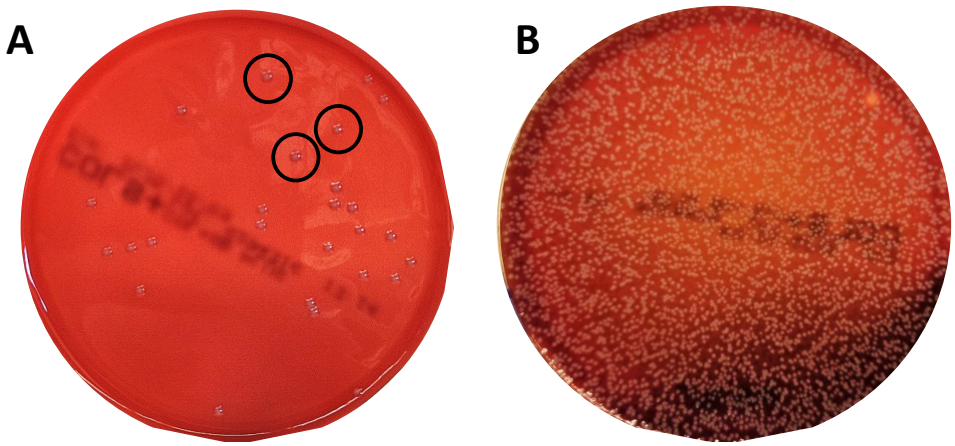

Figure 5. Examples for bacterial growth of *E. coli* on Columbia agar plates with 5% sheep blood.

A Plate shows single colonies of *E. coli* grown on a sheep blood agar plate. Each colony represents a colony forming unit (black circles). **B** Plate shows overgrowth of *E. coli* colonies grown on a sheep blood agar plate. Pictures taken by Janine Hebel.

Universal formula to calculate CFU/100 µg of organ:

$$\frac{\text{CFU}}{100\ \mu\text{g organ}} = \text{number of counted CFUs} \times (\text{dilution factor} \times \text{plating factor})$$

Dilution factor = e.g. 100 (for a 1:100 dilution)

Plating factor = 10 (100 µl of 1 ml total volume were plated; 1000/100 = 10)

To determine the concentration of CFU/g, CFU/100 µg was multiplied by 10 (100 µg × 10 = 1 g) (or multiplied times 20 for spleen). Bacterial concentration in the blood was calculated the same way.

For neonatal mice, the weight of each organ was determined using a precision scale, and one half of each organ was used to determine bacterial load in neonatal mice. Due to this technique, the weight of each organ used to determine bacterial load varied between animals. This was taken into account when calculating bacterial load later (see below). Organs were homogenized and pushed through a 100 µm filter on top of a 1.5 ml Eppendorf Tube using a syringe plunger and 200µl DPBS. Organ solutions were then diluted to reach dilutions of 1:10, 1:200 and 1:4000 of the original. For blood samples, 20 µl of blood were diluted in 180 µl DPBS to obtain a 1:10 dilution. The blood solution was then also diluted multiple times to reach dilution factors of 1:100, 1:200 and 1:4000. 100 µl of each dilution were plated onto Columbia agar plates with 5% sheep blood and incubated at 37°C for 24h. After 24h, CFUs for each organ solution were counted and bacterial load of organs was calculated in CFU/g and, for blood, in CFU/ml. Examples for these calculations are shown below.

Universal formula to calculate CFU/$\frac{1}{2}$ organ:

$$\frac{\text{CFU}}{\frac{1}{2}\,\text{organ}} = \text{number of counted CFUs} \times (\text{dilution factor} \times \text{plating factor})$$

Dilution factor = e.g. 10 (for a 1:10 dilution)

Plating factor = 2 (100 µl of 200 µl total volume were plated; 200/100 = 2)

Universal formula to calculate CFU/mg organ:

$$\frac{\text{CFU}}{\text{mg}} = \frac{\text{CFU}}{\frac{1}{2}\ \text{organ}} \div \text{weight of } \frac{1}{2} \text{organ (mg)}$$

To determine the concentration of CFU/g, CFU/mg needs to be multiplied by 1000.

3.3. Cell isolation from murine and human samples

Blood samples of adult and neonatal **mice** were centrifuged at 3000 rcf for 5 minutes at 4°C to separate the plasma from the cellular components of the blood. Plasma was then transferred into a new tube, frozen and stored at -80°C. Due to the different size, density and cell numbers of organs from adult and neonatal mice, two slightly different protocols were used to prepare single cell suspensions of murine organs for flow cytometry. For neonatal mice, aged postnatal day 1 to 8 (P1 - P8), spleens, lungs and livers were homogenized and pushed through a 40 µm cell strainer using a 1 ml-syringe plunger and DPBS. Cells were washed by centrifugation at 500 rcf and 4°C for 10 minutes. Supernatant was removed and the cell pellets were resuspended in 50 µl DPBS for each antibody panel measured with flow cytometry (s. 3.5).

Organs of adult mice (P21 and up) were first homogenized and pushed through a 100 µm cell strainer using a 1 ml-syringe plunger and DPBS. Cells were washed by centrifugation at 500 rcf and 4°C for 10 minutes. Supernatant was removed and remaining red blood cells (erythrocytes) were lysed by resuspending the cell pellet in an ammonium chloride (ACK) solution for eight minutes at room temperature. Erythrocytes can negatively impact the analysis of leucocytes in flow cytometry due to the auto-fluorescent signal of hemoglobin [223]. The cell solutions were then again pushed through a 40 µm filter with a syringe plunger and DPBS and washed a second time. Lung and spleen cell pellets were resuspended in 50 µl DPBS for each antibody panel measured with flow cytometry (s. 3.5). Due to the high number of cells isolated from livers, liver samples were resuspended in 5 ml DPBS.

For isolation of **human** cord blood mononuclear cells (CBMCs) or peripheral blood mononuclear cells (PBMCs) from whole blood samples. Cells were isolated using density gradient centrifugation. For this process, a minimum of 10 ml and a maximum of 15 ml whole blood were diluted with DPBS up to 35 ml total volume and then slowly layered on top of 15 ml Pancoll (density 1.077 g/ml). Due to the small volume of peripheral blood samples from premature infants, this process was scaled down. To isolate PBMCs from blood of premature infants, up to 200 µl of whole blood were diluted with DPBS up to 1 ml total volume and layered on top of 1 ml Pancoll. Cells were separated via centrifugation at 400 rfc and 20°C for 25 minutes (premature PBMCs were only centrifuged for nine minutes). Due to the lower density of PBMCs and CBMCs compared to Pancoll, the cells sediment between the plasma and Pancoll in a yellow-white layer. The cells were carefully collected and washed with DPBS at 500 rcf and 4°C for 10 minutes. Additionally, remaining erythrocytes in the CBMC suspension were lysed for eight minutes using 10 ml ACK-solution (1:10 deionized water) and washed again as described before. The supernatant was removed, and cells were counted using an automated hemocytometer. PBMCs and CBMCs were used for multiple different experiments and therefore, cell concentration and media to resuspend the cells were chosen based on the follow-up experiment.

Isolated cells could be frozen -80°C after isolation in 500 µl PRMI-medium (+ 10% fetal bovine serum (FBS), 1% glutamine (Glu), 1% penicillin/streptomycin (P/S)) and 500 µl freezing medium (RPMI + 20% FBS + 20% dimethyl sulfoxide (DMSO)) in cryo-tubes. To thaw the cells, the cryo-tube containing the cells was quickly put in a water bath set to 37°C until most of the cells were thawed. Cells were then transferred into ice cold RPMI-medium. Cells were centrifuged at 310 rcf at 4°C for 5 minutes to remove the freezing media. They were then resuspended in warm (37°C) RPMI-medium and counted using a Neubauer counting chamber and then adjusted to the desired concentration in media depending on the follow-up experiment. For determination of cell numbers, cells were stained with trypan blue (ratio 1:2), a dye that enters dead or damaged cells, coloring them blue and leaving viable cells colorless. For this reason, trypan blue staining is used to determine cell viability. The dyed cells were pipetted onto the Neubauer counting chamber and counted under a microscope. The number of cells per ml was calculated using the following equation:

$$\frac{\text{cells}}{\text{ml}} = \frac{\text{number of counted cells}}{\text{number of counted squares}} \times 2\ (\text{dilution factor}) \times 10^4\ (\text{chamber factor})$$

3.4. *In vitro* assays

To determine the expression patterns of CD200 and CD200R of different immune cells from neonates and adults, various analyses were performed. Additionally, to uncover potential implications of CD200 and CD200R expression on immune cell functions, multiple functional experiments were performed, including stimulation of cells with rCD200 and blocking of CD200 and CD200R using antibodies.

Analysis of CD200 and CD200R expression on human monocytes and T-cells

To reveal potential differences in the expression pattern of CD200 or CD200R on neonatal and adult monocytes and T-cells, their expression was analyzed using flow cytometry. For this experiment, immune cells were isolated from peripheral blood of adults and premature infants and from cord blood of full-term and premature infants (s. 3.3). Cells were adjusted to $1x10^6$ cells/ml in RPMI-medium (+10% FBS + 1% Glu) and seeded into 24- or 48-well plates depending on the number of isolated cells. To determine the potential impact of infections (like sepsis) on CD200 and CD200R expression on monocytes and T-cells, they were additionally stimulated with *E. coli* at a MOI 10:1 (s. 3.1), for 24h at 37°C and 5% CO_2. Unstimulated cells served as a control to determine baseline CD200 and CD200R expression. After 24 hours, cells were transferred into FACS-tubes and labeled for flow cytometric analysis using antibodies against the monocyte cell surface marker CD14 PE-Cy7 T-cell marker $CD3^+$ FITC and CD200 PE and CD200R APC as described below (s. 3.5). A representative gating strategy for this analysis is shown in **Figure 6**. Further, CD200 and CD200R expression on T-cell sub-sets were analyzed. An example for the gating strategy for these cells is shown below (**Figure 7**). CD200 and CD200R expression on monocytes and T-cells from adults, full-term and premature infants was analyzed with the BD FACS Canto II™ flow cytometer. Analysis of flow cytometry data was performed using FlowJo™ software. To determine the percentage of Th1, Th2 and Th17 T-cells from $CD4^+$ T-cells, results were calculated as follows:

Calculation of % of $CD4^+$ T-cells:

$$\%\ CCR4^- \text{ of } CD4^+ = \frac{100}{\%\ CD4^+} \times \%\ CCR4^-$$

$$\%\ CCR4^+ \text{ of } CD4^+ = \frac{100}{\%\ CD4^+} \times \%\ CCR4^+$$

Calculation of % Th1, Th2 and Th17 of CD4$^+$:

$$\%\ \text{Th1 of CD4}^+ = \frac{\%\ \text{CCR4}^-\ (\text{of CD4}^+)}{100} \times \%\ \text{Th1}$$

$$\%\ \text{Th2 of CD4}^+ = \frac{\%\ \text{CCR4}^+\ (\text{of CD4}^+)}{100} \times \%\ \text{Th2}$$

$$\%\ \text{Th17 of CD4}^+ = \frac{\%\ \text{CCR4}^+\ (\text{of CD4}^+)}{100} \times \%\ \text{Th17}$$

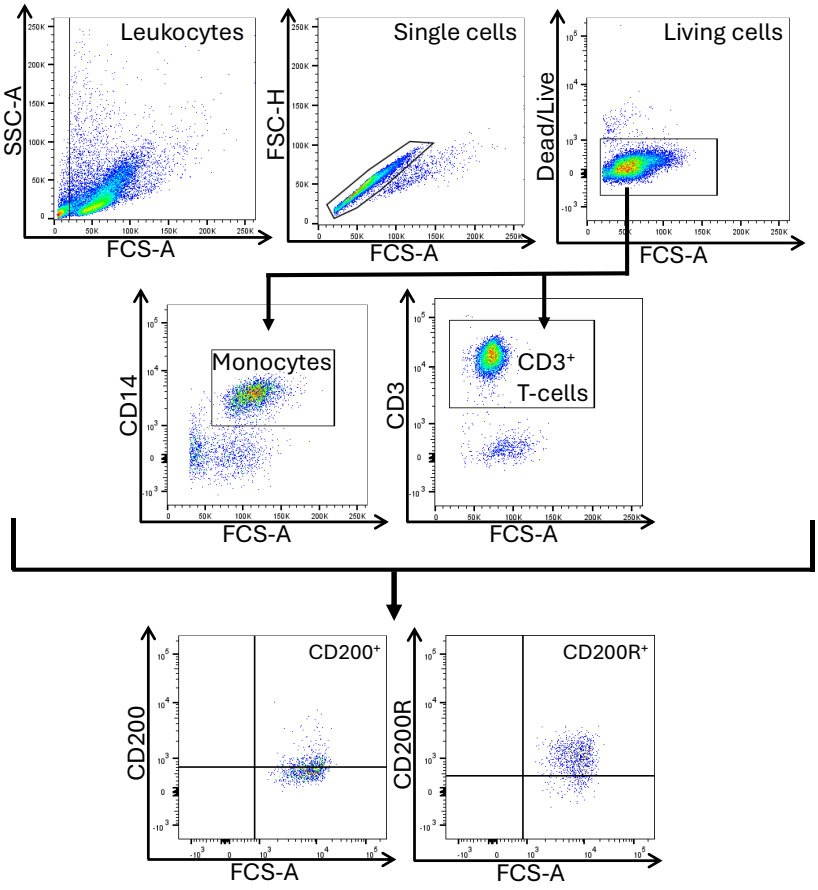

Figure 6. Gating strategy for human blood monocytes and T-cells.

Figure shows representative gating strategy for PBMC and CBMC monocytes and T-cells and their CD200 and CD200R expression. CD200 and CD200R gates were set to the corresponding fluorescence minus one (FMO) control of each sample.

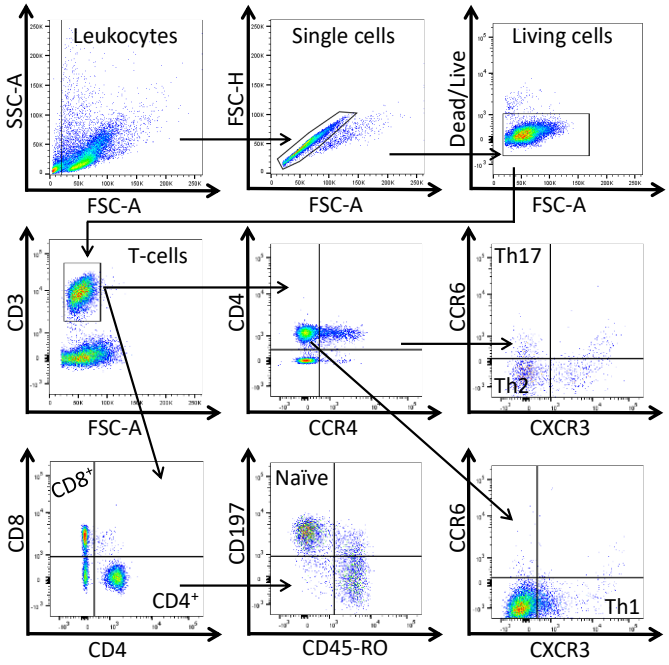

Figure 7. Gating strategy for T-cell sub-sets.

Figure shows representative dot plots of the gating strategy for T-cell sub-types of flow cytometry data.
NaïveT-cells:
$CD3^+ \rightarrow CD4^+$ or $CD8^+ \rightarrow CD197^+/CD45\text{-}RO^-$
Th1cells:
$CD3^+ \rightarrow CD4^+/CCR4^- \rightarrow CCR6^-/CXCR3^+$
Th2cells:
$CD3^+ \rightarrow CD4^+/CCR4^+ \rightarrow CCR6^-/CXCR3^-$
Th17cells:
$CD3^+ \rightarrow CD4^+/CCR4^+ \rightarrow CCR6^+/CXCR3^-$

Effect of CD200 or CD200R blockade on human immune cells

To study the effect of reduced CD200/CD200R expression on human immune cells, CD200 and/or CD200R expression on PBMCs from adults and CBMCs from full-term neonates was blocked using anti-CD200 and anti-CD200R antibodies. Immune cells were isolated from peripheral blood of adults and cord blood of newborns as described in chapter 3.3. Immune cells were adjusted to $1x10^6$ cell/ml in RPMI-medium (without P/S) CD200 and CD200R were blocked for 30 minutes at 37°C and 5% CO_2 by adding 5 µg/ml Ultra-LEAF™ purified anti human CD200 antibody and/or 5 µg/ml Ultra-LEAF™ purified anti human CD200R antibody (Biolegend). Cells treated with 5 µg/ml Ultra-LEAF™ purified mouse IgG1 isotype antibody (Biolegend) and untreated cells served as controls. After 30 minutes of blocking, cells were stimulated with *E. coli* (MOI 10:1) and incubated at 37°C and 5% CO_2 for 4 hours (cytokines) or 24 hours depending on the experiment. For analysis of intracellular cytokines, brefeldin A (c = 10 µg/ml) was added to each well for 4 hours. Brefeldin A inhibits the transport of proteins within cells, therefore preventing the secretion of proteins such as cytokines [224]. This leads to an accumulation of cytokines inside the cell that can be measured using flow cytometry (s. 3.5). For the analysis of co-stimulatory molecules (list of markers **Table 9**) cells were incubated for 24h. Then, cell surface expression of co-stimulatory molecules was analyzed via flow cytometry (s. 3.5).

Table 9. List of antibodies for analysis of co-stimulatory molecules on monocytes and T-cells.

Marker for co-stimulatory molecules on monocytes	Fluorochrome
CD80	FITC
CD86	PE
HLA-DR	FITC
TLR4	PE

3.4.1. Human T-cell proliferation assay

To determine the potential effect of CD200 and/or CD200R blockade on T-cell proliferative capacity, a T-cell proliferation assay was performed. For this assay, immune cells from adult peripheral blood and full-term infant cord blood were isolated (s. 3.3). Cells were adjusted to $1x10^7$ cells/ml in DPBS and labeled with carboxyfluorescein diacetate succinimidyl ester (CFDA-SE) (2.5 µM/ml) for 10 minutes at room temperature. CFDA-SE is a cell dye that diffuses into cells. There, it is cleaved by intracellular enzymes to the fluorescent dye carboxyfluorescein succinimidyl ester (CFSE). CFSE binds to intracellular molecules and is passed onto the daughter cells during cell division, allowing tracking of cell proliferation of stained cells [225]. FBS was added for 1 minute to capture unbound CFDA-SE and stop the labeling process. Cells were washed with RPMI-medium and centrifuged at 310 rcf and 4°C for 5 minutes. Afterwards, the cell pellet was resuspended at $1x10^6$ cells/ml in RPMI-medium. CD200 and/or CD200R expression was blocked for 30 minutes with 5 µg/ml anti-CD200 and/or 5 µg anti-CD200R antibodies. As a control, cells were incubated with 5 µg/ml isotype control antibody. After 30 minutes, T-cell proliferation was induced by adding 0.01 µg/ml OKT3 and 100 U/ml human IL-2. For the assay, cells were plated at 100 µl/well in a 96 U-bottom plates and supplemented with 100 µl/well RMPI-medium ($1x10^5$ cell/well). The plate was incubated for four days at 37°C and 5% CO_2. To analyze differences in level of T-cell proliferation, cells were labeled with an anti-CD4 antibody (s. 3.6.1). and analyzed by flow cytometry and FlowJo™. A gating strategy for analysis of T-cell proliferation is shown in **Figure 8**.

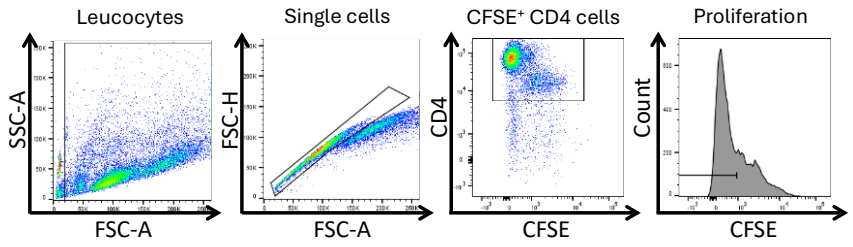

Figure 8. Gating strategy for T-cell proliferation assay. Density plots and histogram show the gating strategy for stimulated $CD4^+$ T-cells. Gate for the histogram was set to the histogram of the unstimulated control.

3.5. Labeling of cells for flow cytometry

Flow cytometry is a method to analyze cell characteristics including size, granularity and cell surface antigens. For flow cytometric analysis, cells suspended in a fluid pass through a laser beam. Light scattered by cells is detected and provides information on size (forward scatter, FSC) and granularity (sideward scatter, SSC) of cells. To analyze cell surface antigens, cells are labeled with antibodies bound to various fluorochromes. The laser beams of the flow cytometer excite the fluorochromes, who then emit light at a specific wavelength that is detected and processed [226].

3.5.1. Extracellular labeling of immune cells

Isolated cells from spleens, livers and lungs of adult and neonatal **mice** (s. 3.3) or PBMCs and CBMCS isolated from **human** blood (s. 3.3) were labeled for flow cytometric analysis of immune cells using combinations of different antibodies. For each extracellular antibody panel, 50 µl of cell solution (~2-5x10^5 cells) was labeled for 10 minutes at 4°C in a FACS (fluorescent activated cell sorting)-tube. To remove unbound antibodies that could provide a false positive signal during analysis, cells were washed with 1 ml FACS-flow (BD) solution, centrifuged at 310 rcf at 4°C for 5 minutes and the supernatant was removed. Murine cells were fixed by resuspension of the pellet in 200 µl formaldehyde (4.5%) and incubated for 10 minutes in the dark. Then, FACS-flow was added, cells were washed once more, and the supernatant was removed. Fixed cells were stored for up to 24 hours at 4°C before analysis. Analysis was performed using a FACS Canto II flow cytometer and the DIVA™ software. The data was evaluated using FlowJo™. Gating strategy for human immune cells can be found in chapter 3.2.

Gating strategies for **murine** immune cells are shown below (**Figure 9** myeloid cells**, Figure 10** lymphoid cells):

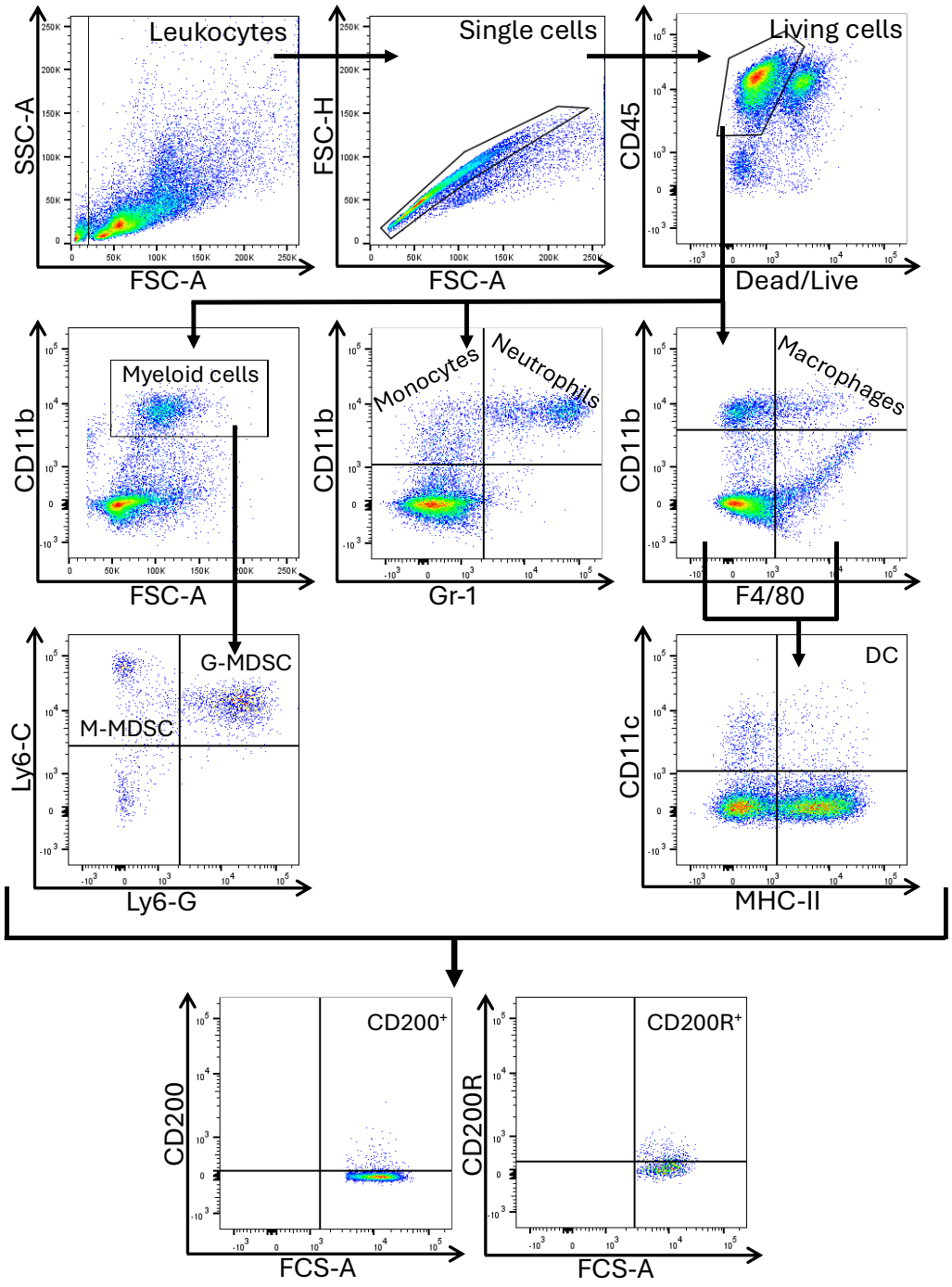

Figure 9. Gating strategy for murine myeloid immune cells.

Representative dot plots show gating strategy of splenic myeloid cells and their CD200 and CD200R expression. CD200 and CD200R gates were set on the corresponding FMO controls of each sample and can therefore differ between samples.

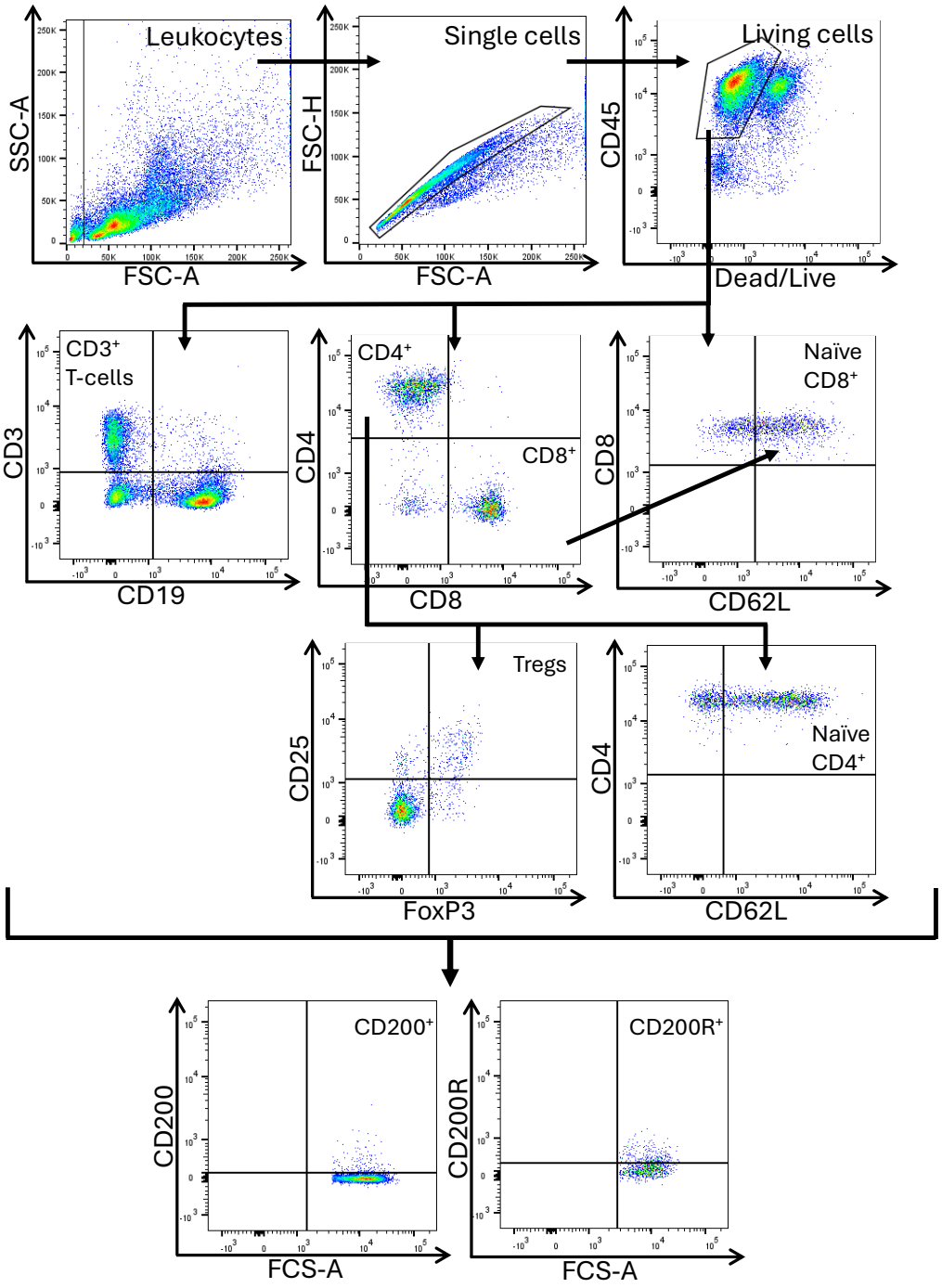

Figure 10. Gating strategy for murine lymphoid immune cells.

Representative dot plots show gating strategy of splenic lymphoid cells and their CD200 and CD200R expression. CD200 and CD200R gates were set on the corresponding FMO controls of each sample and can therefore differ between samples.

3.5.2. Intracellular labeling of immune cells

For the analysis of the intracellular protein FoxP3 in **murine** Tregs, intracellular antibody labeling was performed using a Foxp3/Transcription Factor Staining Buffer Set (Invitrogen). First, cells were stained extracellularly for 30 minutes with antibodies against anti-CD3, anti-CD4 and anti-CD25 as described above. Cells were washed in 1 ml DPBS + 1% FBS and centrifuged at 310 rcf and 4°C for 5 minutes, to remove unbound antibodies. Cells were permeabilized in 200 µl Fixation/Permeabilization concentrate (c = 1:3 Fixation solution/Permeabilization Diluent) for 30 minutes at room temperature in the dark. Cells were washed in 500 µl Permeabilization Buffer (10X) (c = 1:9 deionized water) at 310 rfc and 4°C for 5 minutes. The cell pellet was resuspended in 100 µl Permeabilization Buffer and cells were stained with the intracellular antibody for anti-FoxP3 PE for 30 minutes at room temperature in the dark. Cells were washed in 1 ml FACS-flow at 310 rcf, 4°C for 5 minutes and the supernatant was discarded.

To analyze intracellular cytokine expression of **human** immune cells blocked with anti-CD200 and/or anti-CD200R antibodies (s. 3.4), cells were transferred into FACS-tubes after stimulation with *E. coli* and brefeldin A for 4 hours, centrifuged at 310 rcf at 4°C for 5 minutes and resuspended in DPBS. Then, they were stained with the extracellular marker for monocytes CD14 PE-Cy7 for 10 minutes at 4°C. Unbound antibodies were removed by washing the cells with 1 ml FACS-flow and centrifugation at 310 rcf for 5 minutes at 4°C. Afterwards, cells were permeabilized using 200 µl of the Cytofix/Cytoperm™ Fixation and Permeabilization Solution (BD) for 10 minutes at 37°C, washed with Perm/Wash™ Buffer (BD) (diluted 1:10 with deionized water) at 310 rcf for 5 minutes at 4°C, resuspended in Perm/Wash™ Buffer (BD) and labeled with intracellular antibodies against different cytokines (**Table 10**) for 30 minutes at room temperature in the dark. Unbound antibodies were removed.

Table 10. Overview of intracellular cytokine antibodies.

Marker	Fluorochrome
TNF-α	PE
IL-10	PE
TGF-β	PE
IL-6	PE
IL-1β	APC
IL-2	APC
IL-4	APC
IL-17A	APC
IFNγ	APC

All samples for flow cytometry were measured with the BD FACS Canto II™ cytometer. Analysis of flow cytometry data was performed using FlowJo V10.10 software.

3.6. ELISA assays

Enzyme-linked immunosorbent assay (ELISA) is a technique to detect specific substances such as antigens in a sample. Different variations of ELISA protocols exist. One of the most popular variations is the so-called sandwich-ELISA. In this assay, a plate is coated with a capture antibody to the desired target. Then, the sample is added and, if present, the antigens bind to the capture antibody. Afterwards, an enzyme-linked detection antibody is added that binds to the antigen bound to the capture antibodies. In the last step, a color reagent containing a chemical is added that is then converted into a new color by the enzyme bound to the detection antibody. The shift in color and the intensity can then be detected by the absorbance of light using a photometer [227].

For this study, four different murine ELISAs and one human ELISA were performed.

For the **murine** cytokine ELISAs (IL-6, TNF-α and CXCL1), protein concentration was first determined using the Pierce™ 660nm Protein Assay according to manufacturer's instructions [219]. For all ELISA assays, plasma from mice stored at -80°C was thawed at room temperature and used for analysis directly after. Determination of protein concentrations and the IL-6, TNF-α and CXCL1 ELISA assays were kindly performed by PD Dr. Trim Lajqi, Department of Neonatology, Heidelberg Children's Hospital, Germany. Murine sCD200 ELISAs were performed by Janine Hebel. Analysis was performed according to manufacturer's instructions for IL-6 [213], TNF-α [212], CXCL1 [216] and CD200 [220] ELISAs. Standard curves were

generated using a four-parameter logistic (4-PL) curve-fit (for IL-6, CXCL1 and sCD200) or by plotting the log of the TNF-α concentration (x-axis) against the log of the absorbance (y-axis) with a best fit line determined by regression. Results for IL6, TNF-α and CXCL1 were calculated based on the previously determined protein concentration for each sample and depicted in ng/g or pg/g protein. sCD200 plasma concentrations were determined based on the standard curve and given in pg/ml plasma.

To determine sCD200 concentrations in **human** plasma samples, the human sCD200 ELISA was used. To collect the plasma for this assay, peripheral blood samples of adults and premature infants and cord blood of full-term and premature infants were centrifuged at 3000 rcf at 4°C for 5 minutes. Plasma was frozen and stored at -80°C. Plasma was thawed at room temperature and used for analysis directly after. The assay was performed according to manufacturer´s instructions [214]. The standard curve was analyzed by plotting the log of the CD200 concentration (x-axis) against the log of the absorbance (y-axis) with a best fit line determined by regression. sCD200 plasma concentrations were determined based on the standard curve and given in pg/ml plasma.

3.7. qPCR

To analyze mRNA expression levels of CD200 and CD200R of isolated monocytes and T-cells from peripheral and cord blood of humans, a quantitative polymerase chain reaction (qPCR) analysis was performed.

3.7.1. Isolation of monocytes and T-cells from PBMCs and CBMCs

Mononuclear cells from peripheral blood of adults and cord blood of full-term newborns were isolated (s. 3.3). Monocytes were isolated using the MojoSort™ Human Pan Monocyte Isolation Kit (Biolegend) according to manufacturer´s instructions [215]. Briefly, up to $1x10^8$ PBMCs or CBMCs were resuspended in 1 ml MojoSort™ Buffer. Then, $1x10^7$ cells were blocked using the kits Fc receptor blocking solution for 10 minutes at room temperature. Cells were labeled with the Biotin-Antibody Cocktail for 15 minutes on ice. Then, Streptavidin Nanobeads were added to the cells and incubated for 15 minutes on ice. Cells were resuspended in 2.5 ml MojoSort™ Buffer, and monocytes were separated using a MojoSort™ magnet (negative

selection). T-cells were isolated using the Pan T-cell Isolation Kit (Miltenyi) according to manufacturer´s instructions [218]. Briefly, up to 1x10^7 mononuclear cells were resuspended in 40 µl MACS-Buffer and labeled with the "Pan T Cell Biotin-Antibody Cocktail" for 5 minutes at 4°C. Then, the Pan T Cell MicroBead Cocktail was added, and cells were incubated for 10 minutes at 4°C. T-cells were isolated using magnetic separation and an LS-Column (negative selection). To determine the purity of the isolated monocytes and T-cells, they were stained with an anti-CD14 PE-Cy7 or anti-CD3 FITC antibody (s. 3.5) and analyzed using flow cytometry. Purity of adult monocytes was on average ~70% and ~45% for neonatal monocytes while adult T-cell purity was on average ~94% and neonatal T-cell purity was ~86% (**Figure 11**).

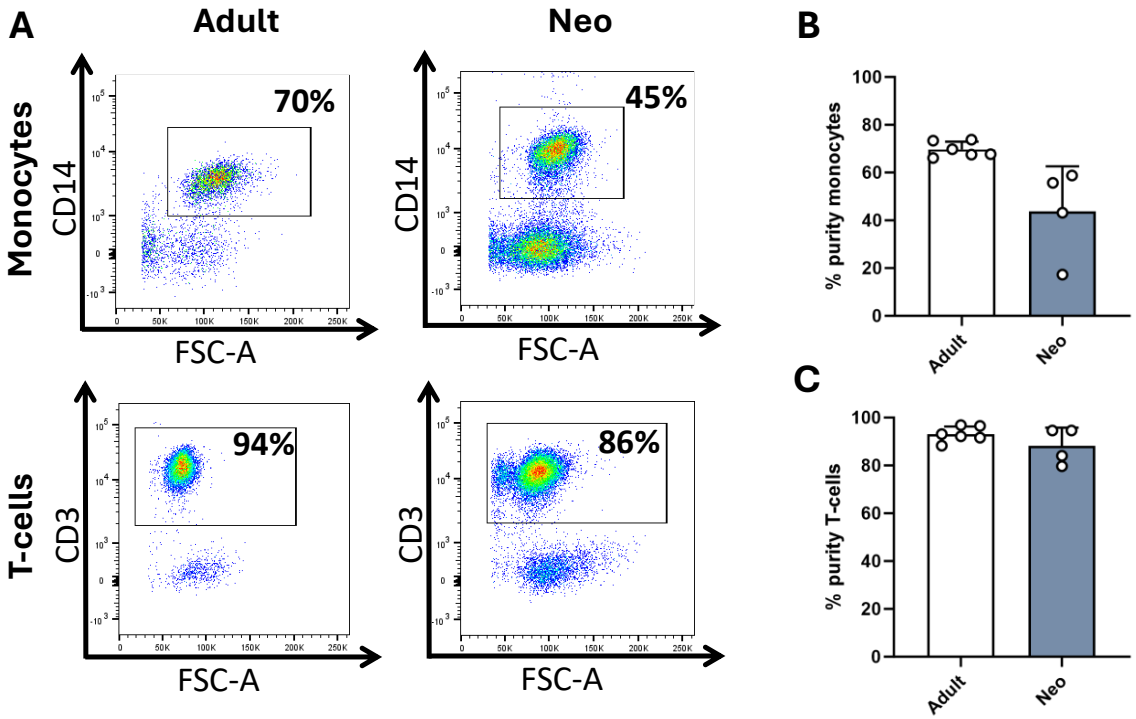

Figure 11. Purity of isolated monocytes and T-cells of adults and neonates.

A Density plots show examples of purity from isolated monocytes of adults (top left) and neonates (top right) and of isolated T-cells of adults (bottom left) and neonates (bottom right) in %. B Bar graph shows purity of isolated monocytes of adults (white) and neonates (blue) in % of all cells. C Bar graph shows purity of isolated T-cells of adults (white) and neonates (blue) in % of all cells

3.7.2. Isolation of RNA

To prepare cells for RNA isolation, isolated monocytes and T-cells were counted (s. 3.7.1) and resuspended in 350 µl RA1 Buffer (from the NucleoSpin RNA kit by Macherey-Nagel) containing 3.5 µl 2-mercaptoethanol (stock solution c = 14.3 M) and stored at -80°C until further use.

RNA isolation of isolated monocytes and T-cells from PBMCs and CBMCs was performed using the NucleoSpin RNA isolation Kit (Macherey-Nagel) according to manufacturer´s instructions [217]. The protocol followed instructions for isolation of RNA from cultured cells and tissue. Briefly, monocyte and T-cell samples stored in RA1 buffer at -80°C were thawed and filtered through a NucleoSpin filter at 11.000 rcf for 1 minute. Then, 70% ethanol was added to the lysate to adjust RNA binding conditions. RNA was bound to a NucleoSpin RNA column by application of the lysate to the column followed by centrifugation at 11.000 rcf for 30 seconds. Then, the silica membrane of the column was desalted using membrane desalting buffer. Next, remaining DNA in the lysate was digested by applying a DNase reaction mix for 15 minutes. After DNA removal, the membrane was washed once with RAW2-Buffer at 11.000 rcf for 30 seconds followed by two wash steps using RA3-Buffer and centrifugation at 11.000 rcf for 1 minute. Lastly, RNA was eluted using RNase-free H_2O and centrifugation at 11.000 rcf for 1 minute.

RNA concentration (in ng/µl) and quality was measured using the Varioskan^{TM} LUX Microplate reader. RNA quality was analyzed using the 260/280 nm ratio, where a value of ~2.0 indicates a pure RNA sample. A value below 1.8 could indicate contamination due to proteins in the sample and a value above 2.1 can indicate RNA degradation. In our experiments, 260/280 ratios of monocytes and T-cells were between 2.0 and 2.1, and all samples were deemed pure enough for complementary DNA (cDNA) synthesis. Isolated RNA was frozen in liquid nitrogen and stored at -80°C until further use.

3.7.3. cDNA synthesis from RNA

cDNA from RNA samples (s. 3.7.2) was synthesized using the ProtoScript™ II First Strand cDNA Synthesis Kit (New England Biolabs) according to manufacturer´s instructions [221]. Briefly, up to 1 µg RNA (in up to 6 µl nuclease free H_2O) was incubated with the Random Primer Mix at 65°C for 5 minutes in a thermocycler to denature the sample. Next, a mix of ProtoScript II Reaction Mix (2x) and ProtoScript II Enzyme Mix (10X) was added to the RNA samples. Samples were incubated at 25°C for 5 minutes followed by 1 hour at 42°C to synthesize the cDNA. Then, enzymes were inactivated by incubation at 80°C for 5 minutes. cDNA samples were adjusted with nuclease free H_2O to a concentration of 5ng/µl and stored at -20°C until further use.

3.7.4. qPCR protocol

Real-time qPCR was performed using the fluorescent dye SYBR Green. qPCR quantifies the formation of double stranded DNA during the PCR amplification process, therefore providing information on the quantity of target DNA in the sample. cDNA samples (s. 3.7.3) of isolated monocytes and T-cells from CBMCs and PBMCs were added into a qPCR reaction mix (**Table 11**) containing primers for CD200, CD200R and the housekeeping gene RPS13 (ribosomal protein S13). Primer sequences are shown below in **Table 12**. Samples were added to a 96-well reaction plate in duplicates. The plate was sealed and centrifuged at 310 rcf and 4°C for 30 seconds to remove bubbles that could interfere with the PCR readings. Then, the qPCR reaction was run as seen in **Figure 12** for 35 cycles using the QuantStudio 3 qPCR machine. Analysis was performed using the Design & Analysis Software (for PCR by Thermofisher Scientific) and Excel. qPCR results were given as Cq (quantification cycle) values, which represents the number of qPCR cycles necessary for the samples fluorescent signal to reach a predefined threshold. This indicates the presence and quantity of the target DNA in the respective sample. Samples were analyzed in relation to the housekeeping gene, and $2^{-\Delta Cq}$ was calculated as described below.

Calculation for $2^{-\Delta Cq}$ of each qPCR sample:

$$\Delta Cq = \text{target gene Cq} - \text{housekeeping Cq}$$

$2^{-\Delta Cq}$= raising 2 to the power of the negative ΔCq

Table 11. Pipetting scheme for qPCR reaction mix.

qPCR reaction mix	Added volume in µl
cDNA (5ng/µl)	3
SYBR Green (2x)	10
Nuclease free H_2O	5.4
Forward Primer (c = 10 µM)	0.8
Reverse Primer (c = 10 µM)	0.8

Table 12. Primer sequences for CD200, CD200R and RPS13 for qPCR.

Primer	Sequence forward	Sequence reverse	NCBI Gene ID
RPS13	GCGTCCCCACTTGGTGAA	AGGAAGATCAGGAGCAAGTCC	
CD200	AAGTGGTGACCCAGGATGAAA	AGGTGATGGTTGAGTTTTGGAG	4345
CD200R	GGAGGATGAAATGCAGCCCTA	CTCAGATGCCTTCACCTTGTTT	131450

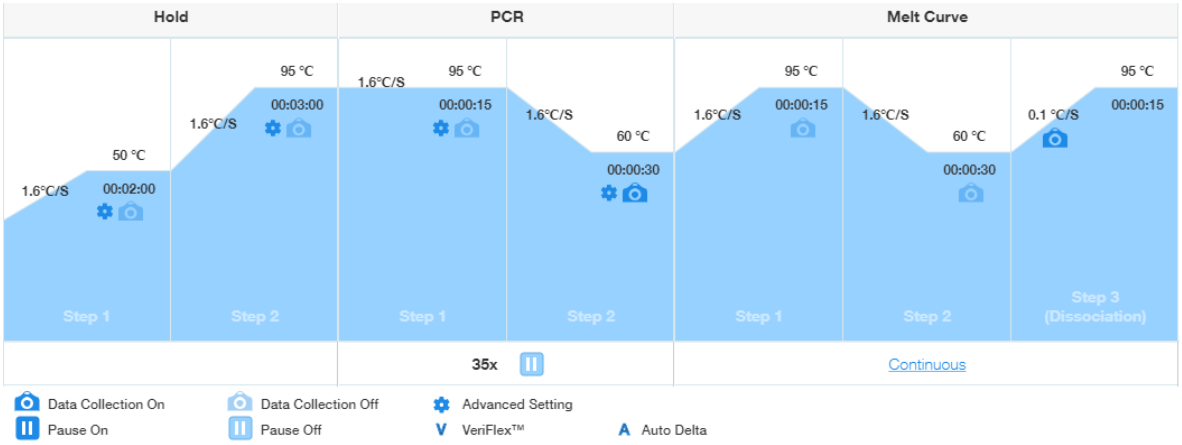

Figure 12. Run protocol for qPCR quantification of CD200 and CD200R in human monocytes and T-cells.

The screenshot from Design & Analysis Software (by Thermofisher Scientific) shows the amplification steps for each qPCR cycle.

3.8. Statistical analysis

Statistical analysis was performed using GraphPad Prism (Version 10.1.1). A p-value of < 0.05 was considered statistically significant (*$p < 0.05$; **$p < 0.01$; ***$p < 0.001$; ****$p < 0.0001$). Values were tested for normal distribution using the Shapiro-Wilk test. To compare more than two unpaired groups of data sets that were normally distributed, a One-Way ANOVA test was performed. If the standard deviation (SD) of data sets was significantly different (tested with the Barlett´s test), the Brown-Forsythe test was performed. To compare more than two unpaired groups of data sets that were not normally distributed, the Kruskal-Wallis test was used. To compare two unpaired groups with normal distribution, a t-test was performed. To compare two unpaired groups that were not normally distributed, the Mann-Whitney test was performed. All analyses were performed using a two-tailed test unless stated otherwise in the respective figure legend. Data are shown as mean ± SD.

4. Results

4.1. The role of CD200 and CD200R in the pathogenesis of murine neonatal and adult *E. coli* sepsis

4.1.1. Murine *E. coli* sepsis progression and outcome differ between adult and neonatal mice

In humans, differences between sepsis susceptibility, severity and disease outcome between adults and especially pre-term infants have been described before, with increased sepsis incidence by up to 40% in pre-term VLBWI and severe disease progression described in neonates (details see introduction chapter 1.1). However, murine sepsis models of neonatal and adult mice have not been directly compared so far.

4.1.1.1. Comparison of adult and neonatal murine *E. coli* sepsis models

To test our hypothesis that *E. coli* induced sepsis in neonatal and adult mice shows similar differences to humans, we set out to establish murine *E. coli* sepsis models for neonatal and adult C57BL/6J mice (see methods chapter 3.2) and compared important markers of sepsis severity including mortality, bacterial load of organs and pro-inflammatory cytokine secretion.

In our experiments, neonatal C57BL/6J mice were more susceptible to sepsis than adult mice and required an ~88 times lower LD30 (lethal dose for 30%) of *E. coli* (neonates ~$2.7x10^4$ vs. adults $2.4x10^6$) per g body weight (**Table 13**, Set-up). We also observed different onset of visible sepsis symptoms, with adult mice showing signs of sepsis as early as six hours after induction while symptoms in neonatal mice were observed earliest after a minimum of 24 hours post sepsis induction. On average, death in adult mice occurred early on between 9.5 and 18.5 hours after sepsis induction in accordance with their early display of symptoms, while death in septic neonatal mice occurred later on between 33 and 37 hours after induction (**Table 13**, Survival-analysis). To compare the efficiency of bacterial clearance by immune cells and a possible accumulation of bacteria in specific organs, we analyzed bacterial load of blood, spleen, lung and liver. In infected adult and neonatal mice, *E. coli* bacteria were found in all

analyzed organs (spleen, liver and lung) as well as in blood with highest concentrations of *E. coli* in adult mice observed in spleen and liver, while the highest bacterial concentrations in neonates were observed in lung and blood. In fact, despite the lower *E. coli* dose given to neonatal mice, we observed similar *E. coli* concentrations in lungs of septic neonatal and adult mice. Additionally, compared to adults, neonatal mice had ~3.8x higher *E. coli* accumulation in their blood than adult mice (**Table 13**, bacterial load). Bacterial load in blood, spleen, lung and liver also differed between animals who survived sepsis and those who didn´t (s. Appendix **Table 19**). Further, to compare sepsis severity mediated by cytokine responses, we analyzed plasma levels of pro-inflammatory cytokines IL-6 and TNF-α in adult and neonatal mice. We found higher plasma levels of the pro-inflammatory cytokines IL-6 and TNF-α in septic neonatal mice, where IL-6 levels were ~3x higher in neonates compared to adults (mean neo 4544 vs. adult 1541 ng/g) and TNF-α levels were ~13x higher (mean neo 7203 vs. adult 544.8 pg/g) (**Table 13**, Cytokines). Plasma IL-6 and TNF-α levels of adult mice euthanized six hours after sepsis induction (6h a.i.) were still ~1.6x to 2x lower than average cytokine levels of neonatal septic mice (**Table 13**, Cytokines). Cytokine levels of IL-6 and TNF-α also differed drastically between animals who survived sepsis and those who died due to their symptoms (s. Appendix **Table 20**).

Table 13. Comparison of severity markers of murine adult and neonatal sepsis.

To compare sepsis progression and severity in an adult and neonatal murine *E. coli* sepsis models, sepsis was induced in adult mice via i.v. injection of *E. coli*. Sepsis was monitored for a maximum of 96 h following induction. Sepsis was induced in neonatal mice via s.c. injection of *E. coli*. Neonatal sepsis was monitored for a maximum of 48 h following induction. The table shows comparison of markers of sepsis severity and information of baseline experimental set-ups of *E. coli* dosage, analysis of survival, analysis of bacterial load of organs spleen, liver and lung, as well as blood and plasma concentrations of pro-inflammatory cytokines IL-6 and TNF-α. ⌀ = average, a.i. = after induction, n.a. = not available.

		Adults n = 19-27	**Neonates n = 20-30**
Set-up	⌀ weight in g	25.05	1.67
	E. coli ~LD30/mouse	$6x10^7$	$4x10^4$
	⌀ *E. coli*/g mouse	$2.4x10^6$	$2.7x10^4$
Survival-analysis	Survival rate %	67 (18/27)	76.7 (23/30)
	Mortality rate %	33 (9/27)	23.3 (7/30)
	Earliest death (in h)	9.5	33
	Latest death (in h)	18.5	37
	Earliest display of symptoms (in h)	6	24
Bacterial load	⌀ CFU/g spleen	$4.1x10^8$	$1.1x10^6$
	⌀ CFU/g lung	$7.7x10^6$	$6.7x10^6$
	⌀ CFU/g liver	$2.1x10^8$	$5.9x10^5$
	⌀ CFU/g blood	$1.2x10^6$	$4.6x10^6$
Cytokines	⌀ IL-6 ng/g protein	1541	4544
	6h a.i. ⌀ IL-6 ng/g protein	2814.9	n.a.
	⌀ TNF-α pg/g protein	544.8	7203
	6h a.i. ⌀ TNF-α pg/g protein	*3329.1*	*n.a.*

4.1.1.2. Effect of weight and litter size on survival in septic adult and neonatal mice

To study the potential effect of other factors than bacterial dose on sepsis survival we analyzed the effect of weight (adults and neonates) and litter size (neonates) on sepsis survival in our *E. coli* sepsis models. In neonatal mice aged P2, average weight significantly decreased with increasing litter size (six: 1.79 ± 0.24 g vs. seven: 1.56 ± 0.17 g vs. eight: 1.48 ± 0.1 g, 6 vs. 7 p = 0.02; 6 vs. 8 p = 0.0007) (**Figure 13**, A). However, litter size did not significantly impact probability of sepsis survival for litters with six (81,2%), seven (77,8%) and eight (88.8%) (p = 0.5) pups (**Figure 13**, B). On average, weight did not significantly differ between neonatal animals who survived sepsis and those who died (1.65 ± 0.3 g vs. 1.64 ± 0.4 g, p = 0.99) (**Figure 13**, C). When comparing survival of neonatal mice below or above their average weight of 1.6 g and therefore a higher or lower *E. coli* dose per g mouse, lower average body weight did also not impact probability of sepsis survival compared to higher average body weight (low body weight 80% vs. high body weight 73.3%, p = 0.6) (**Figure 13**, D). In adult mice with sepsis, weight at the time of sepsis induction did also not significantly differ between surviving and deceased animals (survived 26.1 ± 2.7 g vs. deceased 26.9 ± 4.3 g, p = 0.6) (**Figure 13**, E). However, adult mice with a starting weight below the average of all animals in our experiments of 24.5 g, had a significantly lower probability of sepsis survival compared to adult mice with a starting weight above 24.5 g (lower body weight 57.8% vs. higher body weight 88.9%, p = 0.1) (**Figure 13**, F).

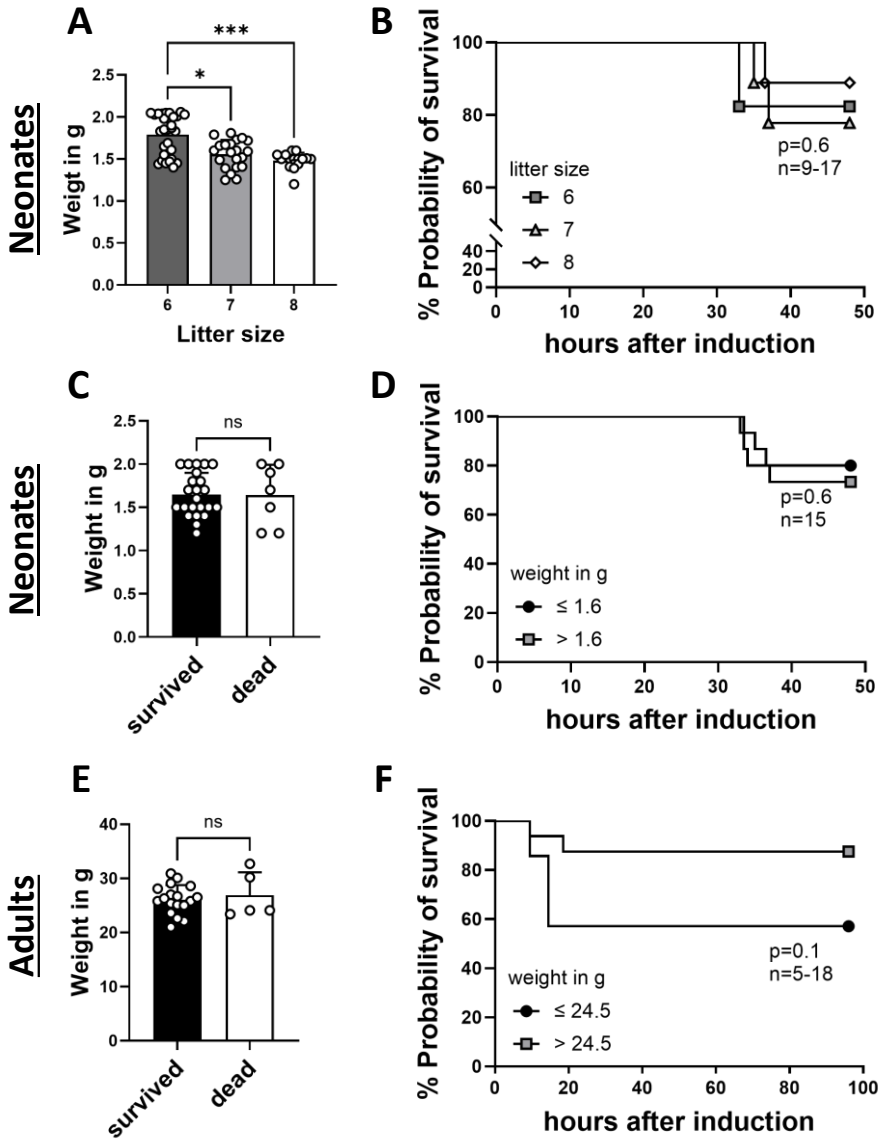

Figure 13. Impact of weight and litter size on *E. coli* sepsis mortality in neonatal and adult mice.

To assess the effect of weight (adults and neonates) and litter size (neonates) on *E. coli* sepsis induced mortality, sepsis was induced in neonatal (age P2) and adult (age 8-12 weeks) C57BL/6J mice. Litter size of neonatal mice, weight and mortality (adults and neonates) was recorded over the course of sepsis (48 h for neonates, 96 h for adults). **A** Bar graph shows individual weight in g of neonatal mice at hour 0 of sepsis induction grouped by litter size. n=9-30, Kruskal-Wallis test. **B** Survival curve shows probability of survival in % of neonatal mice grouped by litter size. n=9-17, p=0.5, Log-rank (Mantel-Cox) test. **C** Bar graph shows weight of neonatal mice in g grouped by surviving animals (black) or dead animals (white). n=7-23, Mann-Whitney test. **D** Survival curve shows probability of survival in % for neonatal animals based on average weight. Average weight of all animals was 1.6 g, and animals were grouped into groups (weight below average and weight above average). n=15, Log-rank (Mantel-Cox) test. **E** Bar graph shows weight of adult mice in g grouped by surviving animals (black) or dead animals (white). n=5-18, unpaired t-test. **F** Survival curve shows probability of survival in % for adult animals based on weight. Average weight of all animals was 24.5 g, and animals were grouped into two groups (weight below average and weight above average). n=5-18, Log-rank (Mantel-Cox) test. p=ns (not significant), *p < 0.05, ***p < 0.001.

4.1.2. Analysis of the role of CD200 and CD200R in murine adult and neonatal *E. coli* sepsis

Neonates' susceptibility and severity of disease progressions in sepsis most likely stem from immune adaptations in early life (see introduction chapter 1.2.1 and 1.3.1). Immune checkpoint molecules are important regulators of pro- and anti-inflammatory immune responses during infections, and differential regulations of ICMs like PD-1 in sepsis have been reported before [140,150]. Based on this knowledge we hypothesized that the differences in clinical course between adult and neonatal sepsis in mice could, at least partially, be caused by differential regulation of immune-checkpoint molecules. In our experiments, we focused on the anti-inflammatory ICM CD200 and its receptor CD200R.

4.1.2.1. Age impacts CD200 and CD200R expression on murine immune cells

To determine if age impacts the expression patterns of CD200 and CD200R on murine immune cells, we measured CD200 and CD200R expression on various splenic immune cell types of mice aged P1, P3, P8, P21 and adults (8 weeks old) (**Figure 14**). On splenic myeloid cells, we observed intermediate CD200 expression in early stages of life (on e.g. neutrophils: P1 48.7 ± 3.20%, P3 49.3 ± 4.62%**,** P8 41.7 ± 6.76%) and a significant drop in CD200 expression at P21 (for e.g. neutrophils 21.5 ± 2.55%) compared to age P1, P3 and P8. In adults, CD200 expression on myeloid cells was overall higher than in younger mice and was significantly increased again after the drop at P21 (monocytes: P21 43.7 ± 6.48% vs. adult 57.3 ± 5.52%, p = 0.007; neutrophils: P21 21.5 ± 2.55% vs. adult 54.8 ± 14.36%, p = 0.007) (**Figure 15**, A + B). In contrast, we observed overall higher CD200R expression on splenic myeloid cells of mice aged P1, P3 and P8 compared to their CD200 expression levels (for e.g. monocytes P1 CD200 46.6 ± 5.07% vs. CD200R 86.8 ± 3.22%). This effect was not observed in mice aged P21 and adults, who had lower overall CD200R expression levels on myeloid cells compared to mice aged P1-P8, with significantly lower levels at P21 and in adults on monocytes and in some cases on neutrophils (e.g. monocytes P1 86.8 ± 3.22% vs. adult 37.0 ± 6.49%, p <0.0001) (**Figure 15**, E + F). The transition from higher CD200R expression to higher CD200 expression on myeloid cells over the course of live became even more clear, when we analyzed the ratios of CD200 to CD200R expression on myeloid cells (**Figure 15**, I + J).

On lymphoid immune cells like T- and B-cells we observed a different CD200 and CD200R expression pattern compared to myeloid cells. On T-cells we observed comparable levels of CD200 expression at P1, P3, P21 and in adults, which were also higher than on myeloid cells (**Figure 15**, A-C). Interestingly in T-cells we observed a significant peak of CD200 expression at P8 compared to P1, P3 and P21 (e.g. P1 55.9 ± 7.85% vs. P8 80.2 ± 5.68%, $p < 0.0001$) (**Figure 15**, C). On B-cells, CD200 expression levels were already high at the beginning of life (P1) and further increased over the course of life with lowest expression levels at age P1 and highest on adult B-cells (P1 58.2 ± 5.08% vs. adult 96.9 ± 0.60%, $p < 0.0001$) (**Figure 15**, D). Overall, CD200R expression levels on T- and B-cells were much lower than on myeloid cells at every age (**Figure 15**, E-H). However, like on myeloid cells, CD200R levels were higher at earlier ages (P1-P3) when compared to P21 and adults, where almost no detectable CD200R expression on T- and B-cells was observed (e.g. B-cells: P1 20.0 ± 5.88% vs. adult 3.1 ± 1.28%, $p = 0.0012$) (**Figure 15**, G + H). The differential expression patterns of CD200 and CD200R expression on lymphoid versus myeloid cells was also observed when we analyzed to ratio of CD200 to CD200R expression on T- and B-cells who showed overall higher CD200R than CD200 expression over the course of life (**Figure 15**, K + L).

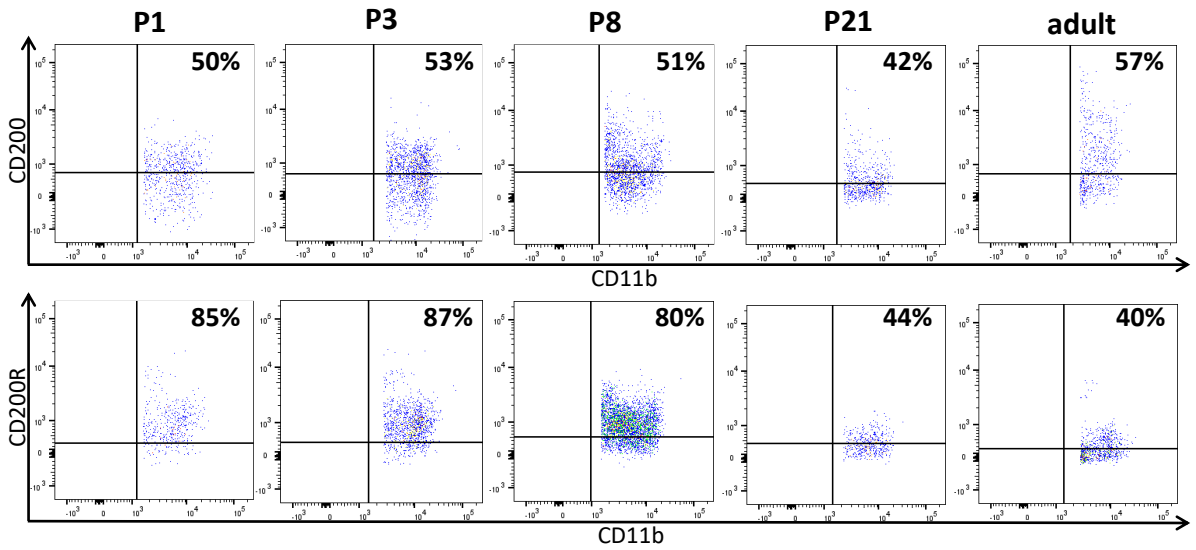

Figure 14. Representative flow cytometry plots for age dependent CD200/CD200R expression on murine monocytes.

Representative dot plots show age dependent CD200 (top) and CD200R (bottom) expression of murine splenic monocytes from mice aged P1, P3, P8, P21 and adults (8 weeks).

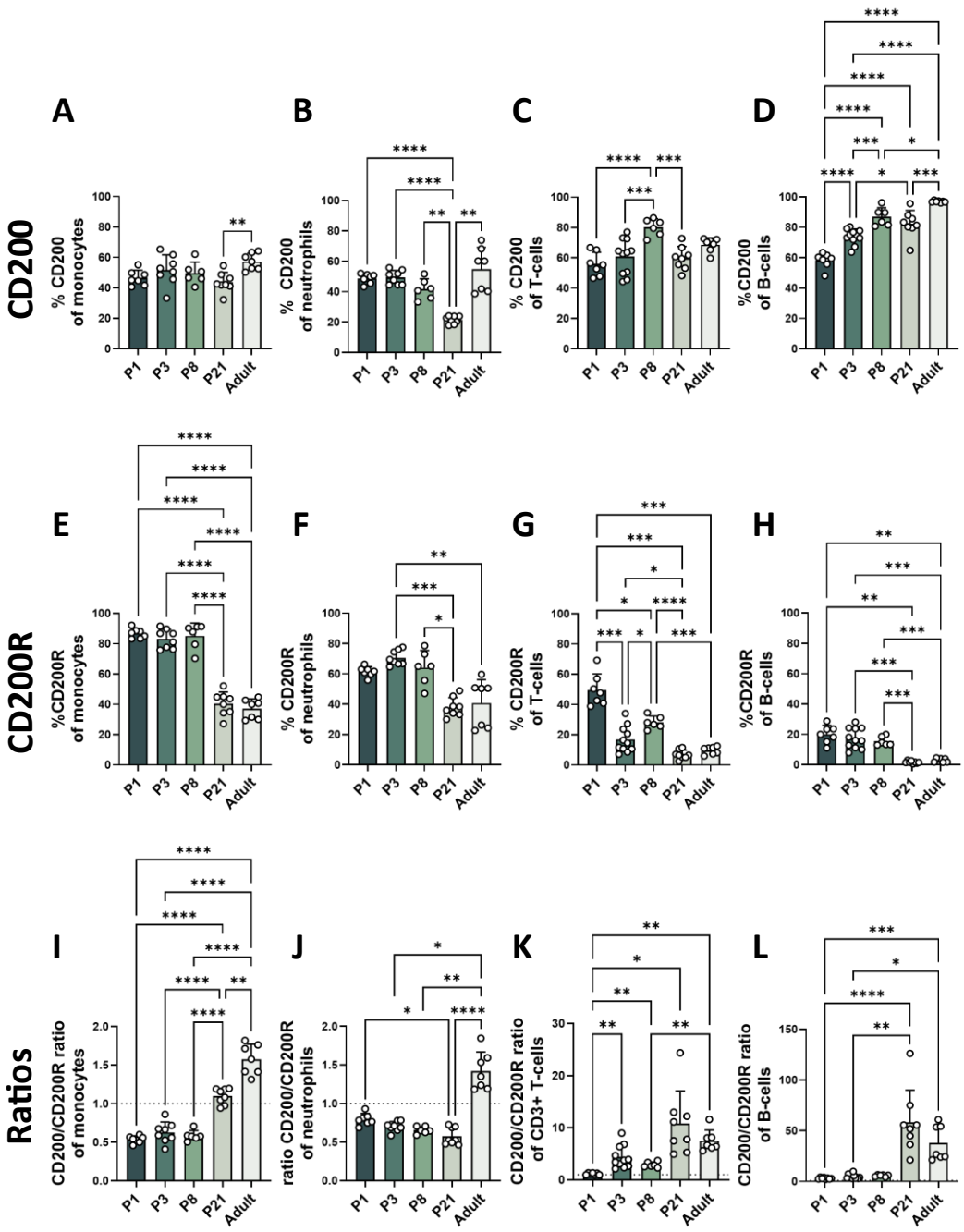

Figure 15. Age dependent CD200 and CD200R expression on splenic immune cells of C57BL/6J mice.

To analyze age dependent CD200 and CD200R expression levels of murine immune cells, spleens of mice aged P1, P3, P8, P21 and 8 weeks (adults) were harvested, homogenized and analyzed for CD200 and CD200R expression using flow cytometry. **A-D** Representative bar graphs show % of CD200 expression on splenic monocytes (**A**), neutrophils (**B**), T-cells (**C**) and B-cells (**D**) of mice aged P1, P3, P8, P21 and adults (left to right). n=6-8, One-Way ANOVA, Kruskal-Wallis test or Brown-Forsythe ANOVA. **E-H** Representative bar graphs show % of CD200R expression on splenic monocytes (**E**), neutrophils (**F**), T-cells (**G**) and B-cells (**H**) of mice aged P1, P3, P8, P21 and adults (left to right). n=6-8, One-Way ANOVA or Brown-Forsythe ANOVA. **I-L** Bar graphs show ratios of CD200 to CD200R expression on monocytes (**I**), neutrophils (**J**), T-cells (**K**) and B-cells (**L**) for mice aged P1, P3, P8, P21 and adults (left to right). CD200/CD200R ratio of 1 ≙ equal CD200 and CD200R expression (indicated with a dotted line). n=6-8, Brown-Forsythe ANOVA or Kruskal-Wallis Test. **Q+R** Representative dot plots show expression of CD200 (top rows) and CD200R (bottom rows) of splenic T-cells (CD3) of adults (**Q**) and neonates (**R**) with (+) or without (-) sepsis. Only significant differences are shown. *p < 0.05, **p < 0.01, ***p < 0.001, ****p < 0.0001.

4.1.3. *E. coli* sepsis impacts CD200 and CD200R expression on splenic neonatal immune cells

The neonatal immune system has been described to be primed towards a primarily suppressive immune response [79–81]. It has also been shown that the regulation of the neonatal immune response to infections is different from that of adults (s. introduction chapter 1.2.1 and 1.3.1). Based on this knowledge and our observations of differential CD200 and CD200R expression patterns over the course of life in mice, we asked whether the regulation of CD200 and CD200R expression differed between adult and neonatal mice when challenged with a severe infection like *E. coli* sepsis. Successful sepsis induction was determined by the occurrence of mortality in both adult and neonatal *E. coli* sepsis models (s. Appendix **Figure 33**). In adult mice, we observed no difference in CD200 expression (monocytes: 37.4 ± 21.25% vs. 45.8 ± 14.81%, p = 0.49; neutrophils: 23.5 ± 12.13% vs. 43.7 ± 15.45%, p = 0.0504; T-cells: 40.7 ± 10.77% vs. 45.6 ± 7.89%, p = 0.44; B-cells: 89.4 ± 9.18% vs. 92.2 ± 4.66%, p = 0.88) (**Figure 16**, A-D), and CD200R expression on splenic immune cells of healthy and septic adult mice (monocytes: 17.9 ± 9.49% vs. 28.5 ± 10.57%, p = 0.13; neutrophils: 22.5 ± 5.73% vs. 25.0 ± 6.49%, p = 0.84; T-cells: 4.4 ± 1.90% vs. 3.5 ± 1.13%, p = 0.39; B-cells: 1.7 ± 1.09% vs. 1.8 ± 0.65%, p = 0.97) (**Figure 16**, E-H). In neonates, we also observed no change in CD200 expression on splenic myeloid immune cells between healthy and septic mice (monocytes: 7.5 ± 1.93% vs. 8.1 ± 3.2%, p = 0.69; neutrophils: 22.5 ± 5.73% vs. 25.0 ± 6.49%, p = 0.84) (**Figure 16**, I + J). However, sepsis led to a significant reduction of CD200 expression on neonatal T-cells (from 14.7 ± 2.69% to 10.2 ± 3.21%, p = 0.04) and a significant increase in CD200 expression on neonatal B-cells (from 40.0 ± 5.18% to 54.1 ± 4.05%, p = 0.0004) (**Figure 16**, K + L). In contrast, CD200R expression was significantly increased on myeloid cells of neonatal septic mice compared to healthy controls (monocytes: from 69.6 ± 4.36% to 81.2 ± 3.52%, p = 0.0005; neutrophils: from 54.6 ± 5.10% to 83.2 ± 5.56%, p < 0.0001), while CD200R expression on lymphoid immune cells of neonatal mice was not affected by sepsis (T-cells: from 55.4 ± 10.91% to 55.4 ± 6.15%, p = 0.99; B-cells: from 2.1 ± 1.04% to 2.4 ± 0.87%, p = 0.62) (**Figure 16**, M-P). Expression of CD200 and CD200R on lung and liver immune cells showed similar results to that of splenic immune cells (not shown).

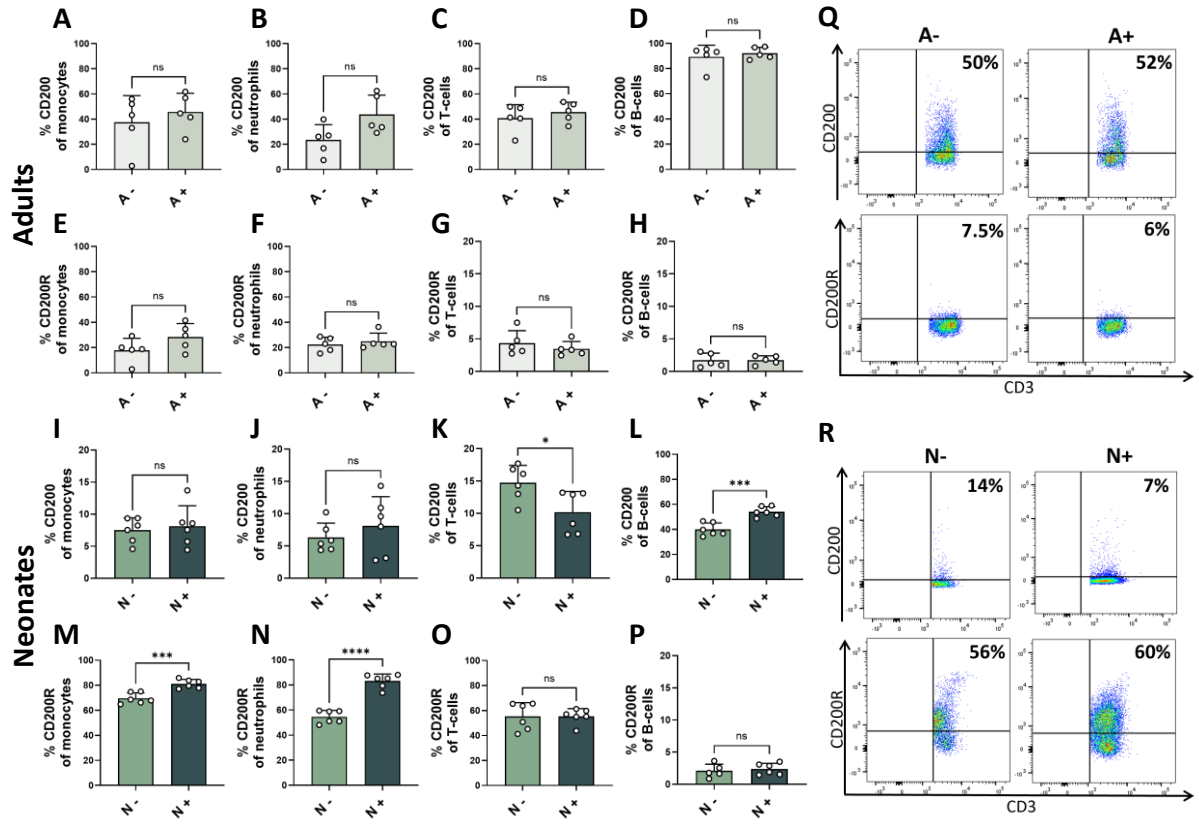

Figure 16. CD200 and CD200R expression on splenic immune cells of adult and neonatal mice with sepsis.

To assess changes in CD200 and CD200R expression on splenic immune cells during sepsis in neonatal and adult mice, we induced sepsis via *E. coli* injection. Spleens were harvested from healthy control mice (-) or septic mice (+) at the end of the experiments (48 h for neonates and 96 h for adults), homogenized and analyzed for CD200 and CD200R expression using flow cytometry. **A-D** Bar graphs show % of CD200 expression on adult (A) splenic immune cells monocytes (**A**), neutrophils (**B**), T-cells (**C**) and B-cells (**D**) for healthy (-) and septic (-) mice. n=5, unpaired t-test and Mann-Whitney test. **E-H** Bar graphs show % of CD200R expression on adult (A) splenic immune cells monocytes (**E**), neutrophils (**F**), T-cells (**G**) and B-cells (**H**) for healthy (-) and septic (-) mice. n=5, unpaired t-test and Mann-Whitney test. **I-L** Bar graphs show % of CD200 expression of neonatal (N) splenic immune cells monocytes (**I**), neutrophils (**J**), T-cells (**K**) and B-cells (**L**) for healthy (-) and septic (-) mice. n=6, unpaired t-test and Mann-Whitney test. **M-P** Bar graphs show % of CD200R expression on adult (N) splenic immune cells monocytes (**M**), neutrophils (**N**), T-cells (**O**) and B-cells (**P**) for healthy (-) and septic (-) mice. n=6, unpaired t-test and Mann-Whitney test. p=ns (not significant), *p < 0.05, ***p < 0.001, ****p < 0.0001.

4.1.4. sCD200 levels change over the course of life but are not affected by sepsis

It is known that a soluble form of the cell surface molecule CD200 exists that can interact with the CD200 receptor and activate its signaling pathway (s. introduction chapter sCD200). Based on our results that revealed differences in CD200 and CD200R expression over the course of life and changes of CD200 or CD200R expression in neonatal mice with sepsis, we wanted to know if these differences are also reflected in sCD200 blood plasma concentrations.

Therefore, we analyzed sCD200 plasma levels of mice aged P1 to adults as well as from adult and neonatal mice with *E. coli* sepsis. We observed no consistent sCD200 plasma concentrations over the course of life in mice. sCD200 levels were higher at earlier stages of life (P1-P21) with peaks at ages P3 and P21 (P1: 327.7 ± 171.5 pg/ml, P3: 434.8 ± 167.0 pg/ml, P8: 297.5 ± 105.2 pg/ml and P21: 464.1 ± 231.3 pg/ml) and a significant drop in sCD200 plasma levels in adult mice compared to mice aged P1, P3 and P21 (e.g. P1 327.7 ± 171.5 pg/ml vs. adult 84.4 ± 63.0 pg/ml, p = 0.03) (**Figure 17**, A). Significantly higher sCD200 levels were also observed in healthy and septic neonatal mice when compared to healthy and septic adult mice (A-: 94.6 ± 77.3 pg/ml vs. N-: 517.2 ± 184.7 pg/ml, p = 0.0002; A+: 41.6 ± 52.1 pg/ml vs. N+: 441.5 ± 113.7 pg/ml, p = 0.0018). For septic mice, we observed a tendency for reduced sCD200 concentrations in both adult and neonatal mice when compared to their healthy controls (A-: 94.6 ± 77.3 pg/ml vs. A+: 41.6 ± 52.1 pg/ml, p = 0.96; N-: 517.2 ± 184.7 pg/ml vs. N+: 441.5 ± 113.7 pg/ml, p = 0.79) (**Figure 17**, B).

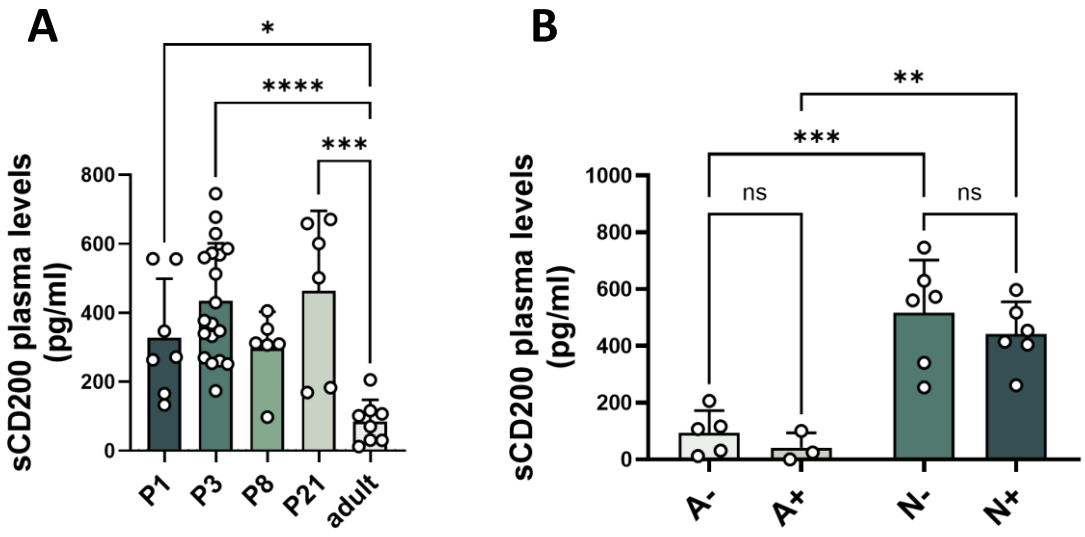

Figure 17. Effect of age and sepsis on sCD200 plasma concentration in neonatal and adult mice.

To analyze changes in sCD200 plasma concentration in mice of different ages, plasma from healthy mice aged P1, P3, P8, P21, 8 weeks (adult) and neonatal and adult mice with *E. coli* sepsis (aged P2 and adults) was analyzed for the sCD200 concentration in plasma by ELISA. **A** Bar graph shows plasma levels of sCD200 in pg/ml plasma for mice aged P1, P3, P8, P21 and for adult animals (left to right). n=6-19, Ordinary One-Way ANOVA, only significant differences are shown. **B** Bar graph shows plasma levels of sCD200 in pg/ml plasma for healthy (-) and septic (+) neonatal (N) and adult (A) mice. n=3-6, Ordinary One-Way ANOVA. p=ns (not significant), *p < 0.05, **p < 0.01, ***p < 0.001, ****p < 0.0001.

4.1.5. Impact of rCD200 treatment on neonatal sepsis

In our previous experiments, we observed overall higher CD200R expression on immune cells of neonatal mice compared to adult mice. Next, we wanted to analyze which potential functions the high CD200R expression on neonatal immune cells could have in the context of sepsis. Therefore, we supplemented recombinant CD200 protein (rCD200) shortly before neonatal sepsis induction to activate the CD200R signaling pathway and analyze the effects of this treatment on neonatal sepsis.

4.1.5.1. rCD200 treatment negatively impacts neonatal sepsis survival

We observed that treatment of neonatal mice with rCD200 shortly before sepsis induction led to a significantly decreased probability of sepsis survival when compared to septic animals without prior rCD200 treatment (control 80% vs. rCD200 36.4%, p = 0.04) (**Figure 18**, A). Mice treated with rCD200 also had reduced average weight gain over the course of the experiment compared to the starting weight normalized to 0% P2 (control 20.7 ± 15.3% vs. rCD200 15.1 ± 10.1%, p = 0.51) (**Figure 18**, B).

To analyze potential differences in bacterial clearance capability of immune cells between untreated and rCD200 treated neonatal sepsis mice, the bacterial load of different organs was analyzed. Overall, the increased mortality of rCD200 treated animals was not reflected in the bacterial load of blood, spleen, lung and liver, which on average, did not significantly differ between control and rCD200 treated animals (blood: $1.2x10^7 \pm 7.9x10^6$ CFU/ml vs. $7.2x10^6 \pm 7.8x10^6$ CFU/ml, p = 0.19; spleen: $2.6x10^6 \pm 3.8x10^6$ CFU/g vs. $2.3x10^6 \pm 2.9x10^6$ CFU/g, p = 0.93; lung: $7.5x10^5 \pm 7.1x10^5$ CFU/g vs. $7.5x10^5 \pm 8.7x10^5$ CFU/g, p = 0.6; liver: $5.6x10^5 \pm 7.4x10^5$ CFU/g vs. $4.9x10^5 \pm 7.4x10^5$ CFU/g, p = 0.99) (**Figure 18**, C-F).

To assess potential differences in the inflammatory response of control and rCD200 treated animals, plasma concentrations of pro-inflammatory cytokines IL-6 and TNF-α were analyzed. Blood plasma levels of IL-6 were slightly but not statistically significant reduced in rCD200 animals compared to the controls while TNF-α levels did not significantly differ between control and rCD200 groups (IL-6: 7711 ± 8086 ng/ml vs. 2297 ± 2482 ng/ml, p = 0.12; TNF-α: 8045 ± 4333 pg/ml vs. 5696 ± 4910 pg/ml, p = 0.15) (**Figure 18**, G + H).

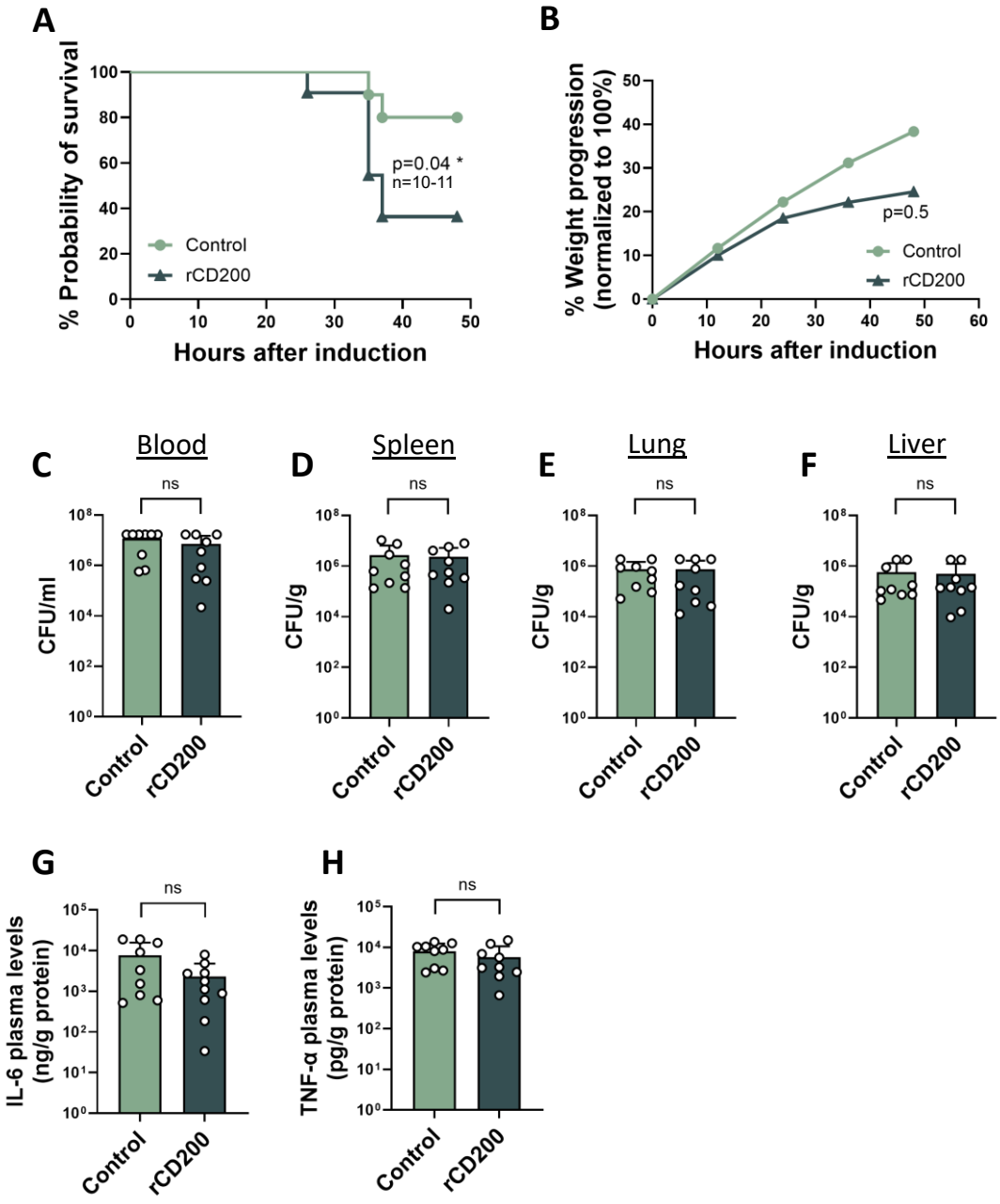

Figure 18. Impact of rCD200 treatment on mortality, bacterial load and cytokine levels in septic neonatal mice.

To analyze the impact of rCD200 treatment and therefore CD200R pathway activation on neonatal sepsis progression, neonatal mice (aged P2) received an i.p. injection with 1 µg rCD200 shortly before sepsis induction via s.c. *E. coli* injection. After a maximum of 48 h, blood and organs (spleen, lung and liver) were harvested and homogenized for analysis of bacterial load. Plasma was analyzed for the expression of pro-inflammatory cytokines via ELISA. **A** Survival graph shows probability of survival in % for control (light green) and rCD200 injected (dark green) neonatal mice. n=10-11, p=0.04, Log-rank (Mantel-Cox) test. **B** Line graph shows weight gain over the course of the experiment normalized to the starting weight at P2 (0 %). **C-F** Bar graphs show bacterial load in blood (**C**), spleen (**D**), lung (**E**) and liver (**F**) of neonatal mice as colony forming units (CFU)/ml for blood or CFU/g for other organs on a logarithmic y-axis for control animals (light green) and animals with rCD200 injection (dark green). n=9, Mann-Whitney test. **G-H** Bar graphs show plasma levels of pro-inflammatory cytokines IL-6 (**G**) in ng/g protein and TNF-α (**H**) in pg/g protein for control (light green) and rCD200 mice (dark green) on a logarithmic y-axis. n=9-10, unpaired t-test or Mann-Whitney test (one-tailed analysis). p=ns (not significant), *p < 0.05.

4.1.5.2. rCD200 treatment does not impact splenic immune cell composition in neonatal sepsis

To determine the impact of rCD200 treatment in neonatal sepsis on immune cell composition, we analyzed percentages of various myeloid and lymphoid immune cell types from spleens of rCD200 treated septic neonatal mice and septic mice without rCD200 treatment. Overall, we observed low numbers of splenic immune cell types for both control and rCD200 treated mice, including monocytes, neutrophils, macrophages, dendritic cells and T-cells (**Figure 19**, A-E). We observed no significant differences in the immune cell composition of control and rCD200 treated neonatal mice for monocytes (control 10.7 ± 3.86% vs. rCD200 11.5 ± 4.02%, p = 0.66), neutrophils (control 7.0 ± 3.39% vs. rCD200 5.2 ± 1.62%, p = 0.18), dendritic cells (control 2.2 ± 1.41% vs. rCD200 1.3 ± 1.50%, p = 0.18) , $CD3^+$ T-cells (control 11.7 ± 1.96% vs. rCD200 12.2 ± 4.85%, p = 0.78), B-cells (control 51.1 ± 6.81% vs. rCD200 57.1 ± 8.93%, p = 0.13), G-MDSCs (control 23.0 ± 13.88% vs. rCD200 16.2 ± 13.71%, p = 0.31) or M-MDSCs (control 36.0 ± 16.66% vs. rCD200 35.1 ± 9.76%, p = 0.71) (**Figure 19**, A + B, D-H). rCD200 treated mice had significantly lower percentages of macrophages compared to control mice (control 6.1 ± 1.01% vs. rCD200 3.2 ± 2.17%, p = 0.015) (**Figure 19**, C). Additionally, we analyzed immune cell composition of T-cell sub-populations. We observed no difference in immune cell composition of control and rCD200 treated neonatal mice for $CD4^+$ and $CD8^+$ T-cells (CD4: control 61.3 ± 6.17% vs. rCD200 62.8 ± 9.89%, p = 0.71; CD8: control 12.4 ± 2.56% vs. rCD200 11.9 ± 4.04%, p = 0.76) (**Figure 19**, I + K). We observed a tendency towards increased naïve $CD4^+$ T-cell numbers in rCD200 treated mice when compared to control animals (control 51.1 ± 21.5% vs. rCD200 64.7 ± 15.7%, p = 0.14), a trend not reflected in naïve $CD8^+$ T-cells (control 42.4 ± 14.57% vs. rCD200 40.2 ± 17.08%, p = 0.86) (**Figure 19**, J + L). Immune cell composition of lung and liver cells showed similar results to that of splenic immune cells (not shown).

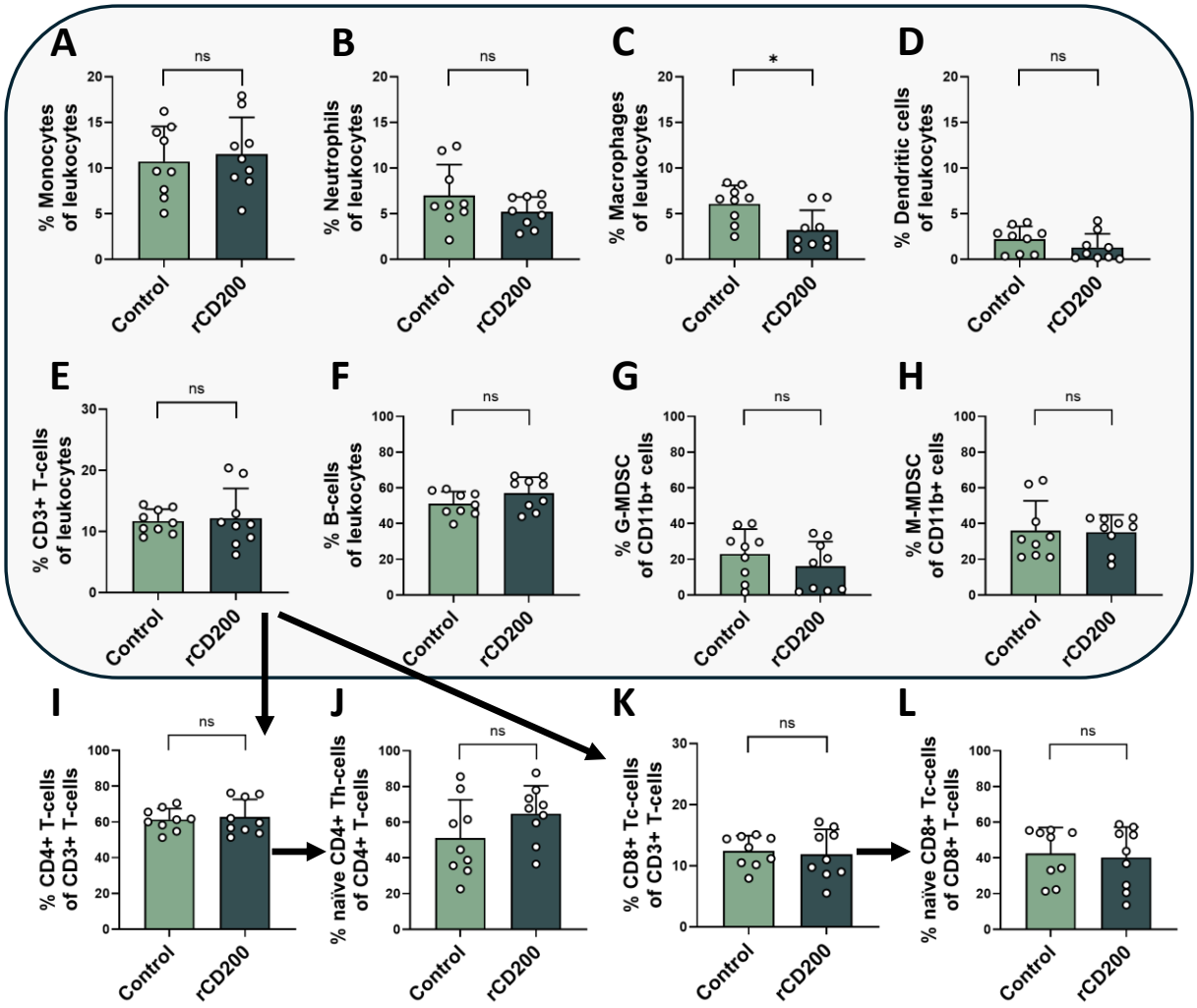

Figure 19. Splenic immune cell composition of neonatal septic mice with or without rCD200 treatment.

To assess the effect of rCD200 treatment on neonatal immune cell composition during sepsis, *E. coli* sepsis was induced in neonatal mice after i.p. injection of PBS (control) or 1µg rCD200. Immune cells were harvested from spleens at the end of the experiment (max. 48 h after induction) and analyzed for immune cell composition using flow cytometry. **A-H** Bar graphs show splenic immune cell composition in % of leukocytes (**A-F**) or $CD11b^+$ cells (**G+H**) for monocytes (**A**), neutrophils (**B**), macrophages (**C**), dendritic cells (**D**), CD3+ T-cells (**E**), B-cells (**F**), G-MDSCs (**G**) and M-MDSCs (**H**) for septic control mice (light green) and rCD200 injected mice (dark green). n=9, unpaired t-test and Mann-Whitney test. **I-L** Bar graphs show splenic immune cell composition of T-cell sub-sets as % of $CD3^+$ T-cells (**I+K**) or $CD4^+$ (**J**)/$CD8^+$ (**L**) T-cells for $CD4^+$ Th-cells (**I**), naïve $CD4^+$ T-cells (**J**), $CD8^+$ T-cells (**K**) and naïve $CD8^+$ T-cells (**L**) for septic control mice (light green) and rCD200 injected mice (dark green). n=9, unpaired t-test and Mann-Whitney test. p=ns (not significant), *$p < 0.05$.

4.1.6. Impact of rCD200 treatment on adult sepsis

Based on our findings, that rCD200 treatment prior to sepsis induction led to increased mortality in neonatal mice, we aimed to assess if a similar effect could be observed in adult mice who had much lower CD200R cell surface expression on immune cells compared to neonatal mice.

4.1.6.1. rCD200 treatment does not affect sepsis mortality in adult mice

To determine the effect of rCD200 treatment shortly before sepsis induction in adult mice, we analyzed different markers of sepsis severity including mortality, weight progression, bacterial load and pro-inflammatory cytokine levels. In adult mice, we observed no change in the probability of sepsis survival between control and rCD200 treated animals (control 83.3% vs. rCD200 87.5%, p = 0.79) (**Figure 20**, A). Further, we observed no difference on average weight progression normalized to the starting weight at 100% over the course of the experiment between control and rCD200 treated animals (control 90.2 ± 4.27% vs. rCD200 89.4 ± 4.58%, p = 0.70) (**Figure 20**, B).

Analysis of bacterial load in blood and different organs to identify potential effects of rCD200 on bacterial clearance revealed no differences in bacterial load of rCD200 treated animals compared to the controls in blood (control $2.0x10^5$ ± $4.8x10^5$ CFU/ml vs. rCD200 $2.0x10^3$ ± $4.5x10^3$ CFU/ml, p = 0.39), spleen (control $2.3x10^7$ ± $5.0x10^7$ CFU/g vs. rCD200 $1.1x10^6$ ± $6.9x10^5$ CFU/g, p = 0.82), lung (control $1.1x10^7$ ± $1.9x10^7$ CFU/g vs. rCD200 $3.9x10^5$ ± $5.0x10^5$ CFU/g, p = 0.31), and liver (control $3.7x10^6$ ± $8.1x10^6$ CFU/g vs. rCD200 $7.4x10^6$ ± $1.3x10^7$ CFU/g, p = 0.94) (**Figure 20**, C-F).

To determine differences in inflammation levels between groups, we analyzed plasma concentrations of pro-inflammatory cytokines IL-6 and CXCL1. We observed no significant differences between control and rCD200 groups for IL-6 (248.2 ± 532.3 ng/g vs. 106.9 ± 207.4 ng/g, p = 0.42) and CXCL1 (510.1 ± 1188 ng/g vs. 201.9 ± 453.2 ng/g, p = 0.47) (**Figure 20**, G + H).

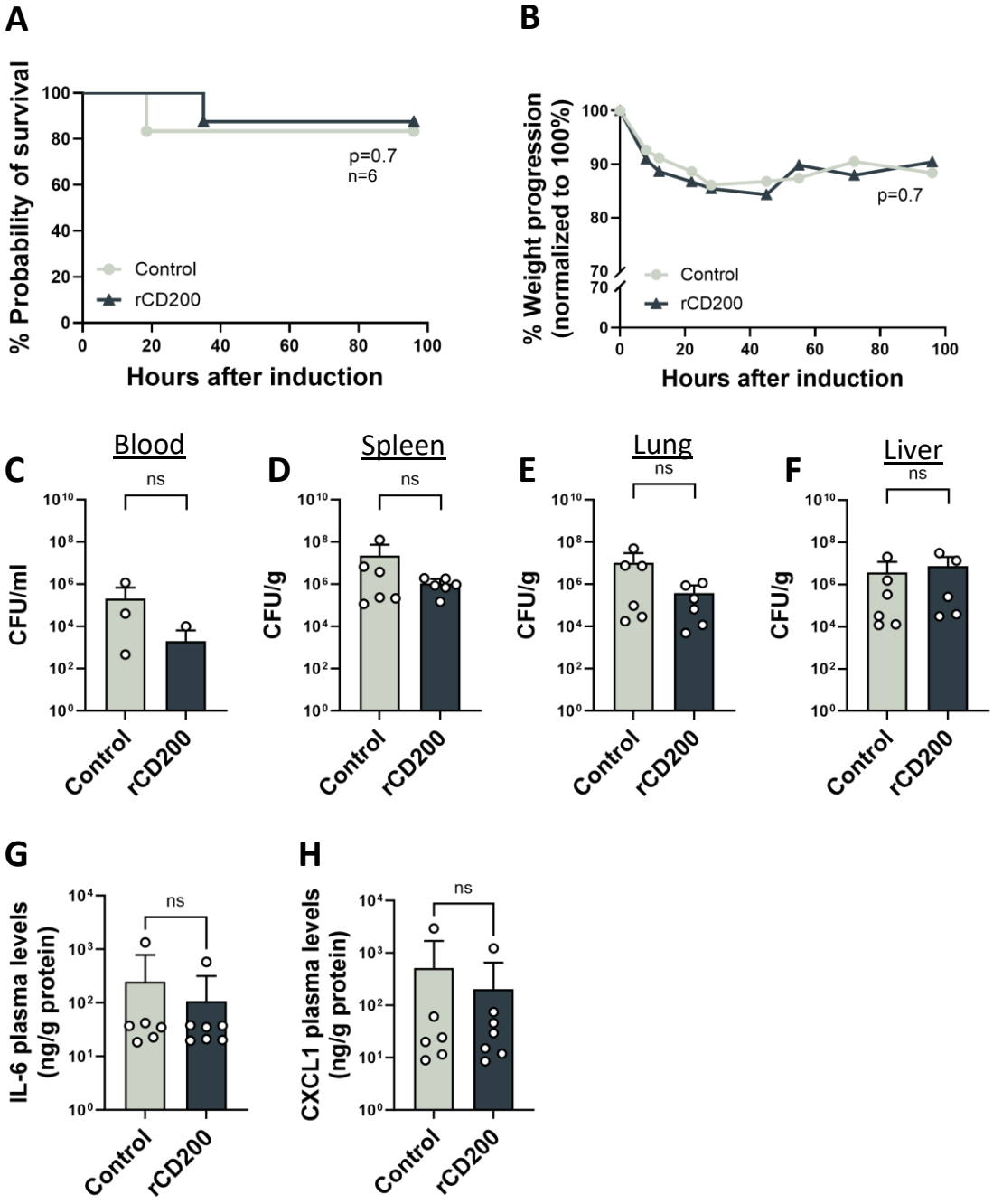

Figure 20. Impact of rCD200 treatment on adult sepsis severity.

To determine the effect of rCD200 treatment on sepsis severity in adult mice, 8–12-weeks-old C57BL/6J mice received an i.v. injection with 10 µg rCD200 shortly before sepsis induction via i.p. *E. coli* injection. After a maximum of 96 h, blood and organs (spleen, lung and liver) were harvested and homogenized for analysis of bacterial load. Plasma was isolated from blood samples for analysis of pro-inflammatory cytokine expression via ELISA. **A** Survival graph shows probability of survival in % for control (light green) and rCD200 injected (dark green) adult mice. n=6, p=0.07, Log-rank (Mantel-Cox) test. **B** Line graph shows weight loss progression over the course of the experiment normalized to the starting weight (100 %). **C-F** Bar graphs show bacterial load in blood (**C**), spleen (**D**), lung (**E**) and liver (**F**) of adult mice as colony forming units (CFU)/ml for blood or CFU/g for other organs on a logarithmic y-axis for control animals (light green) and animals with rCD200 injection (dark green). n=6, Mann-Whitney test. **G-H** Bar graphs show plasma levels of pro-inflammatory cytokines IL-6 (**G**) and CXCL1 (**H**) in ng/g protein for control (light green) and rCD200 mice (dark green) on a logarithmic y-axis. n=6, Mann-Whitney test (one-tailed). p=ns (not significant).

4.1.6.2. rCD200 treatment does not affect immune cell composition in adult mice with *E. coli* sepsis

To assess the effect of rCD200 treatment on immune cell composition of adult mice with sepsis, we analyzed percentages of immune cells from spleens of control and rCD200 treated septic adult C57BL/6J mice. Overall, we observed low percentages of myeloid immune cells of all leukocytes in both control and rCD200 groups (**Figure 21**, A + B). On average we observed no significant differences in immune cell compositions of splenic myeloid and lymphoid immune cells between control and rCD200 animals (monocytes: 3.3 ± 1.22% vs. 2.4 ± 0.28%, p = 0.12; neutrophils: 11.2 ± 9.67% vs. 11.0 ± 3.92%, p = 0.96; T-cells: 19.8 ± 7.46% vs. 18.1 ± 3.59%, p = 0.64; B-cells: 57.8 ± 5.80% vs. 58.7 ± 4.09%, p = 0.73) (**Figure 21**, A-D). Analysis of FoxP3$^+$ Treg composition in three of six animals per group revealed a significant increase in the percentage of splenic FoxP3$^+$ Tregs in rCD200 treated animals compared to control animals (control 9.5 ± 0.83% vs. rCD200 11.1 ± 0.46%, p = 0.04) (**Figure 21**, E). Immune cell composition of lung and liver cells showed similar results to that of splenic immune cells (not shown).

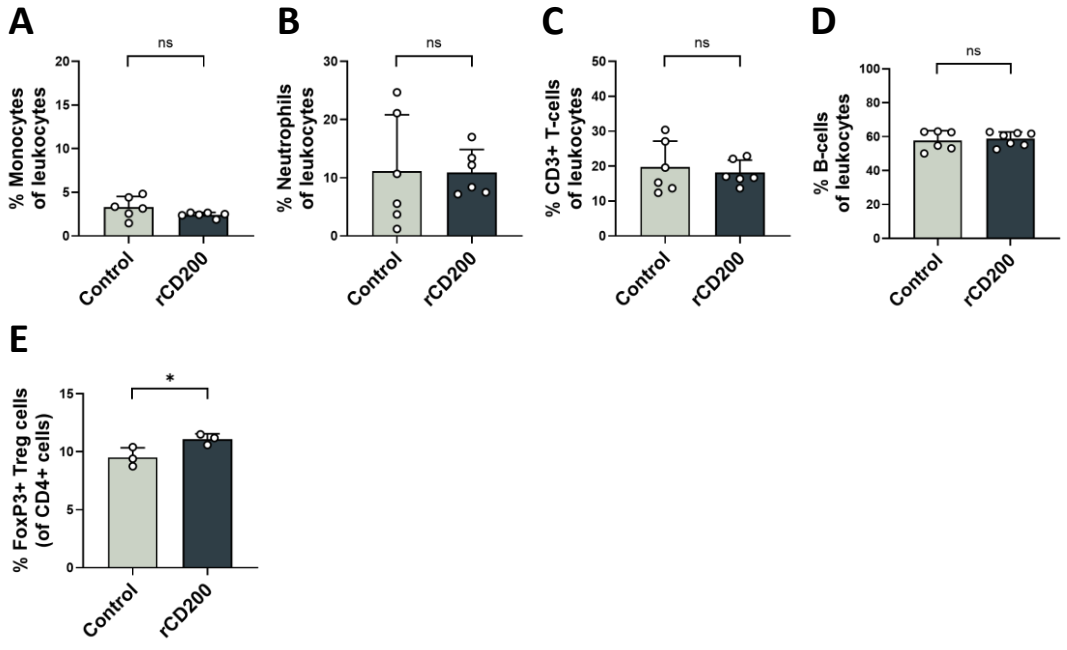

Figure 21. Impact of rCD200 on splenic immune cell composition of adult mice with sepsis.

To assess the effect of rCD200 on splenic immune cell composition of septic adult mice, 8–12-week-old mice received an i.v. injection with 10 µg rCD200 shortly before sepsis induction via i.p. *E. coli* injection. After a maximum of 96 h, spleens were harvested and homogenized to analyze immune cell composition using flow cytometry. **A-E** Bar graphs show % of splenic immune cells for control (light green) and rCD200 injected (dark green) mice for monocytes (**A**), neutrophils (**B**), T-cells (**C**), B-cells (**D**) and FoxP3$^+$ Tregs (**E**). n=3-6, unpaired t-test or Mann-Whitney test. p=ns (not significant), *p < 0.05.

4.1.7. Effect of CD200 blockade in neonatal sepsis

Our previous experiments revealed a negative effect of rCD200 treatment on neonatal sepsis survival in mice. Therefore, we asked whether blockade of CD200 would improve sepsis survival in neonatal mice in a pilot experiment.

4.1.7.1. Blockade of CD200 does not improve neonatal sepsis survival or disease severity

Treatment of neonatal mice with an anti-CD200 antibody to block CD200/CD200R interaction prior to sepsis induction led to a slight decrease in probability of survival compared to the control animals and animals treated with an isotype control antibody (control 100% vs. anti-CD200 71.4%, p = 0.21) (**Figure 22**, A). However, this difference was not significant. In accordance with their lower probability of survival, on average, anti-CD200 treated mice had a reduced percentage of weight gain when compared to control animals (control 22.9 ± 18.29% vs. anti-CD200 14.6 ± 11.27%, p = 0.41) (**Figure 22**, B). To assess whether blockade of CD200 with an anti-CD200 antibody affected the animals ability to clear bacteria, we assessed bacterial load in blood and various organs and found no significant difference in bacterial load between control and anti-CD200 treated neonatal mice for blood ($2.0x10^5 \pm 1.92x10^5$ CFU/ml vs. $4.0x10^5 \pm 6.9x10^5$ CFU/ml, p = 0.54), spleen ($6.8x10^7 \pm 1.22x10^8$ CFU/g vs. $7.2x10^7 \pm 1.15x10^8$ CFU/g, p = 0.23), lung ($2.1x10^7 \pm 4.39x10^7$ CFU/g vs. $1.9x10^7 \pm 2.27x10^7$ CFU/g, p = 0.80) or liver ($2.0x10^7 \pm 4.18x10^7$ CFU/g vs. $6.9x10^7 \pm 1.35x10^8$ CFU/g, p = 0.75) (**Figure 22**, C-F). Next, we analyzed plasma levels of pro-inflammatory cytokines IL-6 and CXCL1 to determine differences in severity of inflammation caused by sepsis between groups. We found no significant differences in the plasma concentrations between control and anti-CD200 treated animals for IL-6 (control 3936 ± 5509 ng/g vs. rCD200 1777 ± 1768 ng/g, p = 0.33) or CXCL1 (control 3043 ± 3594ng/g vs. rCD200 3592 ± 4970 ng/g, p = 0.47) (**Figure 22**, G + H).

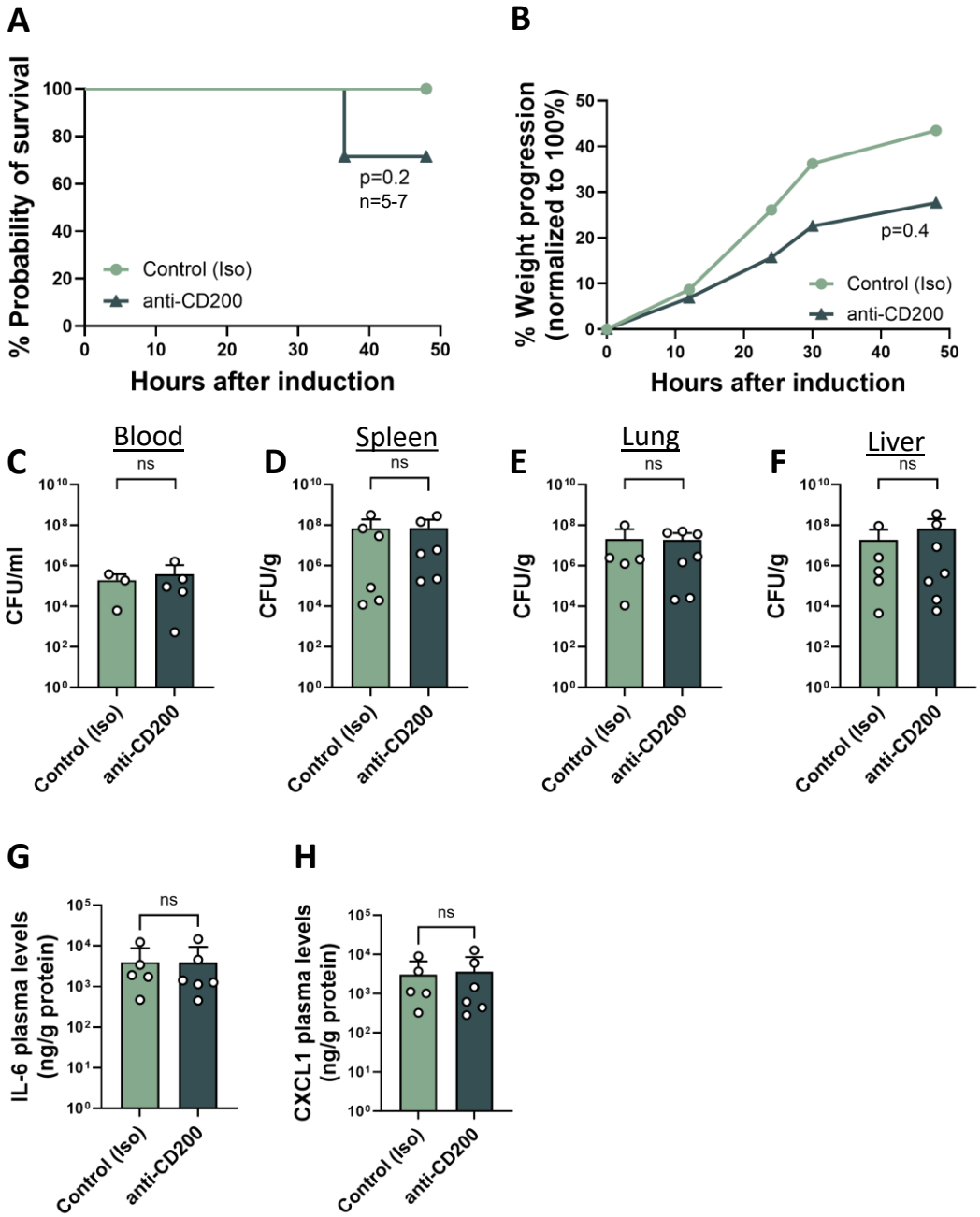

Figure 22. Impact of CD200 blockade on sepsis severity in neonatal mice.

To assess the effect of CD200 blockade on neonatal sepsis survival and severity, neonatal mice (P2) received an i.p. injection with 15 µg anti-CD200-antibody or 15 µg of the corresponding isotype control shortly before sepsis induction via s.c. *E. coli* injection. After a maximum of 48 h, blood and organs were harvested and homogenized for analysis of bacterial load. Plasma was analyzed for expression of pro-inflammatory cytokines by ELISA. **A** Survival graph shows probability of survival in % for control (light green) and anti-CD200 injected (dark green) neonatal mice. n=5-7, p=0.2, Log-rank (Mantel-Cox) test. **B** Line graph shows weight gain over the course of the experiment normalized to the starting weight (0 %) for control (light green) and anti-CD200 treated (dark green) animals. **C-F** Bar graphs show bacterial load in blood (**C**), spleen (**D**), lung (**E**) and liver (**F**) of neonatal mice as colony forming units (CFU)/ml for blood or CFU/g for other organs on a logarithmic y-axis for isotype control animals (light green) and animals with anti-CD200-antibody injection (dark green). n=5-7, Mann-Whitney test. **G-H** Bar graphs show plasma levels of pro-inflammatory cytokines IL-6 (**G**) and CSCL1 (**H**) in ng/g protein for isotype control (light green) and anti-CD200-antibody mice (dark green) on a logarithmic y-axis. n=5-7, Mann-Whitney test (one-tailed). p=ns (not significant).

4.1.7.2. Immune cell composition of septic neonatal mice is not affected by CD200 blockade

To study the effect of CD200 blockade on splenic immune cell composition of septic neonatal mice, we analyzed percentages of myeloid and lymphoid immune cells of spleens from mice treated with an anti-CD200 antibody or and isotype-control antibody. On average, we observed low numbers of myeloid cells (monocytes and neutrophils) and T-cells in spleens of septic neonatal mice of both groups compared to healthy mice (comparison not shown) (**Figure 23**, A-C). We observed a tendency towards increased percentages of monocytes (control 7.5 ± 1.27% vs. anti-CD200 13.5 ± 8.21%, p = 0.07), $CD3^+$ T-cells (control 6.0 ± 2.15% vs. anti-CD200 9.8 ± 5.77%, p = 0.20) and $CD4^+$ T-cells (control 58.6 ± 8.37% vs. anti-CD200 65.0 ± 11.01%, p = 0.30) in anti-CD200 treated neonatal mice when compared to controls, while $CD8^+$ T-cells were significantly decreased (control 16.3 ± 1.68% vs. 13 ± 4.37%, p = 0.048) (**Figure 23**, A + C + E + F). Composition of other immune cells, including neutrophils (control 10.4 ± 3.83% vs. anti-CD200 9.8 ± 5.85%, p = 0.86) and B-cells (control 55.4 ± 10.73% vs. anti-CD200 50.6 ± 10.19%, p = 0.45) did not differ between control and anti-CD200 treated mice (**Figure 23**, B + D). Immune cell composition of lung and liver cells showed similar results to that of splenic immune cells (not shown).

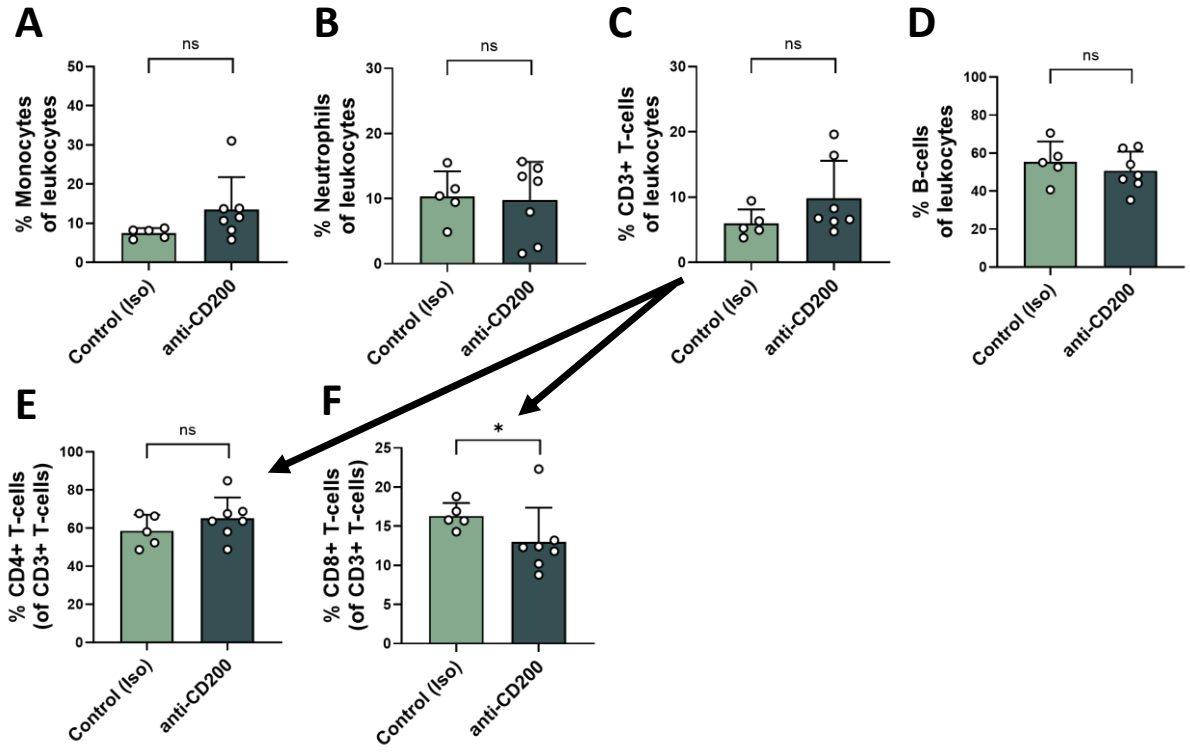

Figure 23. Impact of CD200 blockade on splenic immune cell composition of neonatal mice with sepsis.

To analyze the effect of CD200 blockade on splenic immune cell composition during sepsis, neonatal mice (P2) received an i.p. injection with 15 µg anti-CD200 antibody or 15 µg of the corresponding isotype control shortly before sepsis induction via s.c. *E. coli* injection. After a maximum of 48 h, spleens were harvested and homogenized to analyze immune cell composition using flow cytometry. **A-F** Bar graphs show % of splenic immune cells for isotype control (light green) and anti-CD200 antibody injected (dark green) mice for monocytes (**A**), neutrophils (**B**), $CD3^+$ T-cells (**C**), B-cells (**D**), $CD4^+$ T-cells (**E**) and $CD8^+$ T-cells (**F**). n=5-7, unpaired t-test or Mann-Whitney test. p=ns (not significant), *$p < 0.05$.

4.2. Expression and function of human CD200 and CD200R in neonatal and adult immune cells

Based on the differences in CD200 and CD200R expression and their impact on murine sepsis we observed in our study, we asked whether similar patterns could be observed in human immune cells of neonates and adults. Therefore, we analyzed CD200 and CD200R expression patterns on monocytes and T-cells of adults, full-term neonates and pre-term neonates as well as functional implications of CD200 and CD200R blockade in immune cells from adults and full-term neonates.

4.2.1. CD200 expression differs on human full-term neonatal and adult monocytes and $CD3^+$ T-cells

To analyze potential differences in the expression patterns of CD200 and CD200R on monocytes and T-cells of full-term neonates and adults, we analyzed their expression on untreated cells isolated from whole blood. We observed no significant differences in CD200R expression on monocytes (neo 74.2 ± 9.22% vs. adult 77.5 ± 5.45%, p = 0.23) and T-cells (neo 57.5 ± 8.73% vs. adult 58.5 ± 3.83%, p = 0.70) of neonates and adults (**Figure 24**, C + E). However, we found significantly decreased CD200 expression on neonatal compared to adult monocytes (neo 7.9 ± 6.26% vs. adult 15.6 ± 7.42%, p = 0.0024) and significantly increased CD200 expression on neonatal compared to adult $CD3^+$ T-cells (neo 49.0 ± 10.78% vs. adult 16.3 ± 4.54%, p < 0.0001) (**Figure 24**, B + D). Next, we aimed to analyze if an infectious stimulus impacts the expression of CD200 and/or CD200R on human immune cells. Therefore, we stimulated immune cells of full-term neonates and adults with *E. coli* (MOI 10:1) for 24 h and afterwards, analyzed CD200 and CD200R expression on monocytes and T-cells. Like in the unstimulated immune cells, we observed no significant differences in CD200R expression on neonatal and adult monocytes (neo 87.2 ± 7.63% vs. adult 91.2 ± 5.39%, p = 0.06) and T-cells (neo 59.7 ± 5.09% vs. adult 59.5 ± 3.32%, p = 0.91) after *E. coli* stimulation (**Figure 24**, G + I). CD200 expression on neonatal T-cells still remained significantly higher after *E.coli* stimulation compared to adult T-cells (neo 49.1 ± 14.45% vs. adult 20.4 ± 4.53%, p < 0.0001) (**Figure 24**, H). In contrast to the untreated cells, neonatal monocytes showed significantly higher CD200 expression compared to adult monocytes after *E. coli* stimulation (neo 29.7 ± 17.65% vs. adult

12.8 ± 6.99%, p = 0.0003) (**Figure 24**, F). Considering the ratio of CD200 and CD200R expression on unstimulated versus *E. coli* stimulated monocytes and T-cells we observed a slight upregulation of CD200R on monocytes of neonates and adults (neo 1.2 ± 0.12% vs. adult 1.2 ± 0.06 ratio, p = 0.36) that did not differ between groups, while CD200R expression on T-cells remained unaffected (neo 1.0 ± 0.16% vs. adult 1.0 ± 0.06 ratio, p = 0.61) (**Figure 24**, K + M). Neonatal monocytes significantly upregulated CD200, while adult monocytes did not seem to differentially express CD200 after *E. coli* contact (neo 6.4 ± 4.9% vs. 1.0 ± 0.86 ratio, p = 0.0002) (**Figure 24**, J). In contrast, CD200 expression was significantly upregulated on adult T-cells after *E. coli* stimulation, while neonatal T-cells did not change their expression of CD200 (neo 0.9 ± 0.21% vs. adult 1.3 ± 0.36 ratio, p = 0.002) (**Figure 24**, L).

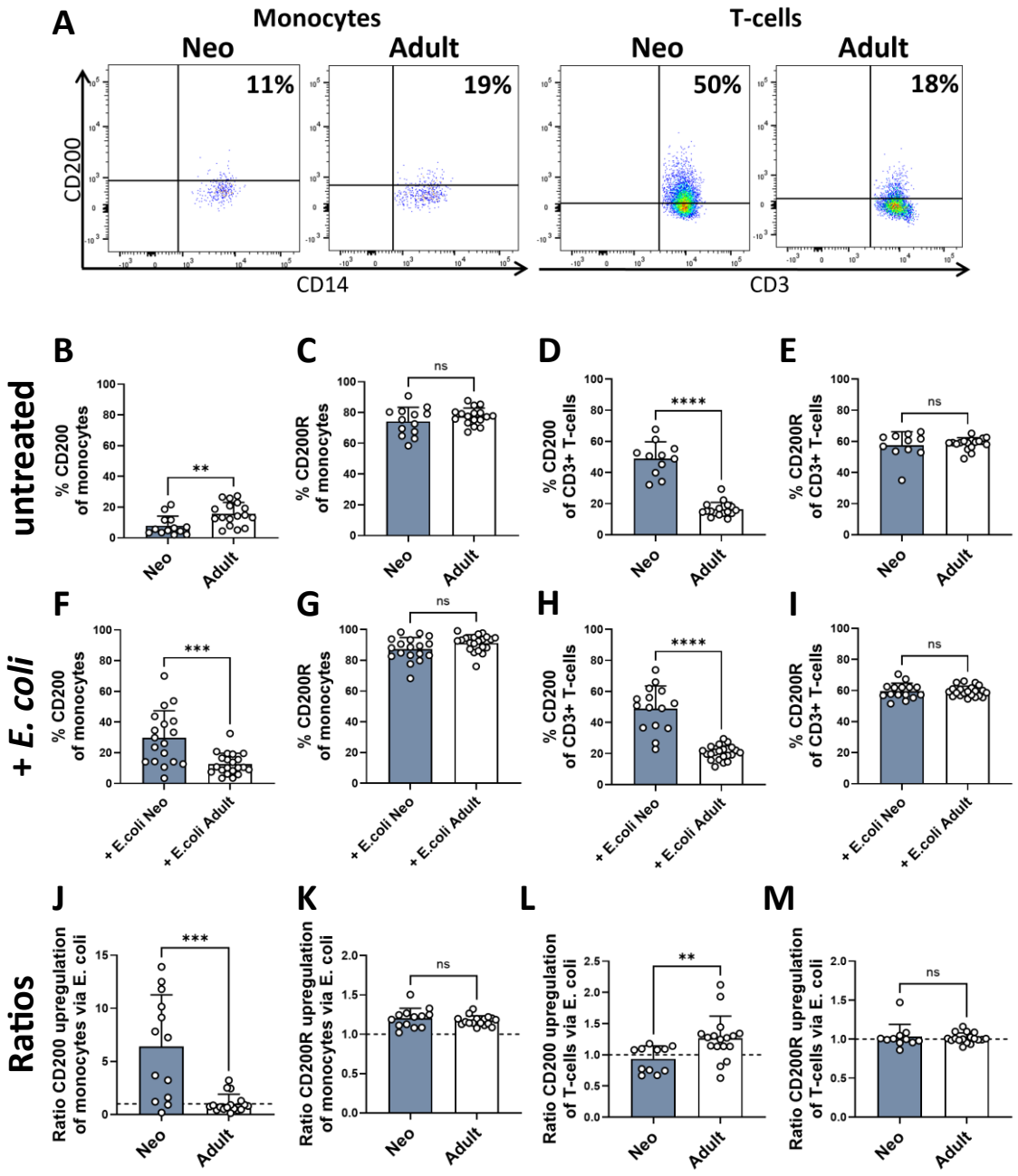

Figure 24. CD200 and CD200R expression on human neonatal and adult monocytes and T-cells.

To assess baseline CD200/CD200R expression on human monocytes and $CD3^+$ T-cells, as well as changes caused by *E. coli* stimulation. Immune cells were isolated from peripheral blood of adults and cord blood of full-term neonates. Cells were left untreated or stimulated with *E. coli* MOI 10:1 for 24 h to analyze changes in CD200/CD200R expression patterns on monocytes and T-cells during infections. **A** Representative dot plots show CD200 expression of monocytes (left) and $CD3^+$ T-cells (right) for adults and neonates. CD200R plots are not shown due to the similarity in CD200R expression of adults and neonates **B-E** Bar graphs show CD200 (**B+D**) and CD200R (**C+E**) baseline expression on monocytes (**B+C**) and $CD3^+$ T-cells (**D+E**) of neonates (light blue) and adults (white) in %. n=13-17, unpaired t-test and Mann-Whitney test. **F-I** Bar graphs show % of CD200 (**F+H**) and CD200R (**G+I**) expression after *E. coli* stimulation on monocytes (**F+G**) and $CD3^+$ T-cells (**H+I)** of neonates (light blue) and adults (white). n=13-17, unpaired t-test and Mann-Whitney. **J-M** Bar graphs show ratios of CD200 (**J+L**) and CD200R (**K+M**) expression of *E. coli* stimulated and unstimulated monocytes (**J+K**) and $CD3^+$ T-cells (**L+M**) of neonates (light blue) and adults (white), no change in CD200/CD200R expression is indicated with a dotted line (at y=1). n=13-17, unpaired t-test and Mann-Whitney test. p=ns (not significant), $^{**}p < 0.01$, $^{***}p < 0.001$, $^{****}p < 0.0001$.

4.2.2. Differences in CD200 mRNA expression of T-cells and monocytes

To confirm differential regulation of CD200 and CD200R expression of CD3+ T-cells and monocytes of adults and full-term neonates, we analyzed CD200 and CD200R mRNA-levels of isolated monocytes and CD3+ T-cells of adults and full-term neonates via qPCR. We found that neonatal CD3+ T-cells had significantly higher CD200 mRNA levels compared to adults (neo 0.01 ± 0.007 vs. adult 0.004 ± 0.002, p = 0.027) (**Figure 25,** B), which matched our previous observation of CD200 cell surface expression (**Figure 24,** C). However, unlike our observation of CD200 cell surface expression on monocytes (**Figure 24**, A), we observed no significant difference in CD200 RNA-levels between neonates and adults (neo 0.004 ± 0.003 vs. adult 0.004 ± 0.004, p = 0.686) (Figure 25, A). Different to what we observed on the cell surface level, we found significantly higher RNA-levels of CD200R in neonatal compared to adult T-cells (neo 0.07 ± 0.22 vs. adult 0.03 ± 0.006, p = 0.008) and a tendency towards higher CD200R RNA-levels on neonatal versus adult monocytes (neo 0.008 ± 0.004 vs. adult 0.005 ± 0.002, p = 0.188) (Figure 25, C + D).

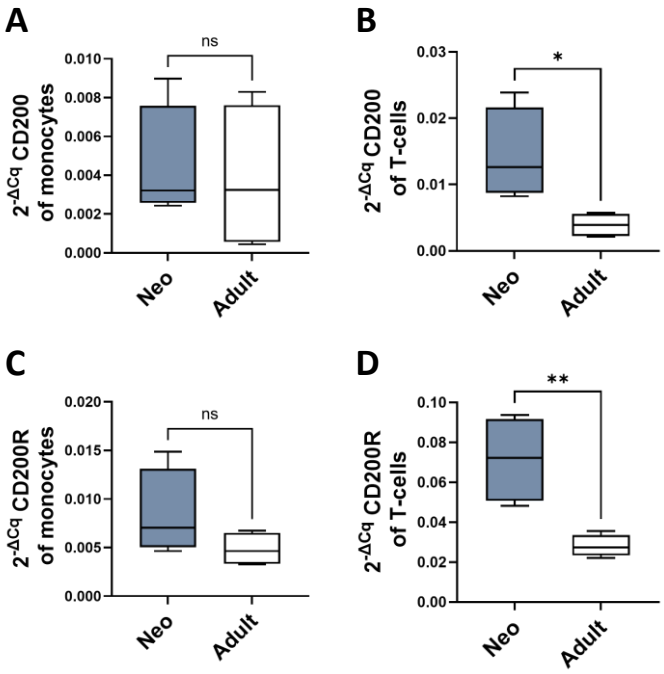

Figure 25. qPCR analysis of CD200 and CD200R mRNA expression on human neonatal and adult monocytes and CD3⁺ T-cells.

To analyze expression of CD200 and CD200R on RNA-level, monocytes and CD3⁺ T-cells were isolated from peripheral blood of adults and cord blood of full-term neonates. RNA was extracted, transcribed into cDNA and the CD200 and CD200R expression on RNA-level was analyzed using qPCR. **A-D** Box graphs show expression of CD200 of monocytes (**A**) and CD3⁺ T-cells (**B**) as well as CD200R of monocytes (**C**) and CD3⁺ T-cells (**D**) of adults (white) and full-term neonates (light blue) in relation to the housekeeping gene (RPS13). n=4, unpaired t-test. p=ns (not significant), *p < 0.05, **p < 0.01.

4.2.3. CD200 expression of adult and neonatal T-cells differs on all T-cell sub-sets

Based on the previous observations of our study, that CD200 expression was significantly increased on full-term neonatal $CD3^+$ T-cells both at the cell surface and RNA-level, we next asked whether this difference stems from a specific T-cell sub-population potentially revealing an important function of CD200 on this sub-type. Therefore, we analyzed CD200 and CD200R cell surface expression on various T-cell sub-populations for full-term neonates and adults. In general, neonates had higher concentrations of mature $CD4^+$ T-cells and naïve $CD4^+$ and $CD8^+$ T-cells compared to adults (not shown). Neonates had lower numbers of mature $CD8^+$, Th1 and Th2 cells in our experiments compared to adults, while γδ-T-cell numbers did not differ (not shown). Except for $CD8^+$ T-cells, we observed significantly higher CD200 expression on all other T-cells sub-populations of neonates compared to adults (including mature and naïve CD4+ T-cells, Th1, Th2 and γδ-T-cells) (**Figure 26**, A, C, E, G and J, Table 14). CD200R expression was significantly lower on neonatal Th1 and Th2 cells compared to adult cells and significantly higher on naïve $CD4^+$ T-cells (**Figure 26**, B, F and H, Table 14). CD200R expression did not differ between neonates and adults on mature and naïve $CD8^+$ T-cells as well as γδ-T-cells, similar to what we observed in $CD3^+$ T-cells before (**Figure 26**, D + K and **Figure 24**, D and **Table 14**). CD200 and CD200R expression on effector memory and central memory T-cells could not be successfully analyzed due to the almost non-existing numbers of these cell types in neonatal cord blood.

Table 14. Percentages of CD200 and CD200R expression of neonatal and adult T-cell sub-populations.

Table shows percentages of CD200 and CD200R expression and p-values of neonatal and adult T-cell sub-sets displayed in **Figure 26**.

	% CD200			% CD200R		
	Neo	**Adult**	**p-value**	**Neo**	**Adult**	**p-value**
$CD4^+$	54.5 ± 2.65	33.27 ± 9.63	0.008	63.03 ± 5.00	59.1 ± 2.72	0.159
naïve $CD4^+$	55.47 ± 2.40	35.38 ± 8.12	0.005	65.4 ± 1.82	60.7 ± 2.83	0.037
$CD8^+$	32.67 ± 13.66	19.26 ± 9.86	0.131	56 ± 16.55	58.47 ± 13.61	0.381
naïve $CD8^+$	26.5 ± 7.80	23.12 ± 6.68	0.518	58.73 ± 14.18	58.48 ± 15.12	0.982
Th1	78.19 ± 5.69	43.48 ± 11.69	< 0.0001	58.93 ± 3.21	66.63 ± 6.00	0.009
Th2	87.66 ± 8.36	40.23 ± 9.90	0.0003	57.61 ± 4.32	75.66 ± 6.31	< 0.0001
γδ-T-cells	64 ± 13.54	38.18 ± 12.93	0.033	79.45 ± 4.97	80.13 ± 4.90	0.853

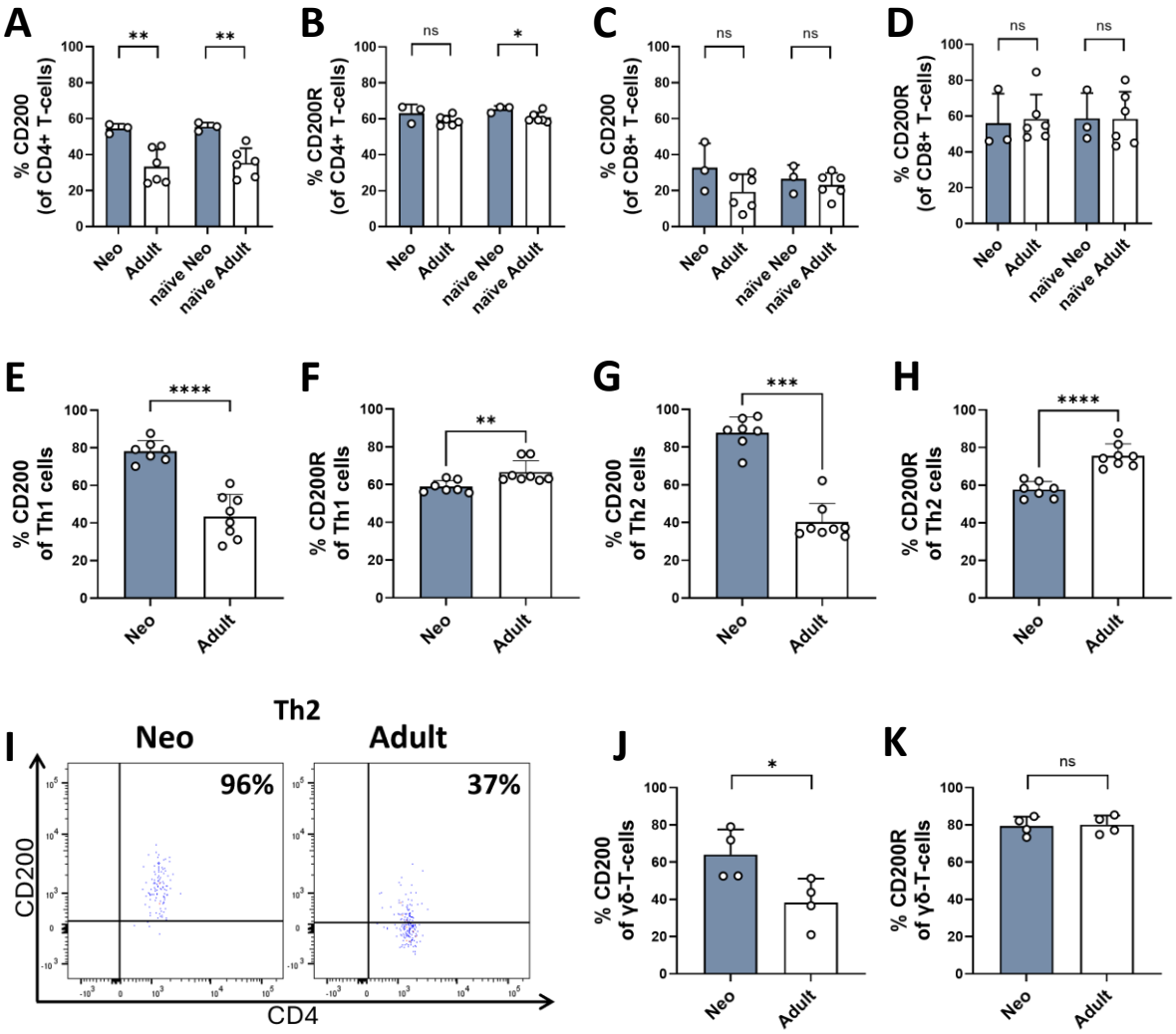

Figure 26. CD200 and CD200R expression on adult and neonatal T-cell sub-populations.

To analyze CD200 and CD200R expression on T-cell sub-populations, PBMCs and CBMCs were isolated from peripheral blood of adults and cord blood of full-term neonates respectively. CD200 and CD200R expression were analyzed using flow cytometry. **A-D** Bar graphs show CD200 (**A+C**) and CD200R (**B+D**) expression on mature and naïve $CD4^+$ (**A+B**) and $CD8^+$ (**C+D**) T-cells for full-term neonates (light blue) and adults (white). Naïve T-cells were defined as $CD45RO^-/CD197^+$. n=3-6, Mann-Whitney and unpaired t-test. **E-I** Bar graphs show CD200 (**E+G**) and CD200R (**F+H**) expression of CD4 T-cell sub-sets Th1 (**E+F**) and Th2 (**G+H**) for full-term neonates (light blue) and adults (white) and **I** shows representative dot plots of CD200 expression on adult and neonatal Th2 cells as an example for CD200 expression on all T-cell sub-sets. Th1 cells were defined as $CD4^+$/CCR4-/$CXCR3^+$/$CCR6^-$ cells and Th2 cells were defined as $CD4^+$/$CCR4^+$/$CXCR3^-$/$CCR6^-$. n=7-8, unpaired t-test, Welsh-t-test and Mann-Whitney test. **J+K** Bar graphs show % of CD200 (**J**) and CD200R (**K**) expression on γδ-T-cells for full-term neonates (light blue) and adults (white). n=4, unpaired t-test and Mann-Whitney test. p=ns (not significant), *p < 0.05, **p < 0.01, ***p < 0.001, ****p < 0.0001.

4.2.4. Blockade of CD200 and/or CD200R does not affect immune response of neonatal and adult monocytes

Overall, we observed higher CD200 expression on neonatal compared to adult T-cells in our experiments. High expression of CD200 on T-cells could lead to increased interaction with other immune cells expressing CD200R like monocytes, impacting their immune response to bacterial stimuli due to the increased anti-inflammatory signaling through the CD200-CD200R pathway. Therefore, we asked if the difference in CD200/CD200R expression on T-cells of neonates and adults would alter cytokine response and regulation of co-stimulatory molecule expression on monocytes. To test this, we isolated PBMCs from adults and CBMCs from full-term neonates, blocked CD200 and/or CD200R expression using anti-CD200 and/or anti-CD200R antibodies and stimulated the cells with *E. coli*.

4.2.4.1. Blockade of CD200 and/or CD200R does not affect cytokine response of neonatal and adult monocytes to *E. coli*

Blockade of CD200, CD200R or both molecules had no effect on cytokine secretion by monocytes of neonates and adults. Shown below are MFIs of four representative cytokines analyzed in this experiment IL-6, TGF- β, IL-2 and IL-4 (**Figure 27**, A-D, **Table 15**). Other cytokines analyzed included IL1-β, IFNγ, TNF-α, IL-17A, and IL-10, that also showed no difference after blockade (not shown). Overall, cytokine expression between untreated (-) neonatal and adult monocytes was similar in our study (**Figure 27**, A-D, **Table 15**).

Table 15. Mean fluorescent intensity of representative graphs for cytokine secretion of neonatal and adult monocytes after CD200 and/or CD200R blockade.

Table shows MFIs of cytokines IL-6, TGF-β, IL-2 and IL-4 of neonatal and adult monocytes left untreated (-), blocked with anti-CD200, anti-CD200R or both antibodies and stimulated with *E. coli* (MOI 10:1) displayed in **Figure 27**.

	IL-6		TGF-β	
	Neo	**Adult**	**Neo**	**Adult**
untreated (-)	3445 ± 4740	2889 ± 3292	626.3 ± 288.8	691 ± 231.6
Anti-CD200	1760 ± 614.5	1949 ± 865.3	662± 216	720.5 ± 219.1
Anti-CD200R	1410 ± 1014	1789 ± 909	588 ± 224.1	704.8 ± 247.5
Anti-CD200+CD200R	2010 ± 1943	1703 ± 898.5	559.3 ± 186.9	684.3 ± 243.6
	IL-2		**IL-4**	
	Neo	**Adult**	**Neo**	**Adult**
untreated (-)	689 ± 391.9	806.8 ± 489.5	226.3 ± 33.6	258.3 ± 117.2
Anti-CD200	688.3 ± 431.8	506 ± 259	245 ± 15	262.7 ± 90.29
Anti-CD200R	678.8 ± 475.3	563.3 ± 205.7	220.7 ± 33.2	280.3 ± 135
Anti-CD200+CD200R	589 ± 341.3	879 ± 642.6	218 ± 32.1	257.7 ± 97.2

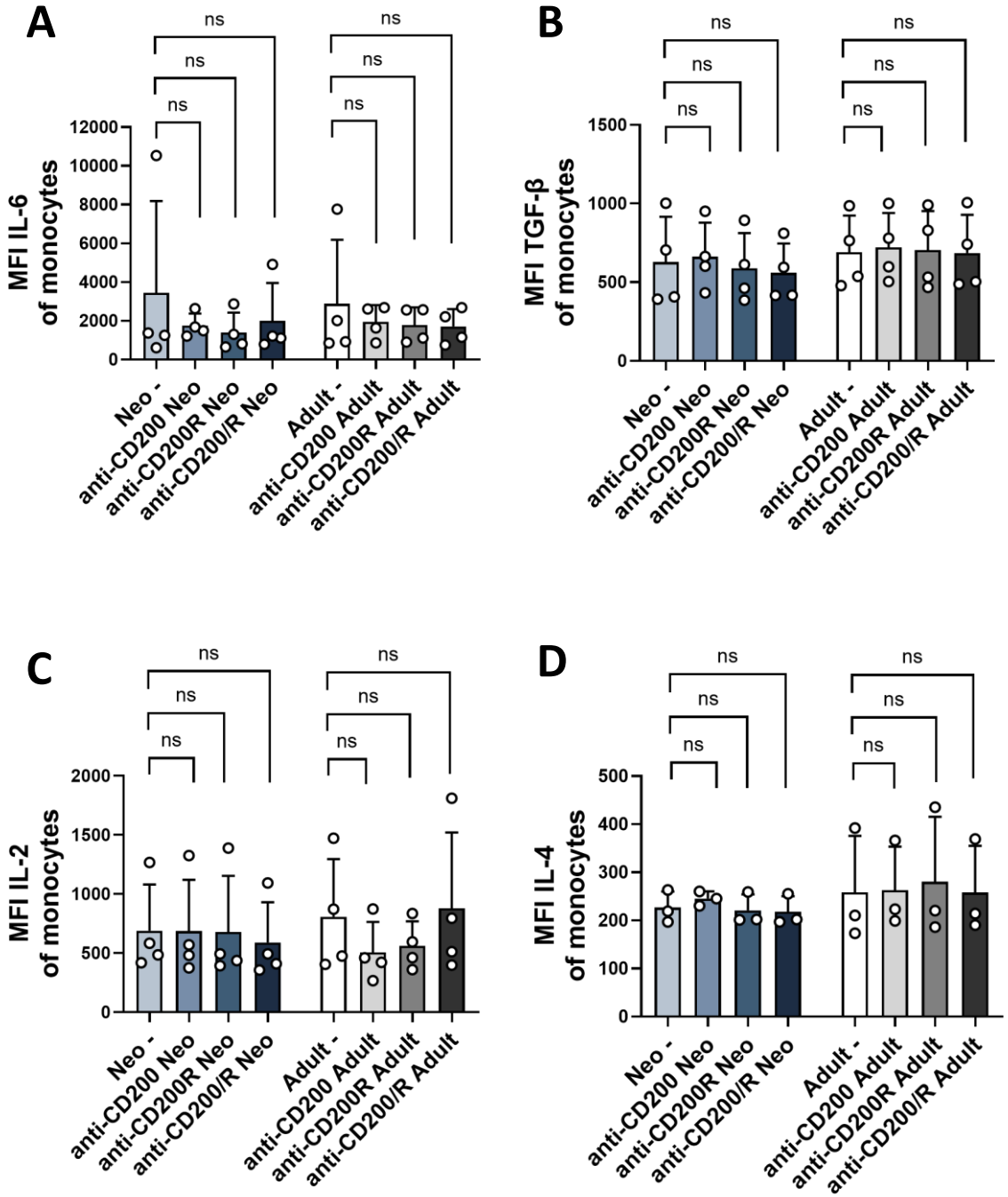

Figure 27. Effect of CD200 and/or CD200R blockade on cytokine secretion of adult and neonatal monocytes.

To assess the effect or blockade of CD200 and/or CD200R signaling on cytokine production of monocytes, PBMCs and CBMCs were isolated from peripheral blood of adults and cord blood of full-term neonates respectively. Cells were blocked with anti-CD200 and/or anti-CD200R antibodies and stimulated with *E. coli* (MOI 10:1) to induce cytokine production of monocytes. **A-D** Bar graphs show Mean fluorescent intensity (MFI) of cytokines IL-6 (**A**), TGF-β (**B**), IL-2 (**C**) and IL-4 (**D**) of monocytes from adults (grey-scale, right) and full-term neonates (blue-scale, left) un-blocked (-), blocked with anti-CD200, anti-CD200R or both (anti-CD200/R) antibodies. n=3-4, Ordinary One-Way ANOVA and Kruskal-Wallis test. p=ns (not significant).

4.2.4.2. Blockade of CD200 and/or CD200R does not affect expression patterns of surface molecules on neonatal and adult monocytes

Immune cell blockade of CD200 and/or CD200 using antibodies followed by stimulation with E. coli did not affect expression of co-stimulatory molecules CD80, CD86, the PAMP receptor TLR4 and the MHC II molecule HLA-DR on neonatal and adult monocytes (**Figure 28**, A-D, **Table 16**). On average, expression of CD80, TLR4 and HLA-DR were slightly higher on untreated adult monocytes compared to neonatal monocytes while expression of CD86 did not differ between groups (**Figure 28**, A-D, **Table 16**).

Table 16. Expression of co-stimulatory molecules on neonatal and adult monocytes after CD200 and/or CD200R blockade.

Table shows % (CD80) and MFIs (CD86, TLR4 and HLA-DR) of neonatal and adult monocytes left untreated (-), blocked with anti-CD200, anti-CD200R or both antibodies and stimulated with *E. coli* (MOI 10:1) displayed in **Figure 28**.

	% CD80		**MFI CD86**	
	Neo	**Adult**	**Neo**	**Adult**
untreated (-)	29.36 ± 16.2	45.33 ± 21.8	3079 ± 1883	3012 ± 1126
Anti-CD200	33.88 ± 20.5	43.98 ± 17.9	3109 ± 2021	2914 ± 1179
Anti-CD200R	32.43 ± 18.3	42.6 ± 19.0	2953 ± 1851	2950 ± 1177
Anti-CD200+CD200R	30.8 ± 19.1	42.35 ± 18.4	3100 ± 2135	2879 ± 1192
	MFI TLR4		**MFI HLA-DR**	
	Neo	**Adult**	**Neo**	**Adult**
untreated (-)	917.3 ± 97.3	1104 ± 265	6549 ± 1664	7624 ± 1868
Anti-CD200	975.3 ± 180.7	1061 ± 272	6360 ± 1720	7206 ± 1433
Anti-CD200R	965 ± 157.2	1027 ± 242.1	6420 ± 2035	7066 ± 794.4
Anti-CD200+CD200R	945.3 ± 165.6	1092 ± 118	6798 ± 1829	6930 ± 1159

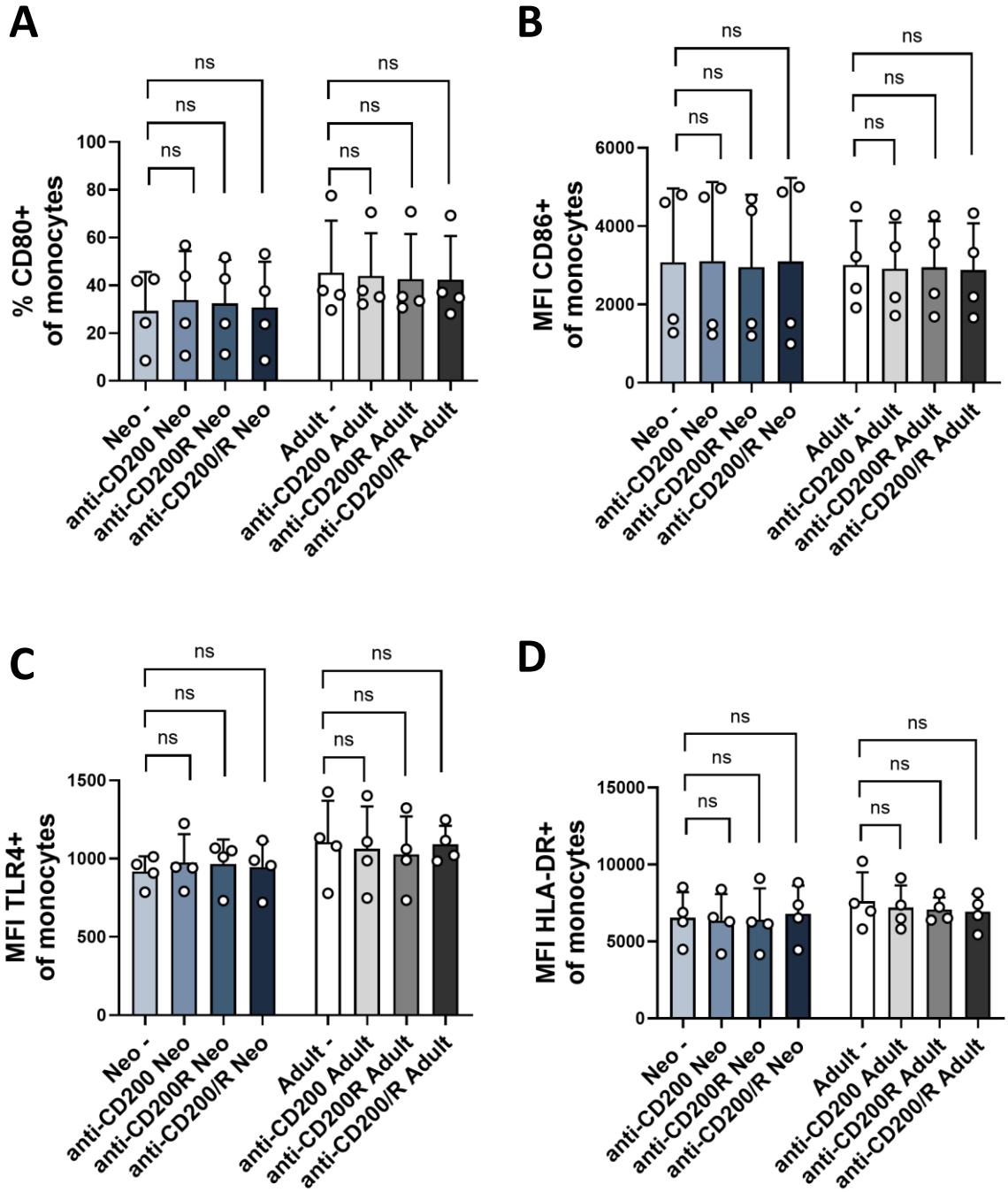

Figure 28. Effect of CD200 and/or CD200R blockade on cell surface molecule expression of adult and neonatal monocytes.

To assess the effect or reduced CD200 and/or CD200R signaling on regulation of cell surface molecule expression of monocytes, PBMCs and CBMCs were isolated from peripheral blood of adults and cord blood of full-term neonates respectively. Cells were blocked with anti-CD200 and/or anti-CD200R antibodies and stimulated with *E. coli* (MOI 10:1) to induce cytokine production of monocytes. A-D Bar graphs show % (A) and Mean fluorescent intensity (MFI) (C-D) of molecules CD80 (A), CD86(B), TLR4 (C) and HLA-DR (D) of monocytes from adults (grey-scale, left) and full-term neonates (blue-scale, right) un-blocked (-), blocked with anti-CD200, anti-CD200R or both (anti-CD200/R) antibodies. n=4, Ordinary One-Way ANOVA and Kruskal-Wallis test. p=ns (not significant).

4.2.5. Adult T-cell proliferation is reduced by CD200 and CD200R blockade while neonatal T-cells are unaffected

To assess whether the differential CD200 expression on adult and neonatal monocytes we observed (**Figure 24**) has an impact on the proliferative capacity of neonatal or adult T-cells, due to due to signaling between monocytes and T-cells, we analyzed T-cell proliferation of adult and neonatal T-cells after blockade of CD200 and/or CD200R with anti-CD200 and/or anti-CD200R antibodies. We observed no significant effect of CD200 and/or CD200R blockade on $CD4^+$ T-cell proliferative capacity in neonates compared to untreated cells (neo- 100% vs. anti-CD200 99.3%, p = 0.99; neo- vs. anti-CD200R 98.1%, p = 0.91; neo- vs. anti-CD200/R 101%, p = 0.99) (**Figure 29**, A). Blockade of CD200 or CD200R individually also did not impact T-cell proliferative capacity of adult $CD4^+$ T-cells (Adult- 100% vs. anti-CD200 94.0%, p = 0.75; Adult- vs. anti-CD200R 88.4%, p = 0.12), while blockade of both CD200 and CD200R at the same time led to significantly reduced $CD4^+$ T-cell proliferation (Adult- 100% vs. anti-CD200/R 81.1%, p = 0.013) (**Figure 29**, A). Analysis of $CD8^+$ T-cell proliferation led to similar results (not shown).

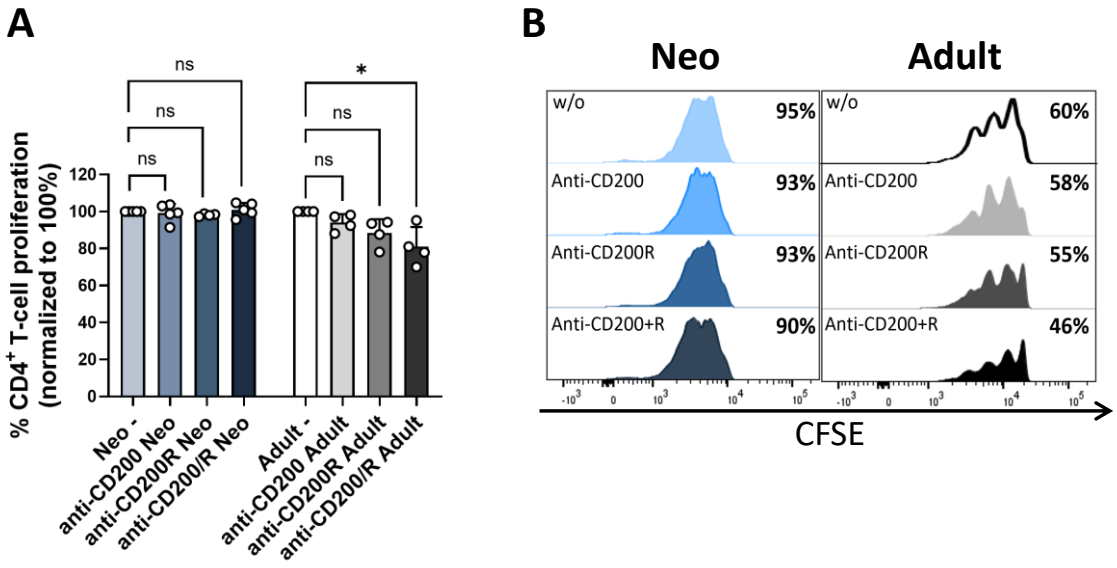

Figure 29. Impact of CD200 or CD200R blockade on $CD4^+$ T-cell proliferation of adults and neonates.

PBMCs of adults and CBMCs of full-term neonates were isolated, and blocked with anti-CD200-antibody, anti-CD200R antibody or both antibodies. T-cell proliferation was induced and measured after 4 days using flow cytometry. **A** Bar graphs show % of $CD4^+$ T-cell proliferation normalized to 100% (stimulated control, unblocked) after blockade with anti-CD200-antibody, anti-CD200R antibody or both antibodies (CD200/R) (left to right) for adults (grey bars, right) and full-term cord blood T-cells (blue bars, left). n=4-5, Ordinary One-way ANOVA and Kruskal-Wallis test. **B** Representative histograms show neonatal and adult $CD4^+$ T-cell proliferations as percentage of stimulated minus unstimulated cells for untreated T-cells (w/o), T-cells blocked with anti-CD200, anti-CD200R or both (anit-CD200 + R) antibodies. p=ns (not significant), *p < 0.05.

4.2.6. CD200 expression differs on human full-term and pre-term neonatal monocytes and $CD3^+$ T-cells

Our analysis of CD200 and CD200R expression on monocytes and T-cells of full-term neonates and adults revealed significant differences in especially the CD200 expression pattern. However, it is known that pre-term neonates are much more susceptible to severe infections like sepsis compared to full-term neonates. Therefore, we asked whether CD200 and/or CD200R expression patterns of full-term and pre-term neonates differ, potentially supporting pre-term neonates' susceptibility to sepsis and severe disease progressions due to different anti-inflammatory signaling. To test this hypothesis, we isolated immune cells from cord blood of full-term neonates and peripheral blood of pre-term neonates and analyzed CD200 and CD200R expression on untreated and *E. coli* stimulated monocytes and $CD3^+$ T-cells. Similarly to what we observed earlier in adults versus full-term neonates, CD200R expression on monocytes of full-term and pre-term neonates did not significantly differ (full-term 74.2 ± 9.22% vs. pre-term 82.1 ± 11.16%, p = 0.053) (**Figure 30**, C). However, we observed significantly higher CD200R expression on T-cells of pre-term compared to full-term neonates (full-term 57.5 ± 8.73% vs. pre-term 65.0 ± 8.12%, p = 0.038) (**Figure 30**, E). We also observed significantly higher CD200 expression on pre-term monocytes compared to full-term neonates (full-term 7.9 ± 6.26% vs. pre-term 33.4 ± 10.30%, p < 0.0001), while CD200 expression on T-cells did not significantly differ between the groups (full-term 49.0 ± 10.78% vs. pre-term 40.6 ± 15.02%, p = 0.124) (**Figure 30**, B + D). Treatment of cells with *E. coli* for 24 hours led to an alignment of CD200 expression on monocytes between groups (full-term 29.7 ± 17.65% vs. pre-term 28.0 ± 18.19%, p = 0.79), while differences in CD200 expression on T-cells (full-term 49.1 ± 14.45% vs. pre-term 46.6 ± 13.1%, p = 0.61) and CD200R expression on monocytes (full-term 87.2 ± 7.63% vs. pre-term 90.3 ± 8.01%, p = 0.28) remained the same (**Figure 30**, J - L). The significantly higher CD200R expression on T-cells of pre-term neonates was even more pronounced after *E. coli* stimulation (full-term 59.7 ± 5.09% vs. pre-term 68.4 ± 9.99%, p = 0.0067) (**Figure 30**, I). To compare differences in CD200 and CD200R up- or down-regulation after *E. coli* stimulation on monocytes and T-cells, we again calculated the ratio of CD200 and CD200R expression between untreated and *E. coli* stimulated cells. Ratios revealed significant upregulation of CD200 on full-term neonatal monocytes compared to pre-term monocytes who slightly downregulated their CD200 expression after *E. coli* contact (full-term 6.4 ± 4.86

vs. pre-term 0.6 ± 0.30 ratio, p = 0.0002) (**Figure 30**, J). On T-cells, full-term neonates downregulated CD200 on average, while pre-term T-cells slightly upregulated CD200 after *E. coli* contact, leading to a significant difference in regulation of CD200 after *E. coli* contact between the two groups (full-term 0.9 ± 0.21 vs. pre-term 1.2 ± 0.25 ratio, p = 0.013) (**Figure 30**, L). CD200R was only marginally upregulated on monocytes of both groups after *E. coli* stimulation with full-term neonates upregulating CD200R significantly higher than pre-term neonates (full-term 1.2 ± 0.13 vs. pre-term 1.1 ± 0.08 ratio, p = 0.0023), while CD200R expression on T-cells did not change after *E. coli* stimulation for both groups (full-term 1.0 ± 0.15 vs. pre-term 1.1 ± 0.13 ratio, p = 0.40) (**Figure 30**, K + M). Due to the small volume of pre-term blood samples, we were able to safely take from these neonates, further analysis of CD200 and CD200R expression on, for example, T-cell sub-populations was not possible so far.

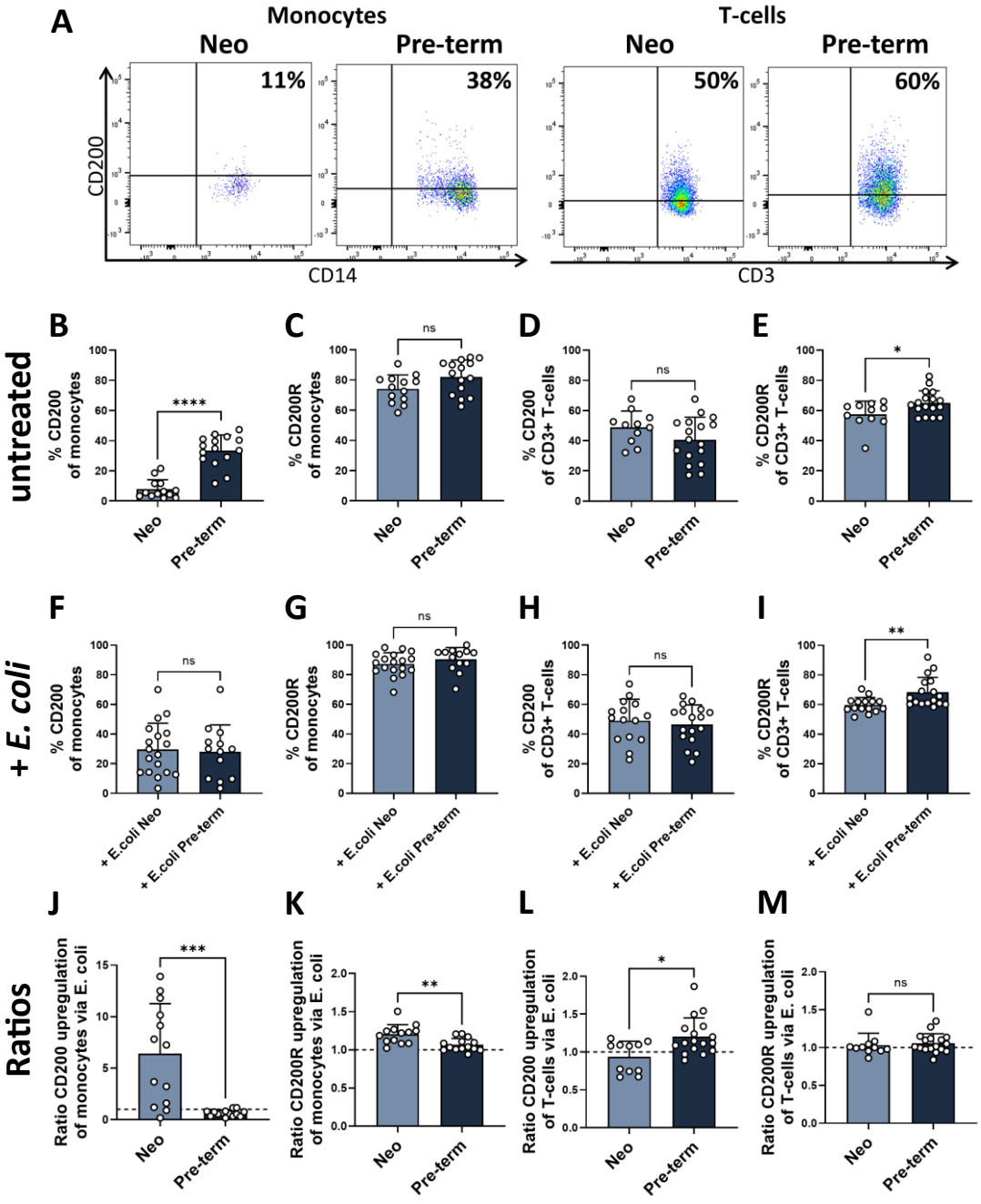

Figure 30. CD200 and CD200R expression on monocytes and T-cells of full-term and pre-term neonates.

To assess baseline CD200 and CD200R expression on human monocytes and T-cells as well as changes after *E. coli* stimulation. PBMCs and CBMCs were isolated from peripheral blood of pre-term neonates and cord blood of full-term neonates. Cells were also stimulated with *E. coli* MOI 10:1 to analyze changes in CD200 and CD200R expression on immune cells during infections. **A** Representative dot plots show CD200 expression of monocytes (left) and $CD3^+$ T-cells (right) for adults and neonates. CD200R expression not shown due to the lack of difference in expression between groups. **B-E** Bar graphs show % of CD200 (**B+D**) and CD200R (**C+E**) baseline expression on monocytes (**B+C**) and $CD3^+$ T-cells (**D+E**) of neonates (light blue) and pre-term neonates (dark blue). n=13-15, unpaired t-test and Mann-Whitney test. **F-I** Bar graphs show % of CD200 (**F+H**) and CD200R (**G+I**) expression after *E. coli* stimulation on monocytes of neonates (light blue) and pre-term neonates (dark blue). n=13-15, unpaired t-test and Mann-Whitney. **J-M** Bar graphs show ratios of CD200 (**J+L**) and CD200R (**K+M**) upregulation after *E. coli* stimulation on monocytes (**J+K**) and T-cells (**L+M**) of neonates (light blue) and pre-term neonates (dark blue). No change in CD200/CD200R expression is indicated with a dotted line (at y=1). n=13-15, unpaired t-test and Mann-Whitney test. p=ns (not significant), *p < 0.05, **p < 0.01, ***p < 0.001, ****p < 0.0001.

4.2.7. Soluble CD200 concentrations are reduced in pre-term neonates

Just like in mice, in humans a functional active soluble form of CD200 (sCD200) has been described (see introduction chapter 1.4.2). Due to its functional implications for induction of CD200R signaling, and the observed differences in CD200 expression on monocytes and T-cells of adults, full-term and pre-term neonates, we aimed to assess if the plasma concentrations of scD200 also differ between these three groups. Therefore, we analyzed plasma from adults, full-term and pre-term neonates for sCD200 using ELISA. Similarly to what we observed at the cell surface level for CD200 expression on monocytes, adults had higher concentrations of sCD200 compared to full-term neonates (adult 1319 ± 3505 to full-term neo 180.9 ± 474.1 pg/ml, p = 0.15). However, this difference was not significant. Compared to adults, sCD200 plasma levels of pre-term neonates were significantly lower (adult 1319 ± 3505 to pre-term 56.0 ± 81.34 pg/ml, p = 0.026). sCD200 plasma levels of pre-term neonates were also lower than those of full-term neonates (full-term neo 180.9 ± 474.1 to pre-term 56.0 ± 81.34 pg/ml, p = 0.156). However, unlike between pre-term neonates and adults, the difference between full-term and pre-term neonates was not significant. (**Figure 31**).

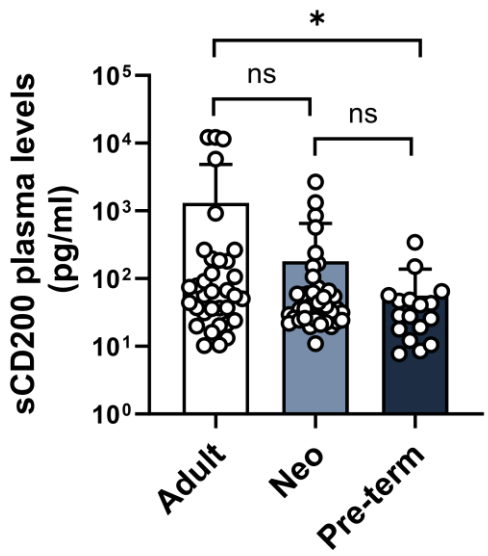

Figure 31. Soluble CD200 levels in plasma of adults, full-term and pre-term neonates.

Plasma was isolated from blood of adults, cord blood of full-term neonates and peripheral blood of pre-term neonates and analyzed for sCD200 levels using ELISA. Bar graph shows plasma concentration of soluble CD200 (sCD200) in pg/ml plasma for adults (white), full-term neonates (Neo, light blue) and pre-term neonates (dark blue). n= 17-40, Kruskal-Wallis test. p=ns (not significant), *p < 0.05.

5. Discussion

Comparison of adult and neonatal murine E. coli sepsis models

Sepsis is a major health concern in adults and especially neonates associated with high mortality rates and its treatment remains challenging. Therefore, many attempts have been made to study sepsis and potential treatments in animal models, with a particular focus on mice. Over the years, many different murine neonatal and adult sepsis models have been developed. Among them, the cecal ligation puncture (CLP) and cecal slurry (CS) methods are the most popular to induce polymicrobial sepsis. In CLP, animals are put under anesthesia to puncture their cecum, resulting in the entry of intestinal contents and bacteria into the abdominal cavity, whereas with the CS method cecal content of a donor mouse is suspended in a solution and intraperitoneally injected into a recipient mouse [151,228–231]. Due to their incomplete intestinal development, small size and the risk of postoperative cannibalism by their mothers, CLP is not the preferred method to induce sepsis in newborn mice [229]. Both CLP and CS models result in symptoms that closely resemble sepsis observed in humans with a gradual increase of sepsis severity and organ damage. Due to the surgical intervention necessary to induce CLP sepsis, this method requires a higher effort than others. Another disadvantage of both CLP and CS methods is the potential variation of sepsis between mice and over the course of a study, due to differences in cecal slurry or cecal content of mice [228]. Another popular way to induce sepsis in mice is the injection of singular pathogens. This method has the advantage of studying the effect of a specific pathogen like GBS or *E. coli* on sepsis progression. This method has been widely used to induce sepsis in both adult and neonatal mice with different injection methods, such as intravenous (i.v.), intraperitoneal (i.p.) or subcutaneous (s.c.) injection [210,228,232–234]. Injection of specific pathogens allows for continuity of sepsis over the course of a study due to the exact injection of the desired concentration of pathogens. However, sepsis can vary depending on bacterial clone, dose, mouse strain and site of injection, which may complicate comparisons between studies [228]. In our experiments, we set out to study *E. coli* induced sepsis, due to it being a leading pathogen of neonatal sepsis. For adult mice we chose the intraperitoneal route, because it is the most commonly used way in the literature [232,235], making our studies comparable to other studies. For neonatal mice, we administered *E. coli* via subcutaneous injection, a method

based on the study of Singh et al. and others [234,236] because, alongside the bacterial injection, additional substances were administered intraperitoneally (rCD200 or anti-CD200 antibodies), and direct interaction with the bacteria was to be avoided. Additionally, i.v. injections in neonatal mice are challenging due to their small size and underdeveloped vascular structures, making this approach less reliable for accurate sepsis induction. In contrast, s.c. injections can be administered with great accuracy in neonatal mice and local subcutaneous infections spread rapidly in neonates, thus providing a reliable approach to induce murine neonatal sepsis [237]. In our study, we observed significant differences between adult and neonatal murine *E. coli* sepsis. These included a ~1500-fold lower *E. coli* dose necessary to induce a LD30 with a body weight only ~15 times lower in neonatal versus adult mice, different timepoints for onset of symptoms and differences in bacterial load of organs. Of note is that we found similar CFU counts in lungs and even higher bacterial load in the blood of neonatal mice, despite the lower relative *E. coli* dose injected. Additionally, we observed drastically higher plasma concentrations of IL-6 and TNF-α in neonatal compared to adult mice after sepsis induction. Similar differences have been observed by others. Mancuso et al. reported a required dose of $5x10^7$ CFU in adult mice and only 60 CFU in neonates to induce a LD90 in a mouse model of GBS sepsis. They also observed a ~100 times higher GBS load in the blood of neonatal mice compared to adults 48h after sepsis induction [233]. The high accumulation of bacteria in the neonatal lung, compared to other organs we observed in our study, has been described before in a GBS sepsis model with neonatal primates, where GBS load in the lung was on average 10- to 100-fold higher than in spleen and liver, and was associated with GBS induced pneumonia in these animals [238]. Other murine sepsis studies also observed the need for reduced bacteria or cecal slurry solutions to induce similar mortality rates in newborn as in adult mice, as well as higher plasma concentrations of IL-6 and TNF-α in neonatal mice, highlighting the increased susceptibility of neonates to develop sepsis and indicating increased levels of inflammation [229,232]. This is consistent with what is observed clinically in neonatology, where reports of the German National Reference Center for Surveillance of Nosocomial Infections (NRZ) show that neonates with a birth weight of 1499 to 499 g have about 4 - 4.5-fold higher device associated sepsis rates compared to adults [9,10].

Phenotypical analysis of murine CD200/CD200R expression reveals differences between adult and neonatal mice at baseline

In our study, we aimed to analyze the role of the ICM CD200 and its receptor CD200R in neonatal sepsis with the question of whether altered expression of this ICM pair might be responsible for the increased susceptibility to infections in neonates and preterm infants. Compared to other ICMs like PD-1 and CTLA-4, CD200 has not been well studied in the context of infections and even less so in neonates. However, there are implications for an important role of CD200/CD200R in regulating immune responses of especially myeloid cells in the context of infections [164,168]. For example, studies reported higher mortality rates in adult CD200 knock-out mice in experimental models of *Neisseria meningitidis* induced sepsis and influenza infection [169,202], suggesting that CD200 dampens inflammation during severe infections, thereby protecting the organism from hyperinflammation.

In our phenotypical analyses, we found overall lower cellular CD200 but higher CD200R expression on myeloid and lymphoid cells of neonatal and young mice. Differences in ICM expression patterns of, for example, PD-1 and CTLA-4 have been reported before, with higher expression levels of these ICMs on $CD4^+$ T-cells of older versus younger mice [161,186,239,240], indicating age dependent regulation of ICMs. In addition, we found significantly elevated levels of soluble CD200 in neonatal mice compared to adult animals, indicating that the CD200/CD200R axis appears overall to be more active in neonates. Interestingly, it has been reported that high levels of CD200 play an important role in maintaining immune tolerance during pregnancy [197,241]. Similar observations have also been reported for the ICM PD-L1, where high levels of soluble PD-L1 have been observed in the blood of pregnant women while decreased PD-L1 expression on, for example, the placenta has been associated with increased fetal rejection in mice and pregnancy complications such as pre-eclampsia in humans [242–244], suggesting an important role of ICMs for maternal-fetal tolerance. The increased activation of the CD200/CD200R axis in newborn mice could therefore be a remnant of pregnancy induced immune adaptations important for fetal survival during pregnancy but on the other hand potentially contribute to increased infection susceptibility in neonates.

We found a significant decrease, especially of CD200R expression on immune cells at P21. The time between P14 and P21 is the time when mice undergo the transition from milk to solid food. This is associated with changes in the intestinal microbiome. Al Nabhani et al. reported the phenomenon of a “weaning reaction” in mice during the transition from milk to solid food, where the expanding microbiota led to a significant immune reaction that reduced the susceptibility to inflammatory pathologies later in life [245]. Based on the observations by Al Nabhani et al., it seems plausible that the changes we observed in the CD200/CD200R expression are also related to diet and/or alterations in the microbiome of growing mice. Further studies, for example in germ-free mice, could provide insights into the mechanisms underlying the changing expression patterns of the CD200/CD200R axis with age.

Impact of E. coli induced sepsis on regulation of CD200 and CD200R expression in mice

We observed no significant difference in the regulation of CD200 on splenic immune cells of adult and newborn mice with *E. coli* sepsis, with the exception of neonatal T-cells who significantly downregulated CD200 during sepsis. The lack of changes in CD200 expression is in line with results of Mukhopadhyay et al. who also found no or small changes in CD200 expression of some murine peritoneal or bone marrow derived macrophage populations after treatment with *Neisseria meningitidis* [202]. In contrast, we observed a significant increase in the expression of CD200R on neonatal monocytes and neutrophils but not adult cells after sepsis induction with *E. coli.* Mukhopadhyay et al. observed a downregulation of CD200R on various elicited murine macrophage populations of adult mice by the gram-negative pathogen *Neisseria meningitides* [202], contrasting our results. One possible explanation for these discrepancies between studies is the known difference in PAMPs and therefore PRR activation between *E. coli* and *Neisseria meningitides*. While *E. coli* derived LPS is a ligand for TLR4, *Neisseria* derived lipoolygosaccharides (LOS) and porin proteins (PorB) bind to TLR4 and TLR2 [246–248]. This dual signaling induced by *Neisseria meningitides* derived PAMPs leads to stronger immune activation and higher pro-inflammatory cytokine secretion compared to *E. coli* induced reactions [249,250]. Regulation of inflammatory signaling cascades have been shown to differ between adults and neonates, altering their immune response to the same stimulus. Ulas et al. showed that neonates had high levels of the alarmins S100A8/A9 who

bind to TLR4 inducing binding to MyD88 and subsequent activation of pathways leading to pro-inflammatory immune responses. Concurrently, TIR-domain adaptor-inducing IFN-β (TRIF) genes (that also interact with TLR4) were silenced and only adapted to the adult phenotype over time, leading to divergence in the TLR4 mediated immune response between neonates and adults [251], which could explain why TLR4 activation, as it occurs during *E. coli* sepsis, affects CD200R expression differently in neonatal compared to adult mice. Upregulation of CD200R in neonatal mice in response to *E. coli* could therefore be a mechanism to increase the anti-inflammatory signaling response thereby preventing hyperinflammation.

Functional implications of CD200 for murine adult and neonatal sepsis

Studies investigating the role of CD200 in adult inflammatory diseases showed that CD200 knock-out mice had a higher mortality rate than wildtype animals in these models, while supplementation of rCD200 in these knock-out mice rescued their survival [169,202], highlighting a beneficial role of CD200 in inflammation in adult mice. In our experiments, administration of rCD200 to neonatal mice before sepsis induction, led to increased mortality, while mortality in adult mice was not affected by administration of rCD200. The distinct reactions of adult and neonatal mice to rCD200 treatment during sepsis could be related to the different levels of CD200R expression with significantly higher CD200R expressed on neonatal immune cells. Our observation that CD200R was further upregulated during *E. coli* sepsis in neonatal and not adult mice, showed that the interaction between receptor and ligand might not be fully saturated with an equal CD200 to CD200R ratio in neonates, and that there was potentially still room for additional CD200 to bind to the CD200R. Further, the fact that adult mice did not respond to *E. coli* sepsis with changes in CD200 and CD200R expression levels compared to neonatal mice, indicates that adult mice might not rely on their CD200R signaling pathway as much as neonatal mice for immune regulation during *E. coli* sepsis. *In vitro* experiments or *in vivo* experiments with sepsis induction by pathogens activating other PRRs than TLR4, such as for example GBS, a Gram-positive pathogen that is recognized by TLR2 receptor or *Neisseria meningitides* could potentially reveal if regulation of CD200 and CD200R

expression on adult immune cells depends on the inflammatory stimulus and if the effect also differs in neonates.

We did not uncover the mechanism by which rCD200 increased the mortality rate in neonatal septic mice, as bacterial load and systemic cytokine secretion were unaffected by rCD200.

CD200 has been reported to play an important role in the regulation of lung homeostasis by binding to the highly expressed CD200R on alveolar macrophages, reducing their activity and preventing lung injury during infections [169,201,252]. Neonatal sepsis is a trigger for the life threatening acute respiratory distress syndrome (ARDS), a lung injury caused by inflammation [253]. Administration of rCD200 in neonatal mice could have led to reduced activation of alveolar macrophages, therefore leading to increased lung injury due to high bacterial load and inflammation in the lung and subsequently the increased mortality observed in our study. Unfortunately, we could not perform histological analyses of the lungs from our experimental animals. This should be done in future experiments to determine whether increased lung failure is responsible for the higher mortality following rCD200 administration.

Unlike in our study, differences in pro-inflammatory cytokine levels were observed in septic adult CD200 knock-out mice who had higher IL-6 plasma levels matching with their increased mortality [202]. Surprisingly, neonatal septic PD-1 knock-out mice, who had reduced sepsis mortality compared to wildtype animals, had higher levels of IL-6 and TNF-α [151,202], suggesting that cytokine levels in murine sepsis models do not always correlate with mortality. Here, a limitation of our study has to be mentioned. Cytokine secretion can change rapidly over time and analysis at a single timepoint, like we did in our study, might lead to overlooking an effect that could have been observed at an earlier or later phase of sepsis. Besides, we analyzed only three (IL-6, TNF-α and CXCL1) out of many possible and commonly analyzed cytokines in sepsis due to the small sample volume that could be obtained from neonatal mice, potentially hiding effects of rCD200 treatment on the secretion of other cytokines such as IL-10 or IL-1β [210,229].

Similar to us, other studies, both in neonatal and adult mice, also found that differences in survival of septic animals does not always lead to variations in bacterial load [151,155,202]. As with the cytokines, analysis of bacterial load at different timepoints after sepsis induction could have potentially revealed an effect that we did not observe since we analyzed only one

timepoint. However, bacterial loads in our studies were comparable to what was observed by others who analyzed bacterial load at different timepoints [229,230,232].

Regarding immune cell composition, we observed no notable variations to controls in immune cell composition in adult and neonatal mice treated with rCD200. However, we focused our analysis on immune cell composition and did not analyze variations in immune cell functions between control and treatments groups like markers of T-cell exhaustion (e.g. PD-1), cell activation (e.g. CD69) or phagocytosis and intracellular killing capabilities of, for example, macrophages. These markers were analyzed in other studies and could reveal an impact of rCD200 treatment on these mice and potential indications for the increased mortality in neonatal rCD200 treated mice [202,229,232,254,255]. Interestingly, we observed a significantly increased number of Tregs in rCD200 treated adult mice compared to controls. A correlation between high CD200 levels and Treg expansion has also been described in human malignancies [192], indicating that administration of additional CD200 into adult mice might have induced Treg expansion during sepsis, a mechanism that could be utilized in the context of other diseases where decreased numbers of Tregs are reported like multiple autoimmune conditions [256].

Further, having observed elevated mortality after CD200 administration, we next blocked CD200 using an anti-CD200 antibody to see whether this might improve sepsis outcome. Similarly to our rCD200 experiments, we observed no impact of CD200 blockade on bacterial load, systemic cytokine secretion of IL-6 and CXCL1 and no notable differences in immune cell composition. These results did not match our assumptions and were in contrast to results from experiments of other groups who blocked PD-1, another anti-inflammatory ICM, and observed improved sepsis rates [151,155]. An important point here is that in our pilot experiments, we only tested one concentration of the anti-CD200 antibody which was based on experiments performed by Snelgrove et al. [169], and adjusted to the weight of neonatal mice. Similarly to us, Snelgrove et al. who used the anti-CD200 antibody to block interaction with CD200R in an influenza model with adult mice, also observed no improved survival [169]. This raises the question of whether the appropriate antibody concentration was used. In addition, we observed differences in the level of CD200R expression between adult and neonatal mice with highly increased CD200R expression on neonatal immune cells that could lead to a need for adjusting the antibody concentration given to neonatal mice. To fully study

the effect of CD200-blockade in neonatal *E. coli* sepsis, a larger number of animals needs to be treated, and different antibody concentrations should be tested [169]. Something that is supported by an interesting observation made by Inoue et al. who found that a high dose of anti-CTLA-4 antibody decreased survival in a CLP sepsis model in mice, while a low anti-CTLA-4 dose increased survival [153], highlighting the need for testing of different antibody concentrations.

Phenotypic analysis of human adult and neonatal CD200 and CD200R expression

In the second part of the project, we analyzed CD200 and CD200R expression on human immune cells. Regarding myeloid cells, we focused on monocytes due to the well reported functions of CD200/CD200R expression in this cell type [168,188,257]. Here, we observed a similar expression pattern of CD200 compared to mice, while human CD200R was highly expressed on adult as well as on neonatal monocytes which differed significantly from our results in mice showing a lower CD200R expression on adult compared to neonatal myeloid cells. On human T-cells we observed significantly higher CD200 expression on neonatal compared to adult T-cells, an effect not seen in murine T-cells. Furthermore, CD200R expression on human T-cells was much higher than on murine T-cells. However, we must note that due to species specific variations, different antibodies were used to analyze immune cells of humans and mice, which could lead to altered baseline expression patterns between humans and mice. Dissimilarities between components of the human and murine immune system have been observed before. One important difference is the composition of blood immune cells. While human blood is rich in neutrophils, murine blood cells are dominated by lymphocytes with lower numbers of neutrophils [258,259]. Furthermore, differences in the expression patterns of molecules other than CD200 and CD200R have been observed between mice and humans, such as low expression of TLR2 on murine peripheral blood lymphocytes but continuously high expression on human leucocytes [259,260]. Additionally, low expression of the B-cell activation marker CD38 on murine germinal center (GC) B-cells and high expression on human GC B-cells and plasma cells [259,261] as well as differential expression of the co-stimulatory molecule CD28 on murine and human $CD4^+$ and $CD8^+$ T-cells [259,262] have been observed. Variations in expression patterns of molecules between humans and

mice may indicate different significances of the molecules for immunoregulation in the two species. Our observation that *E. coli* stimulation barely had any effect on regulating CD200 and CD200R expression on both human adult and neonatal immune cells, similar to what we observed in adult mice with sepsis, while neonatal mice reacted with changes in the CD200/CD200R expression patterns to *E. coli* stimulation, could indicate that CD200/CD200R plays a particular important role in regulating murine neonatal immune responses. On RNA-level we found highly increased levels of CD200 and CD200R on neonatal compared to adult T-cells, while mRNA level of CD200 and CD200R did not significantly differ between adult and neonatal monocytes. When interpreting these results, it must be noted that purity of isolated monocytes for qPCR analysis was much lower than purity of isolated T-cells and results for monocytes should therefore be cautiously interpreted. The increased mRNA levels for CD200R in neonatal compared to adult T-cells were not reflected in the surface expression of CD200R. Such discrepancies have been described before [263] and could be explained, for example, by processing time delays between transcription and translation or due to post-translational processes like targeted degradation of proteins via the ubiquitin-proteasome pathway to remove proteins [264]. However, high mRNA levels of CD200 and CD200R could also indicate that neonates are potentially capable of higher upregulation of their cell surface expression. This could potentially be an important mechanism for suppressing neonatal immune responses and protecting the newborn from hyperinflammation. At the same time, high CD200 expression in neonates could have negative associations as well, as expansion of CD200 expression has been linked to multiple malignant diseases in children and adults [192,194,265], indicating that CD200 induced immunosuppression due to high levels of CD200 could be harmful.

We also found a significantly different expression pattern for sCD200 in humans than in mice. While levels of sCD200 were lower in human neonates than in human adults, the opposite was true in mice. In humans, sCD200 is produced by ectodomain shedding via the metalloproteinase ADAM28. In mice, to our knowledge, the mechanism of sCD200 release has not yet been elucidated [266]. Therefore, it could be speculated that different mechanisms lead to different sCD200 levels in mice and humans.

Functional implications of CD200/CD200R expression on human immune responses

The most striking difference observed between human neonatal and adult immune cells was the significantly higher CD200 expression on neonatal compared to adult $CD3^+$ T-cells. This led us to the analysis of CD200 expression on multiple T-cell sub-populations that differ in number and/or function between adults and neonates. For example, it has been described that newborns have increased numbers of naïve T-cells due to the lack of antigen encounter and a predominance of anti-inflammatory Th2 over pro-inflammatory Th1 immune responses [73,81,267]. In our study, no specific T-cell sub-set could be identified as cause of the high CD200 expression on neonatal $CD3^+$ T-cells, but rather all analyzed T-cell sub-sets (except $CD8^+$) displayed significantly higher CD200 expression in neonates. Our findings agree with results from other studies, who also reported higher CD200 expression on naïve and mature neonatal $CD4^+$ and $CD8^+$ T-cells compared to adult T cells [161,186].

To analyze if the differential expression patterns of CD200 and CD200R between adults and newborns have any functional implications in the context of inflammation, we analyzed different functional aspects of human adult and neonatal monocytes and T-cells. A loss of CD200R signaling has previously been reported to lead to increased activation of myeloid cells [164,168], suggesting that blockade of this pathway followed by cell activation via an inflammatory stimulus should lead to increased secretion of pro-inflammatory cytokines. This phenomenon was observed by Fraser et al. who used anti-CD200 or CD200R antibodies to block their signaling in PBMCs or whole blood cultures and observed increased IL-6 and TNF-α levels in the supernatant after cell activation with phytohemagglutinin (PHA) [268]. However, in our experiments, this effect was not observed, neither in adult nor in neonatal monocytes from PBMC/CBMC cultures blocked with anti-CD200 and/or anti-CD200R followed by *E. coli* stimulation. Contrary to the study of Fraser et al., we analyzed cytokine secretion by monocytes using flow cytometry instead of a supernatant analysis via ELISA. Thus, our analysis did not consider the cytokine secretion of other immune cells potentially leading to different results. Furthermore, we used a different stimulus (*E. coli* instead of PHA) to induce cytokine secretion, which also could lead to a different cytokine response. Another reason for the lack of effects could be that, even though no or weak binding of CD200 to isoforms of CD200R has been reported in previous studies [173,185], there could be an interaction with another CD200R isoform which reverses the effects of CD200R1 blockade.

We also observed no changes in co-stimulatory molecule expression on the cell surface of monocytes from adults and neonates after blockade of CD200 and/or CD200R. We analyzed the surface expression of co-stimulatory molecules four hours after *E. coli* stimulation, potentially leaving not enough time for up- or downregulation to occur. Time series experiments could be useful here in future experiments. For both cytokine and co-stimulatory molecule analysis, it needs to be considered that *in vitro* assays might not accurately reflect the behavior of cells *in vivo.* In another experiment of ours, blocking of CD200 and/or CD200R did not affect cord blood T-cell proliferative capabilities, which aligns with the report of Li et al. who also didn´t observe changes in PBMC $CD4^+$ T-cell proliferation after blockade of CD200R or stimulation with rCD200 [206]. The lack of response from neonatal T-cells in this experiment might indicate that variations in CD200 expression on monocytes between adults and neonates do not impact their signaling capacity to induce proliferation in T-cells.

Due to the fact that pre-term neonates are even more susceptible to sepsis compared to full-term neonates [10,11], we finally compared CD200 and CD200R expression on T-cells and monocytes from neonates born pre-term compared to full-term. Compared to full-term neonates, monocytes and T-cells of pre-term neonates showed slightly higher CD200/CD200R expression levels but a trend towards lower sCD200 plasma concentrations. This again did not match our observations in newborn mice, which can even be considered more similar to pre-term than full-term infants in relation to their developmental stage of organs, such as the lungs and the intestine [269,270]. A limitation is that pre-term infants are a very heterogenous study population, where several factors other than gestational age like birth mode, perinatal infections and maternal inflammatory diseases such as preeclampsia can influence immunity [271–274]. Another limitation is that we used cord blood for analysis of CD200 and CD200R expression on immune cells of term-born infants, while for analysis of CD200 and CD200R expression on pre-term and adult immune cells we used peripheral blood. There are studies showing that cord blood cells react differently than peripheral immune cells, so it cannot be ruled out that our observations can be explained solely by the difference in immune cell sources [275,276].

5.1. Outlook

Taken together, we found significant differences in CD200 and CD200R expression patterns as well as sCD200 plasma concentrations between adult and newborn mice, with newborn mice overall expressing lower levels of CD200 but higher levels of CD200R on their immune cells and exhibiting significantly higher sCD200 levels compared to adult mice. After sepsis induction with *E. coli* neonatal myeloid immune cells upregulated CD200R expression while adult cells did not. We observed a significant impact of rCD200 on neonatal but not adult sepsis mortality, highlighting the CD200/CD200R axis as a potential target for pharmaceutical interventions to improve neonatal sepsis outcome. However, we were unable to replicate the phenotypic effects observed in mice in human immune cells. This leads us to the conclusion that mice might not be the ideal model organism to study the effect of the CD200/CD200R axis on human neonatal sepsis. Further studies should include a detailed expression analysis of cells other than immune cells both in mice and in humans. Even though the different expression patterns of CD200 and CD200R on circulating immune cells make pathogenesis in a systemic disease, such as neonatal sepsis, probably incomparable between mice and humans, it could be possible that pathogenetic mechanisms are similar in newborn mice and humans in individual organs. For example, CD200 and CD200R have been shown to be involved in regulating the brain's immune homeostasis due to their expression on neurons and microglia cells [164,168,277] and its interaction has been shown to have a protective effect on neuroinflammation after ischemic stroke and in neurological diseases including Parkinson's and Alzheimer's [278–280]. CD200 and CD200R signaling could therefore play a role in the neonates' susceptibility to post-inflammatory brain damage, an interesting connection that needs to be studied further. Additionally, the role of CD200 and CD200R signaling in regulating lung immune homeostasis [169,201,252] could be an interesting target for future studies in relation to prevention or treatment of sepsis induced ARDS [253].

The work of this study helps to give a better understanding on cell surface expression and potential functional implications of the ICM CD200 and CD200R during homeostasis and inflammation in adults and neonates both in humans and mice. However, much remains to be uncovered, and further studies will be needed to determine if manipulation of CD200 /CD200R signaling can be used to support treatments of inflammatory diseases in newborns.

6. References

1. Bryce J et al. (2005). WHO estimates of the causes of death in children". *The Lancet*, 365:1147–52.
2. Fleischmann-Struzek C et al. (2018). The global burden of paediatric and neonatal sepsis: a systematic review.
3. Zaidi AKM et al. (2011). Effect of case management on neonatal mortality due to sepsis and pneumonia". *BMC Public Health*, 11:S13.
4. Barton L et al. (1999). Causes of death in the extremely low birth weight infant". *Pediatrics*, 103:446–51.
5. Boghossian NS et al. (2013). Late-onset sepsis in very low birth weight infants from singleton and multiple-gestation births". *The Journal of Pediatrics*, 162:1120–4.
6. Tsai M-H et al. (2014). Incidence, clinical characteristics and risk factors for adverse outcome in neonates with late-onset sepsis". *The Pediatric Infectious Disease Journal*, 33:e7–13.
7. Hammoud MS et al. (2012). Incidence, aetiology and resistance of late-onset neonatal sepsis: A five-year prospective study". *Journal of Paediatrics and Child Health*, 48:604–9.
8. Dong Y & Speer CP. (2015). Late-onset neonatal sepsis:Recent developments. vol. 100. BMJ Publishing Group. F257–63. https://doi.org/10.1136/archdischild-2014-306213.
9. NRZ. (2025). Infektionssurveillance im Modul ITS-KISS, internistisch.
10. NRZ. (2025). Infektionssurveillance im Modul NEO-KISS.
11. NRZ. (2025). Infektionssurveillance im Modul ITS-KISS, pädiatrisch.
12. Singer M et al. (2016). The third international consensus definitions for sepsis and septic shock (Sepsis-3)". *Jama*, 315:801–10.
13. Kim F et al. (2020). Neonatal sepsis". *Bmj*, 371.
14. Shane AL et al. (2017). Neonatal sepsis. vol. 390. Lancet Publishing Group. 1770–80. https://doi.org/10.1016/S0140-6736(17)31002-4.
15. Celik IH et al. (2022). Diagnosis of neonatal sepsis: the past, present and future". *Pediatric Research*, 91:337–50.
16. Köstlin-Gille N et al. (2021). Epidemiology of Early and Late Onset Neonatal Sepsis in Very Low Birthweight Infants: Data from the German Neonatal Network". *Pediatric Infectious Disease Journal*, 40:255–9. https://doi.org/10.1097/INF.0000000000002976.
17. Shah BA & Padbury JF. (2014). Neonatal sepsis an old problem with new insights. vol. 5. Taylor and Francis Inc. 170–8. https://doi.org/10.4161/viru.26906.
18. Tsai C-H et al. (2012). Characteristics of early-onset neonatal sepsis caused by Escherichia coli". *Taiwanese Journal of Obstetrics and Gynecology*, 51:26–30.

19. Shane AL & Stoll BJ. (2014). Neonatal sepsis: Progress towards improved outcomes". *Journal of Infection*, 68. https://doi.org/10.1016/j.jinf.2013.09.011.

20. Wynn JL & Wong HR. (2016). Pathophysiology of neonatal sepsis". *Fetal and Neonatal Physiology*,:1536.

21. Salimi U et al. (2022). Postnatal sepsis and bronchopulmonary dysplasia in premature infants: mechanistic insights into “new BPD”". *American Journal of Respiratory Cell and Molecular Biology*, 66:137–45.

22. Samuels N et al. (2017). Risk factors for necrotizing enterocolitis in neonates: a systematic review of prognostic studies". *BMC Pediatrics*, 17:105.

23. Strunk T et al. (2014). Infection-induced inflammation and cerebral injury in preterm infants". *The Lancet Infectious Diseases*, 14:751–62. https://doi.org/https://doi.org/10.1016/S1473-3099(14)70710-8.

24. Baker P et al. (2023). Skin barrier function: the interplay of physical, chemical, and immunologic properties". *Cells*, 12:2745.

25. Şenel S. (2021). An overview of physical, microbiological and immune barriers of oral mucosa". *International Journal of Molecular Sciences*, 22:7821.

26. Murphy K & Weaver C. (2016). Janeway’s Immunobiology. 9th edition. Garland Science-Taylor & Francis Group.

27. Turvey SE & Broide DH. (2010). Innate immunity". *Journal of Allergy and Clinical Immunology*, 125:S24–32.

28. Mukhopadhyay S et al. (2004). The potential for Toll-like receptors to collaborate with other innate immune receptors". *Immunology*, 112:521–30.

29. Taylor PR et al. (2005). Macrophage receptors and immune recognition". *Annu Rev Immunol*, 23:901–44.

30. Jutras I & Desjardins M. (2005). Phagocytosis: at the crossroads of innate and adaptive immunity". *Annu Rev Cell Dev Biol*, 21:511–27.

31. Tosi MF. (2005). Innate immune responses to infection". *Journal of Allergy and Clinical Immunology*, 116:241–9.

32. Murray JS et al. (1989). MHC control of CD4+ T cell subset activation.". *The Journal of Experimental Medicine*, 170:2135–40.

33. Bonilla FA & Oettgen HC. (2010). Adaptive immunity". *Journal of Allergy and Clinical Immunology*, 125:S33–40.

34. Santana MA & Rosenstein Y. (2003). What it takes to become an effector T cell: the process, the cells involved, and the mechanisms". *Journal of Cellular Physiology*, 195:392–401.

35. Kallies A. (2008). Distinct regulation of effector and memory T-cell differentiation". *Immunology and Cell Biology*, 86:325–32.

36. McHeyzer-Williams LJ & McHeyzer-Williams MG. (2005). Antigen-specific memory B cell development". *Annu Rev Immunol*, 23:487–513.

37. Headland SE & Norling L V. (2015). The resolution of inflammation: Principles and challenges. Semin Immunol, vol. 27, Elsevier, p. 149–60.

38. Köstlin N et al. (2014). Granulocytic myeloid derived suppressor cells expand in human pregnancy and modulate T-cell responses". *European Journal of Immunology*, 44:2582–91. https://doi.org/10.1002/eji.201344200.

39. Köstlin N et al. (2016). Granulocytic Myeloid-Derived Suppressor Cells Accumulate in Human Placenta and Polarize toward a Th2 Phenotype". *The Journal of Immunology*, 196:1132–45. https://doi.org/10.4049/jimmunol.1500340.

40. Köstlin N et al. (2017). HLA-G promotes myeloid-derived suppressor cell accumulation and suppressive activity during human pregnancy through engagement of the receptor ILT4". *European Journal of Immunology*, 47:374–84. https://doi.org/10.1002/eji.201646564.

41. Dietz S et al. (2019). Cord blood granulocytic myeloid-derived suppressor cells impair monocyte T cell stimulatory capacity and response to bacterial stimulation". *Pediatric Research*, 86:608–15. https://doi.org/10.1038/s41390-019-0504-7.

42. Köstlin-Gille N et al. (2019). HIF-1α-deficiency in myeloid cells leads to a disturbed accumulation of myeloid derived suppressor cells (MDSC) during pregnancy and to an increased abortion rate in mice". *Frontiers in Immunology*, 10. https://doi.org/10.3389/fimmu.2019.00161.

43. Tollin M et al. (2005). Vernix caseosa as a multi-component defence system based on polypeptides, lipids and their interactions". *Cellular and Molecular Life Sciences CMLS*, 62:2390–9.

44. Adkins B. (2007). Heterogeneity in the CD4 T cell compartment and the variability of neonatal immune responsiveness". *Current Immunology Reviews*, 3:151–9.

45. Dowling DJ & Levy O. (2014). Ontogeny of early life immunity. vol. 35. Elsevier Ltd. 299–310. https://doi.org/10.1016/j.it.2014.04.007.

46. Salzman NH. (2014). The role of the microbiome in immune cell development". *Annals of Allergy, Asthma & Immunology*, 113:593–8. https://doi.org/https://doi.org/10.1016/j.anai.2014.08.020.

47. Kollmann TR et al. (2017). Protecting the Newborn and Young Infant from Infectious Diseases: Lessons from Immune Ontogeny. vol. 46. Cell Press. 350–63. https://doi.org/10.1016/j.immuni.2017.03.009.

48. Kumar SKM & Bhat BV. (2016). Distinct mechanisms of the newborn innate immunity. vol. 173. Elsevier B.V. 42–54. https://doi.org/10.1016/j.imlet.2016.03.009.

49. Canaday DH et al. (2006). Class II MHC antigen presentation defect in neonatal monocytes is not correlated with decreased MHC-II expression". *Cellular Immunology*, 243:96–106.

50. Nguyen M et al. (2010). Acquisition of Adult-Like TLR4 and TLR9 Responses during the First Year of Life". *PLOS ONE*, 5:e10407-.

51. Tsafaras GP et al. (2020). Advantages and Limitations of the Neonatal Immune System. vol. 8. Frontiers Media S.A. https://doi.org/10.3389/fped.2020.00005.

52. De Wit D et al. (2003). Impaired responses to toll-like receptor 4 and toll-like receptor 3 ligands in human cord blood. J Autoimmun, vol. 21, Academic Press, p. 277–81. https://doi.org/10.1016/j.jaut.2003.08.003.

53. Hunt DWC et al. (1994). Studies of Human Cord Blood Dendritic Cells: Evidence for Functional Immaturity.

54. Borràs FE et al. (2001). Identification of both myeloid CD11c+ and lymphoid CD11c− dendritic cell subsets in cord blood". *British Journal of Haematology*, 113:925–31.

55. De Vries E et al. (2000). Neonatal blood lymphocyte subpopulations: a different perspective when using absolute counts". *Neonatology*, 77:230–5.

56. Dalle J-H et al. (2005). Characterization of cord blood natural killer cells: implications for transplantation and neonatal infections". *Pediatric Research*, 57:649–55.

57. Guilmot A et al. (2011). Natural killer cell responses to infections in early life". *Journal of Innate Immunity*, 3:280–8.

58. Yost CC et al. (2009). Impaired neutrophil extracellular trap (NET) formation: A novel innate immune deficiency of human neonates". *Blood*, 113:6419–27. https://doi.org/10.1182/blood-2008-07-171629.

59. Filias A et al. (2011). Phagocytic ability of neutrophils and monocytes in neonates". *BMC Pediatrics*, 11:29.

60. Miller ME. (1979). Phagocyte Function in the Neonate: Selected Aspects". *Pediatrics*, 64:709–12. https://doi.org/10.1542/peds.64.5.709.

61. Köstlin-Gille N & Gille C. (2020). Myeloid-Derived Suppressor Cells in Pregnancy and the Neonatal Period. vol. 11. Frontiers Media S.A. https://doi.org/10.3389/fimmu.2020.584712.

62. Schwarz J et al. (2018). Granulocytic myeloid-derived suppressor cells (GR-MDSC) accumulate in cord blood of preterm infants and remain elevated during the neonatal period". *Clinical and Experimental Immunology*, 191:328–37. https://doi.org/10.1111/cei.13059.

63. Köstlin N et al. (2017). Granulocytic myeloid-derived suppressor cells from human cord blood modulate T-helper cell response towards an anti-inflammatory phenotype". *Immunology*, 152:89–101. https://doi.org/10.1111/imm.12751.

64. Moynagh PN. (2005). TLR signalling and activation of IRFs: revisiting old friends from the NF-κB pathway". *Trends in Immunology*, 26:469–76.

65. Takeda K. (2005). Toll-like receptors and their adaptors in innate immunity". *Current Medicinal Chemistry-Anti-Inflammatory & Anti-Allergy Agents*, 4:3–11.

66. Levy O et al. (2004). Selective Impairment of TLR-Mediated Innate Immunity in Human Newborns: Neonatal Blood Plasma Reduces Monocyte TNF-Induction by Bacterial Lipopeptides, Lipopolysaccharide, and Imiquimod, but Preserves the Response to R-8481.

67. Yan SR et al. (2004). Role of MyD88 in diminished tumor necrosis factor alpha production by newborn mononuclear cells in response to lipopolysaccharide". *Infection and Immunity*, 72:1223–9.

68. Angelone DF et al. (2006). Innate immunity of the human newborn is polarized toward a high ratio of IL-6/TNF-α production in vitro and in vivo". *Pediatric Research*, 60:205–9. https://doi.org/10.1203/01.pdr.0000228319.10481.ea.

69. Sadeghi K et al. (2007). Immaturity of Infection Control in Preterm and Term Newborns Is Associated with Impaired Toll-Like Receptor Signaling. vol. 195.

70. Han P & Hodge G. (1999). Intracellular cytokine production and cytokine receptor interaction of cord mononuclear cells: Relevance to cord blood transplantation". *British Journal of Haematology*, 107:450–7. https://doi.org/10.1046/j.1365-2141.1999.01696.x.

71. Chelvarajan RL et al. (2004). Defective macrophage function in neonates and its impact on unresponsiveness of neonates to polysaccharide antigens". *Journal of Leukocyte Biology*, 75:982–94. https://doi.org/10.1189/jlb.0403179.

72. Khaertynov KS et al. (2017). Comparative assessment of cytokine pattern in early and late onset of neonatal sepsis". *Journal of Immunology Research*, 2017:8601063.

73. Wilson CB & Lewis DB. (1990). Basis and Implications of Selectively Diminished Cytokine Production in Neonatal Susceptibility to Infection". *Reviews of Infectious Diseases*, 12:S410–20. https://doi.org/10.1093/clinids/12.Supplement_4.S410.

74. Clapp DW. (2006). Developmental regulation of the immune system. Semin Perinatol, vol. 30, Elsevier, p. 69–72.

75. Krampera M et al. (2000). Intracellular cytokine profile of cord blood T-, and NK-cells and monocytes". *Haematologica*, 85:675–9.

76. Lau AS et al. (1996). Interleukin-12 Induces Interferon-γ Expression and Natural Killer Cytotoxicity in Cord Blood Mononuclear Cells". *Pediatric Research*, 39:150–5. https://doi.org/10.1203/00006450-199601000-00023.

77. Piccinni MP et al. (1995). Progesterone favors the development of human T helper cells producing Th2-type cytokines and promotes both IL-4 production and membrane CD30 expression in established Th1 cell clones". *The Journal of Immunology*, 155:128–33. https://doi.org/10.4049/jimmunol.155.1.128.

78. Hilkens CMU et al. (1995). Differential modulation of T helper type 1 (Th1) and T helper type 2 (Th2) cytokine secretion by prostaglandin E2 critically depends on interleukin-2". *European Journal of Immunology*, 25:59–63. https://doi.org/https://doi.org/10.1002/eji.1830250112.

79. Wilson CB et al. (1986). Decreased production of interferon-gamma by human neonatal cells. Intrinsic and regulatory deficiencies.". *The Journal of Clinical Investigation*, 77:860–7.

80. Maródi L et al. (1994). Candidacidal mechanisms in the human neonate. Impaired IFN-gamma activation of macrophages in newborn infants.". *The Journal of Immunology*, 153:5643–9. https://doi.org/10.4049/jimmunol.153.12.5643.

81. Adkins B et al. (2000). Exclusive Th2 Primary Effector Function in Spleens but Mixed Th1/Th2 Function in Lymph Nodes of Murine Neonates 1. vol. 164.

82. Ndure J & Flanagan KL. (2014). Targeting regulatory T cells to improve vaccine immunogenicity in early life". *Frontiers in Microbiology*, 5:477.

83. Kollmann TR et al. (2009). Neonatal Innate TLR-Mediated Responses Are Distinct from Those of Adults". *The Journal of Immunology*, 183:7150–60. https://doi.org/10.4049/jimmunol.0901481.

84. Andrade EB et al. (2013). TLR2-Induced IL-10 Production Impairs Neutrophil Recruitment to Infected Tissues during Neonatal Bacterial Sepsis". *The Journal of Immunology*, 191:4759–68. https://doi.org/10.4049/jimmunol.1301752.

85. Gille C et al. (2013). The CD95/CD95L pathway is involved in phagocytosis-induced cell death of monocytes and may account for sustained inflammation in neonates". *Pediatric Research*, 73:402–8.

86. Humberg A et al. (2020). Preterm birth and sustained inflammation: consequences for the neonate. Semin Immunopathol, vol. 42, Springer, p. 451–68.

87. Allgaier B et al. (1998). Spontaneous and Fas-mediated apoptosis are diminished in umbilical cord blood neutrophils compared with adult neutrophils". *Journal of Leukocyte Biology*, 64:331–6. https://doi.org/10.1002/jlb.64.3.331.

88. Koenig JM et al. (2005). Neonatal neutrophils with prolonged survival exhibit enhanced inflammatory and cytotoxic responsiveness". *Pediatric Research*, 57:424–9. https://doi.org/10.1203/01.PDR.0000153945.49022.96.

89. Song C et al. (2011). Human Neonatal Neutrophils Are Resistant to Apoptosis with Lower Caspase-3 Activity". *The Tohoku Journal of Experimental Medicine*, 225:59–63. https://doi.org/10.1620/tjem.225.59.

90. Hotchkiss RS & Karl IE. (2003). The pathophysiology and treatment of sepsis". *New England Journal of Medicine*, 348:138–50.

91. Mayr FB et al. (2014). Epidemiology of severe sepsis". *Virulence*, 5:4–11.

92. van der Poll T et al. (2017). The immunopathology of sepsis and potential therapeutic targets". *Nature Reviews Immunology*, 17:407–20.

93. Monneret G et al. (2004). The anti-inflammatory response dominates after septic shock: association of low monocyte HLA-DR expression and high interleukin-10 concentration". *Immunology Letters*, 95:193–8.

94. Tamayo E et al. (2011). Pro-and anti-inflammatory responses are regulated simultaneously from the first moments of septic shock". *Eur Cytokine Netw*, 22:82–7.

95. Munoz C et al. (1991). Dysregulation of in vitro cytokine production by monocytes during sepsis.". *The Journal of Clinical Investigation*, 88:1747–54.

96. Hotchkiss RS et al. (2013). Sepsis-induced immunosuppression: From cellular dysfunctions to immunotherapy. vol. 13. 862–74. https://doi.org/10.1038/nri3552.

97. Boomer JS et al. (2011). Immunosuppression in patients who die of sepsis and multiple organ failure". *Jama*, 306:2594–605.

98. Hotchkiss RS et al. (1999). Apoptotic cell death in patients with sepsis, shock, and multiple organ dysfunction". *Critical Care Medicine*, 27:1230–51.

99. Hotchkiss RS et al. (2001). Sepsis-induced apoptosis causes progressive profound depletion of B and CD4+ T lymphocytes in humans". *The Journal of Immunology*, 166:6952–63.

100. Hotchkiss RS et al. (2002). Depletion of dendritic cells, but not macrophages, in patients with sepsis". *The Journal of Immunology*, 168:2493–500.

101. Andreu-Ballester JC et al. (2013). Association of γδ T cells with disease severity and mortality in septic patients". *Clinical and Vaccine Immunology*, 20:738–46.

102. Guisset O et al. (2007). Decrease in circulating dendritic cells predicts fatal outcome in septic shock". *Intensive Care Medicine*, 33:148–52.

103. Monneret G et al. (2003). Marked elevation of human circulating CD4+ CD25+ regulatory T cells in sepsis-induced immunoparalysis". *Critical Care Medicine*, 31:2068–71.

104. Hotchkiss RS et al. (2013). Immunosuppression in sepsis: a novel understanding of the disorder and a new therapeutic approach". *The Lancet Infectious Diseases*, 13:260–8.

105. Venet F et al. (2008). Regulatory T cell populations in sepsis and trauma". *Journal of Leukocyte Biology*, 83:523–35. https://doi.org/10.1189/jlb.0607371.

106. Wan YY. (2010). Regulatory T cells: immune suppression and beyond". *Cellular & Molecular Immunology*, 7:204–10.

107. Uhel F et al. (2017). Early expansion of circulating granulocytic myeloid-derived suppressor cells predicts development of nosocomial infections in patients with sepsis". *American Journal of Respiratory and Critical Care Medicine*, 196:315–27.

108. Hamers L et al. (2015). Sepsis-induced immunoparalysis: mechanisms, markers, and treatment options". *Minerva Anestesiol*, 81:426–39.

109. George RL et al. (2003). The association between gender and mortality among trauma patients as modified by age". *Journal of Trauma and Acute Care Surgery*, 54:464–71.

110. Xu J et al. (2019). Association of Sex with Clinical Outcome in Critically Ill Sepsis Patients: A Retrospective Analysis of the Large Clinical Database MIMIC-III". *Shock*, 52:146–51. https://doi.org/10.1097/SHK.0000000000001253.

111. Frink M et al. (2007). Influence of sex and age on mods and cytokines after multiple injuries". *Shock*, 27:151–6.

112. Zellweger R et al. (1997). Females in proestrus state maintain splenic immune functions and tolerate sepsis better than males". *Critical Care Medicine*, 25:106–10.

113. Das A et al. (2024). Identifying immune signatures of sepsis to increase diagnostic accuracy in very preterm babies". *Nature Communications*, 15. https://doi.org/10.1038/s41467-023-44387-5.

114. Fotopoulos S et al. (1999). The monocyte HLA-DR expression of healthy and infected premature neonates". *Pediatric Research*, 45:763.

115. Gervassi AL & Horton H. (2014). Is infant immunity actively suppressed or immature?". *Virology: Research and Treatment*, 5:VRT-S12248.

116. Pagel J et al. (2016). Regulatory T cell frequencies are increased in preterm infants with clinical early-onset sepsis". *Clinical and Experimental Immunology*, 185:219–27. https://doi.org/10.1111/cei.12810.

117. Iroh Tam P-Y & Bendel CM. (2017). Diagnostics for neonatal sepsis: current approaches and future directions". *Pediatric Research*, 82:574–83.

118. Sharma D et al. (2018). Biomarkers for diagnosis of neonatal sepsis: a literature review". *The Journal of Maternal-Fetal & Neonatal Medicine*, 31:1646–59.

119. Christensen RD & Rothstein G. (1980). Exhaustion of mature marrow neutrophils in neonates with sepsis". *The Journal of Pediatrics*, 96:316–8. https://doi.org/https://doi.org/10.1016/S0022-3476(80)80837-7.

120. Scumpia PO et al. (2005). CD11c+ Dendritic Cells Are Required for Survival in Murine Polymicrobial Sepsis". *The Journal of Immunology*, 175:3282–6. https://doi.org/10.4049/jimmunol.175.5.3282.

121. Gille C et al. (2009). Phagocytosis and postphagocytic reaction of cord blood and adult blood monocyte after infection with green fluorescent protein-labeled Escherichia coli and group B Streptococci". *Cytometry Part B: Clinical Cytometry: The Journal of the International Society for Analytical Cytology*, 76:271–84.

122. Khaertynov KS et al. (2017). Comparative assessment of cytokine pattern in early and late onset of neonatal sepsis". *Journal of Immunology Research*, 2017:8601063.

123. Rittirsch D et al. (2008). Harmful molecular mechanisms in sepsis. vol. 8. 776–87. https://doi.org/10.1038/nri2402.

124. Segura-Cervantes E et al. (2016). Inflammatory response in preterm and very preterm newborns with sepsis". *Mediators of Inflammation*, 2016:6740827.

125. Silveira-Lessa AL et al. (2016). TLR expression, phagocytosis and oxidative burst in healthy and septic newborns in response to Gram-negative and Gram-positive rods". *Human Immunology*, 77:972–80.

126. Zhao J et al. (2008). Hyper innate responses in neonates lead to increased morbidity and mortality after infection". *Proceedings of the National Academy of Sciences*, 105:7528–33.

127. Savva A & Roger T. (2013). Targeting toll-like receptors: promising therapeutic strategies for the management of sepsis-associated pathology and infectious diseases". *Frontiers in Immunology*, 4:387.

128. Hamilton FW et al. (2023). Therapeutic potential of IL6R blockade for the treatment of sepsis and sepsis-related death: A Mendelian randomisation study". *PLoS Medicine*, 20:e1004174.

129. Alsabani M et al. (2022). Reduction of NETosis by targeting CXCR1/2 reduces thrombosis, lung injury, and mortality in experimental human and murine sepsis". *British Journal of Anaesthesia*, 128:283–93.

130. Shane AL & Stoll BJ. (2013). Recent developments and current issues in the epidemiology, diagnosis, and management of bacterial and fungal neonatal sepsis". *American Journal of Perinatology*, 30:131–41. https://doi.org/10.1055/s-0032-1333413.

131. Polat G et al. (2017). Sepsis and septic shock: current treatment strategies and new approaches". *The Eurasian Journal of Medicine*, 49:53.

132. Pardoll DM. (2012). The blockade of immune checkpoints in cancer immunotherapy. vol. 12. 252–64. https://doi.org/10.1038/nrc3239.

133. Pesce S et al. (2020). Cancer immunotherapy by blocking immune checkpoints on innate lymphocytes". *Cancers*, 12:3504.

134. Mariotti FR et al. (2019). Innate lymphoid cells: expression of PD-1 and other checkpoints in normal and pathological conditions". *Frontiers in Immunology*, 10:910.

135. Weyand CM & Goronzy JJ. (2021). The immunology of rheumatoid arthritis". *Nature Immunology*, 22:10–8.

136. Dunne MR et al. (2016). Enrichment of inflammatory IL-17 and TNF-α secreting CD4+ T cells within colorectal tumors despite the presence of elevated CD39+ T regulatory cells and increased expression of the immune checkpoint molecule, PD-1". *Frontiers in Oncology*, 6:50.

137. Keir ME et al. (2008). PD-1 and its ligands in tolerance and immunity. vol. 26. 677–704. https://doi.org/10.1146/annurev.immunol.26.021607.090331.

138. Alvarez IB et al. (2010). Role played by the programmed death-1-programmed death ligand pathway during innate immunity against Mycobacterium tuberculosis". *Journal of Infectious Diseases*, 202:524–32. https://doi.org/10.1086/654932.

139. Eddens T et al. (2024). PD-1 signaling in neonates restrains CD8+ T cell function and protects against respiratory viral immunopathology". *Mucosal Immunology*, 17:476–90. https://doi.org/10.1016/j.mucimm.2023.12.004.

140. Zasada M et al. (2017). Analysis of PD-1 expression in the monocyte subsets from non-septic and septic preterm neonates". *PLoS ONE*, 12. https://doi.org/10.1371/journal.pone.0186819.

141. Dietz S et al. (2023). Expression of immune checkpoint molecules on adult and neonatal T-cells". *Immunologic Research*, 71:185–96. https://doi.org/10.1007/s12026-022-09340-6.

142. Bretscher P & Cohn M. (1970). A Theory of Self-Nonself Discrimination: Paralysis and induction involve the recognition of one and two determinants on an antigen, respectively.". *Science*, 169:1042–9.

143. Francisco LM et al. (2009). PD-L1 regulates the development, maintenance, and function of induced regulatory T cells". *Journal of Experimental Medicine*, 206:3015–29.

144. Ma CJ et al. (2011). PD-1 negatively regulates interleukin-12 expression by limiting STAT-1 phosphorylation in monocytes/macrophages duringchronic hepatitis C virus infection". *Immunology*, 132:421–31. https://doi.org/10.1111/j.1365-2567.2010.03382.x.

145. Wherry EJ & Kurachi M. (2015). Molecular and cellular insights into T cell exhaustion". *Nature Reviews Immunology*, 15:486–99.

146. Walker LSK & Sansom DM. (2011). The emerging role of CTLA4 as a cell-extrinsic regulator of T cell responses". *Nature Reviews Immunology*, 11:852–63.

147. Ribas A & Wolchok JD. (2018). Cancer immunotherapy using checkpoint blockade". *Science*, 359:1350–5.

148. Bader LI et al. (2017). Assays for infliximab drug levels and antibodies: a matter of scales and categories". *Scandinavian Journal of Immunology*, 86:165–70.

149. Zou W. (2005). Immunosuppressive networks in the tumour environment and their therapeutic relevance". *Nature Reviews Cancer*, 5:263–74.

150. Shao R et al. (2016). Monocyte programmed death ligand-1 expression after 3-4 days of sepsis is associated with risk stratification and mortality in septic patients: A prospective cohort study". *Critical Care*, 20. https://doi.org/10.1186/s13054-016-1301-x.

151. Young WA et al. (2017). Improved survival after induction of sepsis by cecal slurry in PD-1 knockout murine neonates". *Surgery (United States)*, 161:1387–93. https://doi.org/10.1016/j.surg.2016.11.008.

152. Patil NK et al. (2017). Targeting immune cell checkpoints during sepsis. vol. 18. MDPI AG. https://doi.org/10.3390/ijms18112413.

153. Inoue S et al. (2011). Dose-dependent effect of anti-CTLA-4 on survival in sepsis". *Shock*, 36:38–44.

154. Huang X et al. (2009). PD-1 expression by macrophages plays a pathologic role in altering microbial clearance and the innate inflammatory response to sepsis.

155. Fallon EA et al. (2021). Survival and Pulmonary Injury After Neonatal Sepsis: PD1/PDL1's Contributions to Mouse and Human Immunopathology". *Frontiers in Immunology*, 12. https://doi.org/10.3389/fimmu.2021.634529.

156. Zhang Y et al. (2010). PD-L1 blockade improves survival in experimental sepsis by inhibiting lymphocyte apoptosis and reversing monocyte dysfunction". *Critical Care*, 14. https://doi.org/10.1186/cc9354.

157. Yang L et al. (2024). PD-L1 Blockade Improves Survival in Sepsis by Reversing Monocyte Dysfunction and Immune Disorder". *Inflammation*, 47:114–28. https://doi.org/10.1007/s10753-023-01897-0.

158. Hotchkiss RS et al. (2019). Immune checkpoint inhibition in sepsis: a Phase 1b randomized study to evaluate the safety, tolerability, pharmacokinetics, and pharmacodynamics of nivolumab". *Intensive Care Medicine*, 45:1360–71.

159. Hotchkiss RS et al. (2019). Immune checkpoint inhibition in sepsis: a phase 1b randomized, placebo-controlled, single ascending dose study of antiprogrammed cell death-ligand 1 antibody (BMS-936559)". *Critical Care Medicine*, 47:632–42.

160. Watanabe E et al. (2020). Pharmacokinetics, pharmacodynamics, and safety of nivolumab in patients with sepsis-induced immunosuppression: a multicenter, open-label phase 1/2 study". *Shock*, 53:686–94.

161. Walk J et al. (2012). Inhibitory receptor expression on neonatal immune cells". *Clinical and Experimental Immunology*, 169:164–71. https://doi.org/10.1111/j.1365-2249.2012.04599.x.

162. BARCLAY AN & WARD HA. (1982). Purification and Chemical Characterisation of Membrane Glycoproteins from Rat Thymocytes and Brain, Recognised by Monoclonal Antibody MRC OX 2". *European Journal of Biochemistry*, 129:447–58. https://doi.org/10.1111/j.1432-1033.1982.tb07070.x.

163. Clark MJ et al. (1985). MRC OX-2 antigen: a lymphoid/neuronal membrane glycoprotein with a structure like a single immunoglobulin light chain. vol. 4.

164. Barclay AN et al. (2002). CD200 and membrane protein interactions in the control of myeloid cells". *Trends in Immunology*, 23:285–90.

165. Mccaughan GW et al. (1987). Characterization of the Human Homolog of the Rat MRC OX-2 Membrane Glycoprotein. vol. 25.

166. Borriello F et al. (1998). Characterization and localization of Mox2, the gene encoding the murine homolog of the rat MRC OX-2 membrane glycoprotein. vol. 9.

167. Wright GJ et al. (2001). The unusual distribution of the neuronal/lymphoid cell surface CD200 (OX2) glycoprotein is conserved in humans". *Immunology*, 102:173–9. https://doi.org/10.1046/j.1365-2567.2001.01163.x.

168. Hoek RM et al. (2000). Down-regulation of the macrophage lineage through interaction with OX2 (CD200)". *Science*, 290:1768–71.

169. Snelgrove RJ et al. (2008). A critical function for CD200 in lung immune homeostasis and the severity of influenza infection". *Nature Immunology*, 9:1074–83. https://doi.org/10.1038/ni.1637.

170. Coles SJ et al. (2011). CD200 expression suppresses natural killer cell function and directly inhibits patient anti-tumor response in acute myeloid leukemia". *Leukemia*, 25:792–9. https://doi.org/10.1038/leu.2011.1.

171. Conticello C et al. (2013). CD200 expression in patients with Multiple Myeloma: Another piece of the puzzle". *Leukemia Research*, 37:1616–21. https://doi.org/10.1016/j.leukres.2013.08.006.

172. Gorczynski RM et al. (2000). Receptor engagement on cells expressing a ligand for the tolerance-inducing molecule OX2 induces an immunoregulatory population that inhibits alloreactivity in vitro and in vivo". *The Journal of Immunology*, 165:4854–60.

173. Wright GJ et al. (2003). Characterization of the CD200 Receptor Family in Mice and Humans and Their Interactions with CD200 1. vol. 171.

174. Wright GJ et al. (2000). Lymphoid/Neuronal Cell Surface OX2 Glycoprotein Recognizes a Novel Receptor on Macrophages Implicated in the Control of Their Function). N-CAM and L1 are involved in mediating The OX2 protein (CD200) belongs to a group of leukocyte Results Production of a Monoclonal Antibody that Binds Rat Resident Peritoneal Cells and Blocks OX2 Binding In a previous study, a receptor for OX2 was identified. vol. 13.

175. Daëron M et al. (2008). Immunoreceptor tyrosine-based inhibition motifs: a quest in the past and future". *Immunological Reviews*, 224:11–43.

176. Mihrshahi R et al. (2009). Essential Roles for Dok2 and RasGAP in CD200 Receptor-Mediated Regulation of Human Myeloid Cells". *The Journal of Immunology*, 183:4879–86. https://doi.org/10.4049/jimmunol.0901531.

177. Vieites JM et al. (2003). Characterization of human cd200 glycoprotein receptor gene located on chromosome 3q12-13". *Gene*, 311:99–104. https://doi.org/10.1016/S0378-1119(03)00562-6.

178. Zhang S & Phillips JH. (2005). Identification of tyrosine residues crucial for CD200R-mediated inhibition of mast cell activation". *Journal of Leukocyte Biology*, 79:363–8. https://doi.org/10.1189/jlb.0705398.

179. Zhang S et al. (2004). Molecular Mechanisms of CD200 Inhibition of Mast Cell Activation. vol. 173.

180. Mihrshahi R & Brown MH. (2010). Downstream of Tyrosine Kinase 1 and 2 Play Opposing Roles in CD200 Receptor Signaling". *The Journal of Immunology*, 185:7216–22. https://doi.org/10.4049/jimmunol.1002858.

181. Hatherley D et al. (2005). Recombinant CD200 protein does not bind activating proteins closely related to CD200 receptor". *The Journal of Immunology*, 175:2469–74.

182. Voehringer D et al. (2004). CD200 receptor family members represent novel DAP12-associated activating receptors on basophils and mast cells". *Journal of Biological Chemistry*, 279:54117–23.

183. Kojima T et al. (2007). Mast cells and basophils are selectively activated in vitro and in vivo through CD200R3 in an IgE-independent manner". *The Journal of Immunology*, 179:7093–100.

184. Gorczynski R et al. (2004). CD200 Is a Ligand for All Members of the CD200R Family of Immunoregulatory Molecules 1. vol. 172.

185. Hatherley D & Barclay AN. (2004). The CD200 and CD200 receptor cell surface proteins interact through their N-terminal immunoglobulin-like domains". *European Journal of Immunology*, 34:1688–94.

186. Rijkers ESK et al. (2008). The inhibitory CD200R is differentially expressed on human and mouse T and B lymphocytes". *Molecular Immunology*, 45:1126–35. https://doi.org/10.1016/j.molimm.2007.07.013.

187. Choueiry F et al. (2020). CD200 promotes immunosuppression in the pancreatic tumor microenvironment". *Journal for Immunotherapy of Cancer*, 8. https://doi.org/10.1136/jitc-2019-000189.

188. Jenmalm MC et al. (2006). Regulation of Myeloid Cell Function through the CD200 Receptor". *The Journal of Immunology*, 176:191–9. https://doi.org/10.4049/jimmunol.176.1.191.

189. Taylor N et al. (2005). Enhanced Tolerance to Autoimmune Uveitis in CD200-Deficient Mice Correlates with a Pronounced Th2 Switch in Response to Antigen Challenge1.

190. Gorczynski L et al. (1999). Evidence that an OX-2-positive cell can inhibit the stimulation of type 1 cytokine production by bone marrow-derived B7-1 (and B7-2)-positive dendritic cells". *The Journal of Immunology*, 162:774–81.

191. Gorczynski RM et al. (2005). Augmented induction of CD4+CD25+ treg using monoclonal antibodies to CD200R". *Transplantation*, 79:488–91. https://doi.org/10.1097/01.TP.0000152118.51622.F9.

192. Memarian A et al. (2013). Upregulation of CD200 is associated with Foxp3+ regulatory T cell expansion and disease progression in acute myeloid leukemia". *Tumor Biology*, 34:531–42. https://doi.org/10.1007/s13277-012-0578-x.

193. Coles SJ et al. (2012). Increased CD200 expression in acute myeloid leukemia is linked with an increased frequency of FoxP3 + regulatory T cells. vol. 26. 2146–8. https://doi.org/10.1038/leu.2012.75.

194. Aref S et al. (2017). Upregulation of CD200 is associated with regulatory T cell expansion and disease progression in multiple myeloma". *Hematological Oncology*, 35:51–7. https://doi.org/10.1002/hon.2206.

195. Bissonnette EY et al. (2020). Cross-Talk Between Alveolar Macrophages and Lung Epithelial Cells is Essential to Maintain Lung Homeostasis. vol. 11. Frontiers Media S.A. https://doi.org/10.3389/fimmu.2020.583042.

196. Jiang-Shieh YF et al. (2010). Distribution and expression of CD200 in the rat respiratory system under normal and endotoxin-induced pathological conditions". *Journal of Anatomy*, 216:407–16. https://doi.org/10.1111/j.1469-7580.2009.01190.x.

197. Gorczynski RM et al. (2002). The same immunoregulatory molecules contribute to successful pregnancy and transplantation". *American Journal of Reproductive Immunology*, 48:18–26. https://doi.org/10.1034/j.1600-0897.2002.01094.x.

198. Tonks A et al. (2007). CD200 as a prognostic factor in acute myeloid leukaemia [7]. vol. 21. Nature Publishing Group. 566–8. https://doi.org/10.1038/sj.leu.2404559.

199. Mora A et al. (2019). CD200 is a useful marker in the diagnosis of chronic lymphocytic leukemia". *Cytometry Part B - Clinical Cytometry*, 96:143–8. https://doi.org/10.1002/cyto.b.21722.

200. Moreaux J et al. (2006). CD200 is a new prognostic factor in multiple myeloma". *Blood*, 108:4194–7. https://doi.org/10.1182/blood-2006-06-029355.

201. Patoine D et al. (2022). Specificity of CD200/CD200R pathway in LPS-induced lung inflammation". *Frontiers in Immunology*, 13. https://doi.org/10.3389/fimmu.2022.1092126.

202. Mukhopadhyay S et al. (2010). Immune Inhibitory Ligand CD200 Induction by TLRs and NLRs limits macrophage activation to protect the host from meningococcal septicemia". *Cell Host and Microbe*, 8:236–47. https://doi.org/10.1016/j.chom.2010.08.005.

203. Wong KK et al. (2012). Soluble CD200 is critical to engraft chronic lymphocytic leukemia cells in immunocompromised mice". *Cancer Research*, 72:4931–43. https://doi.org/10.1158/0008-5472.CAN-12-1390.

204. Twito T et al. (2013). Ectodomain shedding of CD200 from the B-CLL cell surface is regulated by ADAM28 expression". *Leukemia Research*, 37:816–21.

205. Wong KK et al. (2016). Characterization of CD200 ectodomain shedding". *PLoS ONE*, 11. https://doi.org/10.1371/journal.pone.0152073.

206. Li Y et al. (2012). Aberrant CD200/CD200R1 expression and function in systemic lupus erythematosus contributes to abnormal T-cell responsiveness and dendritic cell activity". *Arthritis Research and Therapy*, 14. https://doi.org/10.1186/ar3853.

207. Clark DA et al. (2018). Soluble CD200 in secretory phase endometriosis endometrial venules may explain endometriosis pathophysiology and provide a novel treatment target". *Journal of Reproductive Immunology*, 129:59–67.

208. Charles River Laboratories. (2025). C57BL/6 Mice | Charles River". https://www.criver.com/products-services/find-model/c57bl6-mouse?region=23 (accessed August 12, 2025).

209. The Jackson Laboratory. (2025). 000664 - B6 Strain Details". https://www.jax.org/strain/000664# (accessed August 12, 2025).

210. Speer EM et al. (2020). A Neonatal Murine Escherichia coli Sepsis Model Demonstrates That Adjunctive Pentoxifylline Enhances the Ratio of Anti- vs. Pro-inflammatory Cytokines in Blood and Organ Tissues". *Frontiers in Immunology*, 11. https://doi.org/10.3389/fimmu.2020.577878.

211. Miltenyi Biotec. (2020). Anti-FITC MicroBeads, Datasheet". https://static.miltenyibiotec.com/asset/150655405641/document_qal0dblh8t06fcfkru8tg8ht19?content-disposition=inline (accessed August 14, 2025).

212. BioLegend Inc. n.d.Mouse TNF-α ELISA MAX™ Standard Set, Datasheet". https://www.biolegend.com/en-us/products/mouse-tnf-alpha-elisa-max-standard-2242 (accessed August 14, 2025).

213. BioLegend Inc. n.d.Mouse IL-6 ELISA MAX™ Standard Set, Datasheet". https://www.biolegend.com/en-us/products/mouse-il-6-elisa-max-standard-2250 (accessed August 14, 2025).

214. R&D Systems Inc. n.d.DuoSet™ CD200 ELISA Development System, Datasheet". https://www.rndsystems.com/products/human-cd200-duoset-elisa_dy2724#product-datasheets (accessed August 16, 2025).

215. Biolegend. (2025). MojoSort™ Human Pan Monocyte Isolation Kit, Datasheet". https://www.biolegend.com/protocols/mojosort-human-pan-monocyte-isolation-kit-protocol/4312/ (accessed August 21, 2025).

216. R&D Systems Inc. n.d.DuoSet™ CXCL1/KC ELISA, Datasheet". https://resources.rndsystems.com/pdfs/datasheets/dy453-05.pdf?v=20250921&_gl=1*7sxztr*_up*MQ..*_ga*MzA4OTc4MjAzLjE3NTg1Mzg0NTA.*_ga_2T0XXM39JP*czE3NTg1Mzg0NDkkbzEkZzAkdDE3NTg1Mzg0NDkkajYwJGwwJGgw (accessed September 22, 2025).

217. Macherey-Nagel. (2022). Bioanalysis NucleoSpin ® RNAIsolation Kit, Datasheet". https://www.mn-net.com/media/pdf/b0/51/ee/Instruction-NucleoSpin-RNA.pdf (accessed August 21, 2025).

218. Miltenyi Biotec. (2020). Pan T-cell Isolation Kit, Datasheet". https://www.miltenyibiotec.com/DE-en/products/pan-t-cell-isolation-kit-human.html#130-096-535 (accessed August 21, 2025).

219. Thermo Fisher Scientific Inc. n.d.Pierce™ 660nm Protein Assay, Datasheet". https://assets.thermofisher.com/TFS-Assets/LSG/manuals/MAN0016386_Pierce660nmProteinAssay_PI.pdf (accessed August 14, 2025).

220. Boster Biological Technology. n.d.Mouse CD200 ELISA Kit PicoKine®, Datasheet". https://www.bosterbio.com/datasheet?sku=EK1185 (accessed August 14, 2025).

221. New England Biolabs. n.d.ProtoScript II First Strand cDNA Synthesis Kit, Datasheet". https://www.neb.com/en/protocols/2013/01/23/first-strand-cdna-synthesis-protocols-e6560?pdf=true (accessed August 21, 2025).

222. Robbins JB et al. (1974). Escherichia coli K1 capsular polysaccharide associated with neonatal meningitis". *New England Journal of Medicine*, 290:1216–20.

223. Hirstch RE. (2003). Hemoglobin fluorescence. Hemoglobin Disorders: Molecular Methods and Protocols, Springer, p. 133–54.

224. Lippincott-Schwartz J et al. (1990). Microtubule-dependent retrograde transport of proteins into the ER in the presence of brefeldin A suggests an ER recycling pathway". *Cell*, 60:821–36.

225. Lyons AB. (2000). Analysing cell division in vivo and in vitro using flow cytometric measurement of CFSE dye dilution". *Journal of Immunological Methods*, 243:147–54.

226. McKinnon KM. (2018). Flow cytometry: an overview". *Current Protocols in Immunology*, 120:1–5.

227. Shah K & Maghsoudlou P. (2016). Enzyme-linked immunosorbent assay (ELISA): the basics". *British Journal of Hospital Medicine*, 77:C98–101.

228. Cai L et al. (2023). Advances in Rodent Experimental Models of Sepsis. vol. 24. Multidisciplinary Digital Publishing Institute (MDPI). https://doi.org/10.3390/ijms24119578.

229. Wynn JL et al. (2007). Increased mortality and altered immunity in neonatal sepsis produced by generalized peritonitis". *Shock*, 28:675–83. https://doi.org/10.1097/shk.0b013e3180556d09.

230. Brook B et al. (2019). Robust health-score based survival prediction for a neonatal mouse model of polymicrobial sepsis". *PLoS ONE*, 14. https://doi.org/10.1371/journal.pone.0218714.

231. Brudecki L et al. (2012). Myeloid-derived suppressor cells evolve during sepsis and can enhance or attenuate the systemic inflammatory response". *Infection and Immunity*, 80:2026–34. https://doi.org/10.1128/IAI.00239-12.

232. Michels KR et al. (2019). The Role of Iron in the Susceptibility of Neonatal Mice to Escherichia coli K1 Sepsis". *Journal of Infectious Diseases*, 220:1219–29. https://doi.org/10.1093/infdis/jiz282.

233. Mancuso G et al. (2004). Dual Role of TLR2 and Myeloid Differentiation Factor 88 in a Mouse Model of Invasive Group B Streptococcal Disease1.

234. Lieblein-Boff JC et al. (2013). Neonatal E. coli infection causes neuro-behavioral deficits associated with hypomyelination and neuronal sequestration of iron". *Journal of Neuroscience*, 33:16334–45.

235. Zhu Y et al. (2024). Differential neutrophil responses in murine following intraperitoneal injections of Escherichia coli and Staphylococcus aureus". *Heliyon*, 10.

236. Singh K et al. (2010). Inter-alpha inhibitor protein administration improves survival from neonatal sepsis in mice". *Pediatric Research*, 68:242–7.

237. Seman BG et al. (2020). A neonatal imaging model of gram-negative bacterial sepsis". *Journal of Visualized Experiments (JoVE)*,:e61609.

238. Rubens CE et al. (1991). Pathophysiology and Histopathology of Group B Streptococcal Sepsis in Macaca nemestrina Primates Induced after Intraamniotic Inoculation: Evidence for Bacterial Cellular Invasion.

239. Shimada Y et al. (2009). Age-associated up-regulation of a negative co-stimulatory receptor PD-1 in mouse CD4+ T cells". *Experimental Gerontology*, 44:517–22.

240. Jain SS et al. (2024). The Role of Aging and Senescence in Immune Checkpoint Inhibitor Response and Toxicity". *International Journal of Molecular Sciences*, 25:7013.

241. Yu G et al. (2008). LPS-induced murine abortions require C5 but not C3, and are prevented by upregulating expression of the CD200 tolerance signaling molecule". *American Journal of Reproductive Immunology*, 60:135–40.

242. Mach P et al. (2022). Soluble PD-L1 and B7-H4 serum levels during the course of physiological pregnancy". *American Journal of Reproductive Immunology*, 87:e13519.

243. Guleria I et al. (2005). A critical role for the programmed death ligand 1 in fetomaternal tolerance". *The Journal of Experimental Medicine*, 202:231–7.

244. Tripathi S et al. (2025). Role of PD-L1 in the Pathogenesis of Pre-Eclampsia and Its Association with Adverse Fetal Outcomes". *Turk Patoloji Dergisi*, 1.

245. Al Nabhani Z et al. (2019). A Weaning Reaction to Microbiota Is Required for Resistance to Immunopathologies in the Adult". *Immunity*, 50:1276-1288.e5. https://doi.org/10.1016/j.immuni.2019.02.014.

246. Tapping RI et al. (2000). Toll-like receptor 4, but not toll-like receptor 2, is a signaling receptor for Escherichia and Salmonella lipopolysaccharides". *The Journal of Immunology*, 165:5780–7.

247. Massari P et al. (2006). Meningococcal porin PorB binds to TLR2 and requires TLR1 for signaling". *The Journal of Immunology*, 176:2373–80.

248. Pridmore AC et al. (2003). Activation of toll-like receptor 2 (TLR2) and TLR4/MD2 by Neisseria is independent of capsule and lipooligosaccharide (LOS) sialylation but varies widely among LOS from different strains". *Infection and Immunity*, 71:3901–8.

249. Doran KS et al. (2016). Host–pathogen interactions in bacterial meningitis". *Acta Neuropathologica*, 131:185–209.

250. Humphries HE et al. (2005). Activation of human meningeal cells is modulated by lipopolysaccharide (LPS) and non-LPS components of Neisseria meningitidis and is independent of Toll-like receptor (TLR) 4 and TLR2 signalling". *Cellular Microbiology*, 7:415–30.

251. Ulas T et al. (2017). S100-alarmin-induced innate immune programming protects newborn infants from sepsis". *Nature Immunology*, 18:622–32. https://doi.org/10.1038/ni.3745.

252. Holt PG & Strickland DH. (2008). The CD200-CD200R axis in local control of lung inflammation". *Nature Immunology*, 9:1011–3.

253. De Luca D et al. (2017). The Montreux definition of neonatal ARDS: biological and clinical background behind the description of a new entity". *The Lancet Respiratory Medicine*, 5:657–66.

254. Ramonell KM et al. (2017). CXCR4 blockade decreases CD4+ T cell exhaustion and improves survival in a murine model of polymicrobial sepsis". *PloS One*, 12:e0188882.

255. González-Amaro R et al. (2013). Is CD69 an effective brake to control inflammatory diseases?". *Trends in Molecular Medicine*, 19:625–32.

256. Schlöder J et al. (2022). Boosting regulatory T cell function for the treatment of autoimmune diseases–That's only half the battle!". *Frontiers in Immunology*, 13:973813.

257. Koning N et al. (2010). Expression of the inhibitory CD200 receptor is associated with alternative macrophage activation". *Journal of Innate Immunity*, 2:195–200. https://doi.org/10.1159/000252803.

258. Doeing DC et al. (2003). Gender dimorphism in differential peripheral blood leukocyte counts in mice using cardiac, tail, foot, and saphenous vein puncture methods". *BMC Clinical Pathology*, 3:3.

259. Mestas J & Hughes CCW. (2004). Of Mice and Not Men: Differences between Mouse and Human Immunology".

260. Rehli M. (2002). Of mice and men: species variations of Toll-like receptor expression". *Trends in Immunology*, 23:375–8.

261. Gordon J et al. (2001). Modelling the human immune response: can mice be trusted?". *Current Opinion in Pharmacology*, 1:431–5.

262. Lenschow DJ et al. (1996). CD28/B7 system of T cell costimulation". *Annual Review of Immunology*, 14:233–58.

263. Li J et al. (2020). Discrepant mRNA and protein expression in immune cells". *Current Genomics*, 21:560–3.

264. Liu Y et al. (2016). On the Dependency of Cellular Protein Levels on mRNA Abundance. vol. 165. Cell Press. 535–50. https://doi.org/10.1016/j.cell.2016.03.014.

265. Kandeel EZ et al. (2021). Overexpression of CD200 and CD123 is a major influential factor in the clinical course of pediatric acute myeloid leukemia". *Experimental and Molecular Pathology*, 118:104597.

266. Morgan HJ et al. (2022). CD200 ectodomain shedding into the tumor microenvironment leads to NK cell dysfunction and apoptosis". *Journal of Clinical Investigation*, 132. https://doi.org/10.1172/JCI150750.

267. D'Arena G et al. (1998). Flow cytometric characterization of human umbilical cord blood lymphocytes: immunophenotypic features". *Haematologica*, 83:197–203.

268. Fraser SD et al. (2016). Reduced expression of monocyte CD200R is associated with enhanced proinflammatory cytokine production in sarcoidosis". *Scientific Reports*, 6:38689.

269. Stanford AH et al. (2020). A direct comparison of mouse and human intestinal development using epithelial gene expression patterns". *Pediatric Research*, 88:66–76.

270. Miller AJ & Spence JR. (2017). In vitro models to study human lung development, disease and homeostasis". *Physiology*, 32:246–60.

271. Lockwood CJ & Kuczynski E. (1999). Markers of risk for preterm delivery".

272. Sibai BM. (2006). Preeclampsia as a cause of preterm and late preterm (near-term) births. Semin Perinatol, vol. 30, Elsevier, p. 16–9.

273. Berkowitz GS et al. (1998). Risk factors for preterm birth subtypes". *Epidemiology*, 9:279–85.

274. Goldenberg RL et al. (2008). Epidemiology and causes of preterm birth". *The Lancet*, 371:75–84.

275. Eiwegger T et al. (2008). Allergen specific responses in cord and adult blood are differentially modulated in the presence of endotoxins". *Clinical & Experimental Allergy*, 38:1627–34.

276. Alnabhan R et al. (2015). Differential activation of cord blood and peripheral blood natural killer cells by cytokines". *Cytotherapy*, 17:73–85.

277. Lyons A et al. (2007). CD200 ligand–receptor interaction modulates microglial activation in vivo and in vitro: a role for IL-4". *Journal of Neuroscience*, 27:8309–13.

278. Ritzel RM et al. (2019). CD200-CD200R1 inhibitory signaling prevents spontaneous bacterial infection and promotes resolution of neuroinflammation and recovery after stroke". *Journal of Neuroinflammation*, 16. https://doi.org/10.1186/s12974-019-1426-3.

279. Walker DG et al. (2009). Decreased expression of CD200 and CD200 receptor in Alzheimer's disease: A potential mechanism leading to chronic inflammation". *Experimental Neurology*, 215:5–19. https://doi.org/10.1016/j.expneurol.2008.09.003.

280. Zhang S et al. (2011). CD200-CD200R dysfunction exacerbates microglial activation and dopaminergic neurodegeneration in a rat model of Parkinson's disease". *Journal of Neuroinflammation*, 8. https://doi.org/10.1186/1742-2094-8-154.

281. Shrum B et al. (2014). A robust scoring system to evaluate sepsis severity in an animal model". *BMC Research Notes*, 7:233.

7. Contributions

This study was conducted at the University Children´s Hospital Tübingen, department of neonatology, research group for neonatal immunology and immune tolerance. It was supervised by PD Dr. med. Natascha Köstlin-Gille. Prof. Dr. Katja Schenke-Layland served as the second supervisor and was always available for questions and support.

Conceptualization of this study and interpretation of results was done in close collaboration with PD Dr. med. Natascha Köstlin-Gille.

The study was funded by the Jürgen Manchot Foundation.

With the following exceptions, the data in this dissertation originate solely from my own experimental work:

Murine IL-6, TNF-α and CXCL1 ELISAs: Determination of murine plasma protein concentrations and the murine cytokine ELISA assays were performed by PD Dr. Trim Lajqi in cooperation with the Department of Neonatology under the direction of Prof. Dr. med. Christian Gille, Heidelberg Children's Hospital, Germany. Collection of plasma and analysis and interpretation of collected data were done by me.

8. Acknowledgements

Finally, I would like to take the opportunity to thank everyone who supported me throughout my work on this thesis over the past three years.

First, I would like to thank the supervisors of this thesis and members of my thesis advisory committee (TAC) PD Dr. Natascha Köstlin-Gille and Prof. Dr. Katja Schenke-Layland who, together with Prof. Dr. Ivo Bendix (University Hospital Essen), took the time to support me throughout my work on this project with valuable feedback and advice. I especially want to highlight PD Dr. Natascha Köstlin-Gille who, as my primary supervisor, gave me the chance to work on this thesis in her lab as part of the Department of Neonatology at the Children´s Hospital Tübingen. Thank you for believing in me and all your encouragement and guidance throughout, and for the countless hours we spent planning this project, executing it and discussing the results. I learned lots of valuable lessons during my time in your lab and you gave me the chance to learn from you and profit from your extensive knowledge of neonatal immunology which shaped me into the scientist I am today. This thesis would not have been possible without your support. Additionally, I would like to thank Prof. Dr. Christian Gille and Prof. Dr. Christian F. Poets for their guidance and support.

Further, I want to thank all members of the NeoLab who supported me during the experiments and long days of work for this thesis and always took the time to listen, give feedback or lend me their knowledge. So, a special thanks to Steffi, Gabriele, Jessi and all the amazing medical doctoral students who worked in the lab, without you I probably would have quit a long time ago. I also want to thank Juli, who helped and guided me through the first steps of establishing the murine sepsis experiments and who collected all the blood samples of pre-mature neonates for this project. Also, I want to thank Trim from the NeoLab in Heidelberg for his work performing all murine cytokine ELISAs and for his feedback on my experimental setups.

A big thank you also to all the animal caretakers, especially Alisha Huff, who took care of the animals every day and supported all murine experiments. Without you, planning and executing these complex experiments would not have been possible.

I want to thank Libera Lo Presti for helping me to improve my scientific writing skills and for her valuable feedback over the past couple months. I also want to thank her for her kind words and unwavering support throughout my work on this thesis.

I want to thank the Jürgen Manchot Foundation for their financial support of this project.

Lastly, I especially want to thank my family, my parents Michael and Andrea, my sister Jenny and my grandparents Harald und Elfriede, who endlessly supported and encouraged me throughout this thesis project, even when things were though. Thank you for always being there for me and for helping me achieve everything I set out to do in life. And of course, I also want to give a special shoutout to my best friend Sabrina, who has been a great support and a valuable source of comfort in my life and who has had to listen to all my complaints and problems over the past three years, and to my very close friends Lena, Miri, Svenja, Vani, Adri, Basti, Flo and Tobi who supported me endlessly throughout the past twelve years, and who always made sure that we collected many wonderful memories together outside of work.

9. Appendix

9.1. Scoresheets murine sepsis

9.1.1. Score sheet for adult *E. coli* sepsis

Table 17. Score sheet for adult murine *E. coli* sepsis.

Top part shows characteristics of mouse behavior and appearance and the corresponding score points. Bottom part shows adjustments to the surveillance protocol based on score points. The scoresheet was based on the murine sepsis score by Shrum et al. [281].

Score	0	1	2	3
Appearance	Smooth coat	Slightly ruffled fur	Majority of fur on back is ruffled	Piloerection, puffy appearance
Level of consciousness	Active	Active, avoids standing upright	Active only when provoked	Non-responsive, even when provoked
Activity	Normal	Suppressed eating, drinking, or running	Stationary	Stationary, even when provoked
Response to stimulus	Normal	Slowed response to auditory or touch stimuli	No response to auditory, slowed response to touch	No response to touch stimuli
Eyes	Open	Not fully open, potentially secretions	Half closed, potential secretions	Mostly or completely closed
Respiration quality	Normal	Periods of labored breathing	Consistently labored breathing	Labored breathing with gasps
Weight	Normal	Weight loss 5-10%	Weight loss >10 to 20%	Weight loss ≥ 20%
Score 0-2:	no burden, observation every 12h	**Score 6-9:**	moderate burden, observation every 2h	
Score 3-5:	low burden, observation every 6h, adding wet food	**Score ≥ 10:**	high burden, immediate termination of experiment	

9.1.2. Score sheet for neonatal sepsis

Table 18. Score sheet for neonatal murine *E. coli* sepsis.

Top part shows characteristics of neonatal mouse behavior and appearance and the corresponding score points. Bottom part shows adjustments to the surveillance protocol based on score points.

Score	0	1	2
Appearance (JAX Score) (s. Figure 32)	No deviation	Deviation in 1 score	Deviation > 1 score
Activity	Spontaneous movement to teat	Reduced movement to teat	No movement to teat
Vigilance	Normal and normal food uptake	Reduced food uptake	No food uptake
Respiration quality	Normal	Periods of labored breathing	Consistently labored breathing
Behavior of mother	Normal		Rejection of pups
Score 0:	no burden, observation every 6h		
Score ≤ 2	Intensive observation, every 3h		
Score > 2	Immediate termination of experiment		

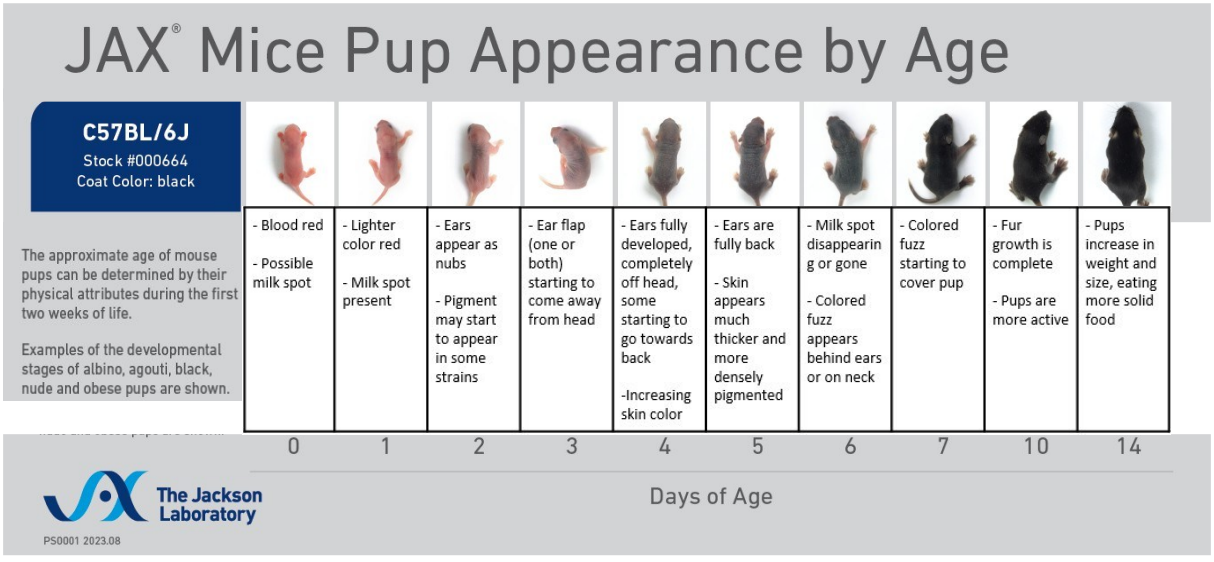

Figure 32. JAX® mice pup appearance by age.

Figure shows the mice pup appearance by age overview for C57BL/6J mice adapted from the original image of the Jackson laboratory used to determine pup appearance of neonatal sepsis mice in our score sheet. Adjusted from: https://jackson.jax.org/rs/444-BUH-304/images/Poster_Pup_Appearance_Age.pdf, by Janine Hebel

9.2. Comparison of adult and neonatal murine sepsis

Additionally, to the severity markers shown in **Table 13**, we analyzed differences in bacterial load of organs and blood **Table 19** and plasma cytokine levels **Table 20** between surviving and deceased animals. On average, mice who survived sepsis had much lower bacterial load in blood and organs compared to animals who succumbed to induced *E. coli* sepsis. Surviving animals had the highest bacterial load in spleens (adults) or blood (neonates), while animals who died had the highest bacterial concentrations in spleens (adults) or lungs (neonates) (**Table 19**). In adult mice, plasma levels of IL-6 was ~70 times higher in mice who died of sepsis compared to surviving animals. In neonatal mice IL-6 levels of surviving animals were ~1.5 times higher than those of neonatal mice who died earlier in the experiment. TNF-α levels could not be compared for adult mice due to the fact that no TNF-α levels were analyzed in adult mice who died of sepsis (instead CXCL1 Was analyzed, not shown). TNF-α levels of neonatal mice were similar between mice who survived and mice who didn´t. However, only one neonatal mouse who died of sepsis was analyzed for TNF-α plasma levels, the other ones were analyzed for CXCL1 levels (not shown) (**Table 20**).

Table 19. Comparison of bacterial load of adult and neonatal septic mice grouped surviving and deceased mice.

To compare sepsis progression and severity in an adult and neonatal murine *E. coli* sepsis models, sepsis was induced in adult mice via i.v. injection of *E. coli*. Sepsis was monitored for a maximum of 96 h following induction. Sepsis was induced in neonatal mice via s.c. injection of *E. coli*. Neonatal sepsis was monitored for a maximum of 48 h following induction. The table shows comparison analysis of bacterial load of organs spleen, liver and lung, as well as blood grouped in animals who survived sepsis and those who didn´t. ⌀ = average.

	Survived	Adults n = 19-27	Neonates n = 20-30		Dead	Adults n = 19-27	Neonates n = 20-30
⌀ Bacterial load	CFU/g spleen	$2.4x10^6$	$9.7x10^5$	⌀ Bacterial load	CFU/g spleen	$2x10^9$	$1.8x10^6$
	CFU/g lung	$1.2x10^6$	$6.0x10^5$		CFU/g lung	$2.1x10^7$	$3.7x10^7$
	CFU/g liver	$6.3x10^5$	$3.4x10^5$		CFU/g liver	$1x10^9$	$1.8x10^6$
	CFU/g blood	$4.1x10^4$	$4.5x10^6$		CFU/g blood	$5.6x10^6$	$5.7x10^6$

Table 20. Comparison of IL-6 and TNF-α plasma cytokine levels in adult and neonatal sepsis mice grouped in surviving and deceased animals.

To compare sepsis progression and severity in an adult and neonatal murine *E. coli* sepsis models, sepsis was induced in adult mice via i.v. injection of *E. coli*. Sepsis was monitored for a maximum of 96 h following induction. Sepsis was induced in neonatal mice via s.c. injection of *E. coli*. Neonatal sepsis was monitored for a maximum of 48 h following induction. The table shows comparison of plasma concentrations of pro-inflammatory cytokines IL-6 and TNF-α. ⌀ = average, n.a. = not available.

		Adults n = 19-27	**Neonates n = 20-30**
Cytokines	**⌀ IL-6 in ng/g SURVIVED**	80.74	4677
	⌀ IL-6 in ng/g DEAD	5631	3215
	⌀ TNF-α in pg/g SURVIVED	544.8	7115.9
	⌀ TNF-α in pg/g DEAD	n.a.	8160.9 (1 mouse only!)

9.3. *E. coli* sepsis induced mortality in adult and neonatal mice

To verify successful induction of sepsis in our murine *E. coli* sepsis models for adult and neonatal mice used to determine changes in CD200 and CD200R expression on immune cells during sepsis (see chapter 4.1.3, **Figure 16**), mortality was analyzed. We observed a significantly reduced probability of survival in adult mice after sepsis induction (A+) compared to adult controls with DPBS injection (A-) (**Figure 33**, A). Sepsis induction in our neonatal model also led to a decreased probability of survival in septic mice (N+) compared to healthy controls (N-) (**Figure 33**, B).

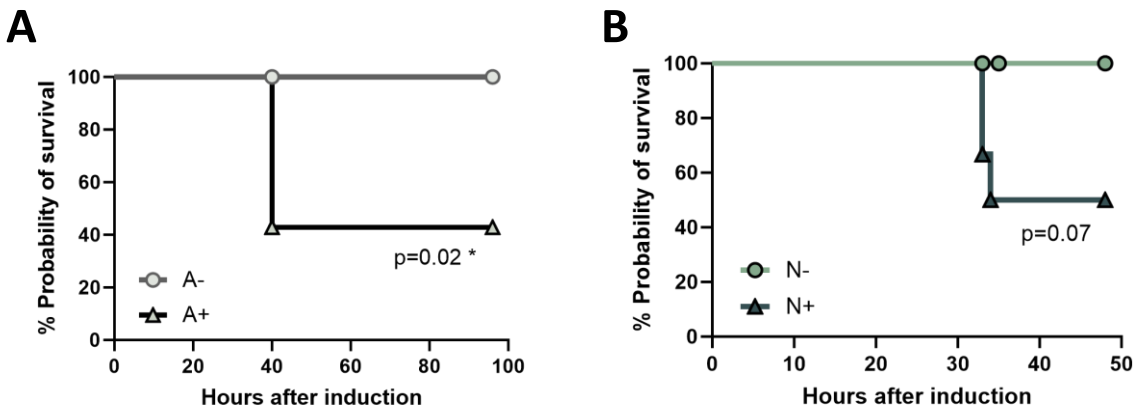

Figure 33. Mortality rate of adult and neonatal mice for the E. coli sepsis model.

To verify successful sepsis induction in adult and neonatal mice in our *E. coli* sepsis models, sepsis was induced via *E. coli* injection and mortality was recorded over the course of the experiment (96h for adults, 48h for neonates). **A** Survival curve shows probability of survival for healthy adult mice (A-) and septic adult mice (A+) in %. n=6, Log-Rank (Mantel-Cox) test. **B** Survival curve shows probability of survival for healthy neonatal (age P2) mice (N-) and septic neonatal mice (N+) in %. n=7, Log-Rank (Mantel-Cox) test. p=ns (not significant), *p < 0.05.